Key Emerging Issues and Recent Progress related to Structural Materials Degradation

Author

Francois Cattant
Plescop, Morbihan, France

A.N.T. INTERNATIONAL®

Advanced Nuclear Technology International
Spinnerivägen 1, Mellersta Fabriken plan 4,
448 51 Tollered, Sweden

info@antinternational.com
www.antinternational.com

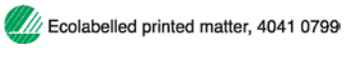
Ecolabelled printed matter, 4041 0799

Disclaimer

The information presented in this report has been compiled and analysed by Advanced Nuclear Technology International Europe AB (ANT International®) and its subcontractors. ANT International has exercised due diligence in this work, but does not warrant the accuracy or completeness of the information. ANT International does not assume any responsibility for any consequences as a result of the use of the information for any party, except a warranty for reasonable technical skill, which is limited to the amount paid for this report.

Quality-checked and authorized by:

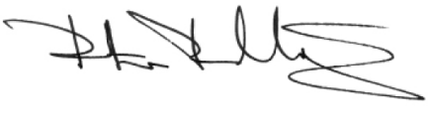

Mr Peter Rudling, President of ANT International

Content

1 Extended summary 1-1

2 Introduction 2-1

3 Workshops 3-1

3.1 Reactor Pressure Vessel Integrity Workshop 3-1
3.2 BWR/PWR in-vessel inspection Workshop 3-5
3.3 Fatigue management training Workshop 3-12

4 PWR chemistry 4-1

5 PWR reactor internals and ageing management 5-1

6 PWR nickel-based alloys 6-1

7 PWR stainless steel and modelling 7-1

8 BWR Major Component issues 8-1

8.1 AREVA solution. 8-3
8.2 GE Hitachi Nuclear Energy solution. 8-6
8.3 Westinghouse solution. 8-7

9 BWR Water Chemistry and Mitigation 9-1

10 BWR Assessment 10-1

11 BWR Inspection/Operating Experience/NDE 11-1

12 Probabilistic Fracture Mechanics/xLPR 12-1

13 Long Term Operations (LTO) 13-1

14 Non-destructive Examination Techniques 14-1

15 Reactor Pressure Vessel Integrity 15-1

16 Peening and Surface Mitigation 16-1

17 Cast Austenitic Stainless Steel 17-1

18 Thermal and Environmentally Assisted Fatigue 18-1

19 Welding Techniques & Residual Stress Modelling 19-1

20 Operational Experience & Plant Component Research 20-1

21 Steam Generator 21-1

References

Nomenclature

List of common abbreviations

Unit conversion

1 Extended summary

This EPRI conference is held every other even year, filling the gap left by the environmental degradation conference (held every odd year) and by the Fontevraud conference (every other even year); these are the three major routine conferences dedicated to materials degradations in NPPs.

The 2016 EPRI conference was two folds: a first day dedicated to workshops, followed by 3 days of "classic" type conference with papers presented in three parallel sessions.

During the Reactor Pressure Vessel Integrity Workshop, a broad review of the fundamental concepts related to RPV integrity, the current regulations and the rationale behind them and the existing and developing technologies / techniques for evaluating and assuring RPV integrity were presented, along with a focus is on the traditional vessel and the degradation mechanisms that impact operating limits (e.g., embrittlement).

With plants ageing, an emphasis is put on thermal ageing. LAS (plate, forging, welds, and HAZ) is susceptible to thermal aging. Thermal aging is caused by slow diffusion and segregation of impurity elements (e.g., primarily phosphorous) into grain boundaries at operating temperature. The result is an increase in DBTT but not yield strength/hardness; also known as a "non-hardening embrittlement". The degree of embrittlement is largely a function of the P content and temperature.

The LAS components susceptible to thermal ageing are:

- RPV LAS components, e.g., RPV flange, nozzle shell ring, and outlet nozzles, they experience temperatures of up to 315°C;
- Vessel heads of some reactors may be near the hot leg temperature of about 315°C;
- Pressurizers experience highest operating temperature at around 343°C.

The HAZ of pressurizer welds is viewed as the area the most susceptible to thermal ageing.

LAS is also susceptible to neutron Irradiation Embrittlement. RPV is fabricated of ferritic low alloy steel, which exhibits good combination of strength and ductility. Carbon and low alloy steels behave in ductile manner at high temperatures but brittle at low temperatures – exhibit a ductile-to-brittle transition over temperature. In the ductile domain, crack propagation consumes large amounts of energy and involves plastic deformation. In the brittle domain, crack propagation is rapid with low energy absorption and little plastic deformation; fracture is sudden and catastrophic. Both failure modes are to be avoided, but brittle fracture warrants special attention.

The BWR/PWR in-vessel inspection workshop started with a report of the recent baffle-former-bolting inspection findings at DC Cook 2, Indian Point 2, Salem 1, Surry 1 and Prairie Island 2.

Intergranular Stress Corrosion Cracking in austenitic piping was a major issue for Boiling Water Reactors in the 1980s – susceptibility of reactor internals to IGSCC was also recognized.

Shroud cracking in 1993-1994 confirmed that IGSCC of internals is a significant issue for BWRs.

Recent BWR internals inspections have detected some indications such as a typical cracking of core shrouds, damage of jet pump assemblies: wedge & rod wear, set screw gaps & damage, restrainer bracket damage, cracking located on riser pipe …

The fatigue management training workshop objectives were: 1) understanding the nature of fatigue and fatigue damage, 2) recognizing typical characteristics of fatigue failure and 3) describing fatigue as a potentially life limiting mechanism for nuclear plants, especially in extended life operation.

The definition of fatigue per the American Society of Testing and Materials is: "the process of progressive localized permanent structure change, occurring in a material subjected to fluctuating stresses and strains...which may culminate in cracks or complete fracture after sufficient number of fluctuations". Note that the reference [Gustin, 2016] states that 50% to 90% of all failures are due to fatigue.

The "western style" PWR chemistry, i.e., the one based on Westinghouse, Babcock & Wilcox, or Combustion Engineering designs and their licensed derivatives, generally use lithium hydroxide enriched in ^{7}Li for primary side pH_T control. Recently there have been interruptions in the ^{7}Li supply and there is a concern that this may become more common in the coming years, thus prompting the evaluation of alternative production sources and an alternative chemical to ^{7}Li for pH_T control. Potassium hydroxide, which has been successfully used for pH_T control in VVERs for a number of years, is one alternative to LiOH. However, there are important differences between VVER and Western PWR experiences such as: 1) materials: titanium-stabilized SS (VVER) vs nickel-based alloys (PWR), 2) fuel cladding: both zirconium alloy (KOH less corrosive), but low crud and lower boiling (VVER) and 3) chemistry: ammonia for hydrogen (VVER) vs dissolved gas (PWR), Li/K new to PWRs. According to the reference [Fruzzetti et al., 2016], it would take at least 8 years to qualify the use of KOH as alternative to LiOH.

Studies on the initiation of irradiation assisted stress corrosion cracking of stainless steels in PWR primary water have shown that the susceptibility to cracking increases, and the critical stress level for initiation decreases, with dose. The existing database on initiation of IASCC mainly consists of data from tests performed in environments with 1,000 or 1,200 ppm B, 2 ppm Li, and 30 cc/kg H_2. However, many reactors operate or consider operating at a higher Li content at the beginning of the reactor cycle. Limited data indicate that the susceptibility to IASCC increases at 3.5 ppm Li compared to 2.1 ppm. Thus, the reference [Jenssen and Smith, 2016] investigates the effect of Li content in PWR primary water on the initiation of IASCC in irradiated stainless steel. Another objective of the study was to expand the current database for initiation of IASCC to doses relevant for the maximum end-of-life dose for 40 years of operation. The main result is that a larger fraction of the specimens tested at 8 ppm of Li initiated cracking, compared to the test at 2 ppm Li. In addition, cracking initiated at a lower stress level in the test with 8 ppm Li.

Regarding PWR reactor internals and ageing management, the reference [Wilson and Malikowski, 2016] reports Westinghouse operating experience of baffle-former bolts. As already mentioned above, recent inspections have uncovered a significant number of bolts that are either visually failed or have ultrasonic examination indications. While the topic of baffle-former bolt degradation is not a new topic for the industry, recent quantities and patterns of degradation and/or UT indications suggests that there are additional factors that may be contributing to the susceptibility of a plant to large groupings (clusters) of baffle-former bolt degradation.

As concerns heads replacements, of the 65 operating PWRs in the U.S., reactor vessel closure heads at 41 units have been replaced so far with heads having Alloy 690 nozzles attached using Alloy 52/152 weld metal. The reference [White et al., 2016a] describes the technical basis for extension of the nominal 10-year interval for periodic volumetric or surface examinations of these components required by ASME Code Case N-729-1 as mandated by U.S. NRC regulations. The technical basis, which was published by EPRI in February 2014 as MRP-375 (EPRI 3002002441), has been cited in licensee submittals requesting extension of the inspection interval for the heads at 15 U.S. PWRs. The U.S. NRC has approved requests by individual plants to extend the interval for volumetric or surface examination to up to 15 years. An expert panel organized by EPRI is currently assessing the laboratory PWSCC crack growth rate data for Alloys 690/52/152. Once that assessment is complete, it is expected that work may be used to support an inspection interval longer than 15 years.

SCC studies over the last dozen years have demonstrated that Alloy 690 is not immune to SCC, even in the most optimal microstructures and without cold work. However, the SCC growth rate can vary by many orders of magnitude, in the worst cases with growth rates as fast as Alloy 600, but in most relevant conditions, exhibiting crack growth rates that fall in the low or very low range. By contrast, in almost all tests of Alloy 152/52/52i weld metals – including in ~ two dozen specimens involving over 200,000 hours of testing at GE – low or very SCC growth rates have been observed. In GE testing, only in a 20% cold worked weld did the growth rates rise into the "high" category, and only one as-welded specimen exhibited a growth rate barely into the medium growth rate range. In general, and despite of tests on specimens with various types of weld defects, the weld metals exhibited excellent resistance to SCC, even when there was a high fraction of intergranular cracking.

Damaged hold down springs were discovered in B&W units in 2007 and 2009. Poolside post-irradiation examination of hold down springs irradiated for two 24-month cycles in a commercial reactor identified numerous instances of severe cracking within each hold down spring assembly. The

Alloy 718 hold down springs are designed such that they operate under high stress levels, close to or even exceeding yield stress, throughout their lifetime.

Since the early 2000's, the U.S. Nuclear Regulatory Commission has maintained an active research program to evaluate the susceptibility of nickel-based alloys used in primary system pressure boundary components to primary water stress corrosion cracking. Extensive crack growth rate measurement testing was performed on low-chromium Alloys 600/82/182 following in-service degradation events at Davis-Besse, V.C. Summer, Wolf Creek, and other plants. In recent years, however, the main testing focus is high-chromium Alloys 690/52/152 used for replacement, repair, or mitigation of reactor vessel head penetrations and dissimilar metal piping welds. A main objective of the NRC testing program is to support the technical bases for updates to in-service inspection requirements, particularly within the context of potential reactor operation up to 80 years.

Concerning austenitic stainless steels behaviour, their service experience in PWR primary chemistry conditions has been good with most of the relatively few failures by stress corrosion cracking which have been observed occurring in occluded locations where the chemistry is less well controlled in than in the main primary circuit such as dead legs, threaded regions and canopy seals. These failures have been linked to local elevated oxygen levels and/or anionic contaminants. Nevertheless, a small number of occurrences of SCC have been reported in flowing coolant, almost all of which were associated with high levels of surface and /or bulk cold work. Cold work can arise from a variety of sources: welding-induced shrinkage, machining or grinding, deformation during installation, etc.

Switching to BWR components issues, jet pump flow induced vibration is a phenomenon that has been prevalent across the BWR fleet. Leakage in the slip joint between the mixer and diffuser has been defined as a major contributor to the flow induced vibrations issue that has resulted in many repairs and extended outage durations that have cost utilities millions of dollars per unit to address. Unfortunately, the current repair approaches have not addressed this leakage. Three vendors (AREVA, GE Hitachi and Westinghouse) have designed a repair that addresses this leakage and stops the major contributor to the damaging flow induced vibrations. Basically, the three vendors came up with a similar mechanical solution. AREVA uses a flow control collar, GE Hitachi Nuclear Energy solution uses a spring-loaded clamp and Westinghouse uses a slip joint extension.

Turning to BWR Water Chemistry and Mitigation, the reference [Andresen, 2016] presents the status of and developments with OnLine NobleChem.

SCC mitigation in BWRs has included eliminating bulk cold worked materials, then crevices, then sensitized SS, then water impurities. This was good, but insufficient mitigation. Corrosion potential mitigation was pursued via hydrogen water chemistry in 1980s, this was most effective in recirculation piping. Then, catalysis conceptualized and initial development done in mid 1980s which was demonstrated with Pt sputtering and electroplated coatings, with noble metals alloys and thermal spray powders and with electroless deposition of Pt in water. NobleChem was first applied at Duane Arnold in 1996. The next step was a continuous improvement as OnLine NobleChem in 2005 which was designed to minimize the critical path time during outages and permit easy, periodic application to address crack flanking. Now, OnLine NobleChem is now the dominant process.

In the history of OLNC deployment, there are many positive indications, but negatives must be addressed. There are many examples of good news with NobleChem, including low ECP in recirculation flanges, NMP-1 jet pump latch, evidence of component mitigation, reasonable Pt size-distribution on some MMS coupons, etc. But to have confidence, to convince ourselves and the NRC that NobleChem provides mitigation at all plants and all locations of interest, the problem areas must be addressed:

- MMS coupons with little or no Pt, or poor Pt distribution;
- Cases where no Pt is found on plant components (Hatch shroud);
- Evidence that crud exists on many (all?) plant surfaces and associated focus on effective OLNC mitigation;
- Injection tap plugging, and deposition along feed water pipe.

In recent years evidence of core shroud indications exhibiting atypical orientations has been reported by utilities following in-vessel visual inspections of the core shroud assembly. Inspection data exhibiting reportable indications that cross weld material and appear to propagate outside of the expected extent of the core shroud weld heat affected zone has generated questions regarding the possible cause and characteristics of the observed indications. One concern is that the indications occur in regions of high fluence on the core shroud such that it is considered possible that the cracking is irradiation assisted stress corrosion cracking. If this is the case then there are potentially significant implications for the manner in which the Boiling Water Reactor utilities must manage degradation of the core shroud and other reactor internal components. Current inspection, flaw evaluation, and repair guidelines are inherently based on the expectation that cracking will occur in the vicinity of the core shroud welds; therefore, if IASCC is beginning to occur in the operating fleet then there exists the possibility that inspection volumes and associated tooling, procedures, and qualifications must change. The Boiling Water Reactor Vessel and Internals Project has completed a project to extract a sample of a 304-stainless steel core shroud, irradiated to approximately 2×10^{21} n/cm^2 (E > 1 MeV), in one of the plants that has reported indications extending across weld material and out into the base material. Metallurgical testing has been performed on the boat sample to investigate the cracking mechanism(s) that may have contributed to the indications reported in the core shroud.

Core shroud cracking due to SCC in the HAZ of the welds is known at KKM since 1990. Typical measures for characterization, assessment and mitigation like UT-inspections, extraction of a plug sample and installation of tie rods were performed in the ‘90s. The special ecologic-political situation in Switzerland led to further actions in the last 20 years, which exceeded the worldwide standard of core shroud assessment. Qualified UT of all affected welds at least every two years offers a high-resolution database of crack growth from which the BWRVIP can profit. The introduction of Noble Metal Chemical Addition and On-Line NobleChem™ treatment since 2000 and 2005, respectively, was conducted in close cooperation with EPRI and the PSI (project NORA), which led to a steady optimization of this technique in the last years. Decreasing crack growth rates as well as stagnating crack depths at the KKM core shroud affirm these beneficial measures of mitigation. Some off-axis crack-like indications were detected in 2014, which however showed no obvious change in 2015. Sophisticated fracture mechanics analyses are performed for the integrity assessment of all cracks. A detailed 3D-Finite-Element model of the core shroud is used assigning all relevant loading combinations including the latest seismic calculations of the whole reactor building with soil-structure-interaction and solid-fluid-interaction as well as acoustic loads from a postulated recirculation-line break. KKM is sure to demonstrate the integrity of the core shroud without further repair until the permanent cessation of operations in 2019.

Probabilities studies are more and more used in the industry. For several years, the NRC and EPRI have been jointly funding an effort to develop the Extremely Low Probability of Rupture V2.0 computational code. The objective of this code is to evaluate the likelihood of piping failure compared with other more likely outcomes such as crack arrest, crack detection during inspection, or the formation and detection of a leaking crack. The initial effort is focusing on the evaluation of dissimilar metal welds in pressurized water reactors subjected to primary water stress corrosion cracking and fatigue, with and without the effect of various mitigation methods, to determine if the rupture probability is sufficiently low to justify continued regulatory credit for leak-before-break in applicable piping systems.

United States and International utilities are actively engaged in assessing the economic and societal benefits of operating nuclear plants beyond their initial license periods. Nuclear plant generated electricity is still the largest contributor to non-carbon dioxide emitting generation. In the US, a majority of operating plants has already received approval for an additional 20 years of operation, and soon it is expected that utilities will begin the process to seek a second 20-year renewal. The keys to successful renewal are to maintain safe and reliable operations by building a sound technical case through the following activities:

- Develop comprehensive understanding of aging degradation issues for systems, structures and components;
- Implement specific plant aging management programs to address aging degradation and
- Confirm behaviour of degradation mechanisms for the entire period of operation.

2 Introduction

This document is an extensive summary of the International Light Water Reactor Materials Reliability Conference and Exhibition 2016 held August 1-4, 2016 in Chicago, Illinois, USA.

The first day of the conference was dedicated to 3 workshops held in parallel: Reactor Pressure Vessel Integrity Workshop, BWR/PWR In-Vessel Inspection Workshop and Fatigue Management Training Workshop.

During days 2 to 4, 104 series of slides were presented in 3 parallel sessions which covered:

- PWR chemistry,
- PWR Reactor Internals and Aging Management,
- PWR Nickel-Based Alloys,
- PWR Stainless Steel and Modelling,
- BWR Major Component issues,
- BWR Water Chemistry and Mitigation,
- BWR Assessment,
- BWR Inspection/Operating Experience/NDE,
- Probabilistic Fracture Mechanics/xLPR,
- Long Term Operation (LTO),
- Non-destructive Examination Techniques,
- Reactor Pressure Vessel Integrity,
- Peening and Surface Mitigation,
- Cast Austenitic Stainless Steel (CASS),
- Thermal and Environmentally Assisted Fatigue,
- Welding Techniques & Residual Stress Modelling,
- Operational Experience & Plant Component Research,
- Steam Generator.

No papers were given at this conference, the proceedings contain only the slides that have been presented. Thus, this report is a summary of some of the most important slides, with little text added.

This report has six sections.

- The first section concerns the workshops presented on August the 1st.
- The second section covers the conference given from August the 2nd to August the 4th.
- The third section is the list of references.
- The fourth section contains the nomenclature.
- The fifth section is a list of abbreviations.
- The last section is a unit conversion table.

3 Workshops

3.1 Reactor Pressure Vessel Integrity Workshop

The purpose of this workshop is two folds:

- Present broad review of:
  - Fundamental concepts related to RPV Integrity;
  - Current regulations and the rationale behind them;
  - Existing and developing technologies / techniques for evaluating and assuring RPV integrity;
- Focus is on the traditional vessel and the degradation mechanisms that impact operating limits (e.g., embrittlement).

The RPV Integrity is paramount because:

- The reactor vessel is one of the four barriers of protection from irradiation release to the general public: ceramic fuel pellets, fuel rods, RPV and containment building;
- Protecting the integrity of the RPV is of the utmost importance to safety because the failure of the vessel is beyond the design basis: the containment building was not designed for RPV failure; therefore, early focus of ASME Section XI (1973) was the RPV;
- Neutrons from the reactor core irradiate the vessel during operation and cause localized embrittlement of the vessel steel;
- Reactor vessel embrittlement is the dominant aging concern that may limit the useful life of a nuclear plant. Note that PWRs are more susceptible than BWRs because PWR vessels receive significantly more neutron irradiation (~10×).

Configuration and functions of the PWR RPV (Figure 3-1).

- Functions: to support and contain the core; to direct the coolant flowing through the fuel bundles;
- Its essential characteristics are:
  - Low alloy steel vessel with stainless steel clad;
  - No penetrations present in the beltline area;
  - Equipped with a removable top head and a nonremovable bottom head;
  - Equipped with control rod penetrations through the top head.

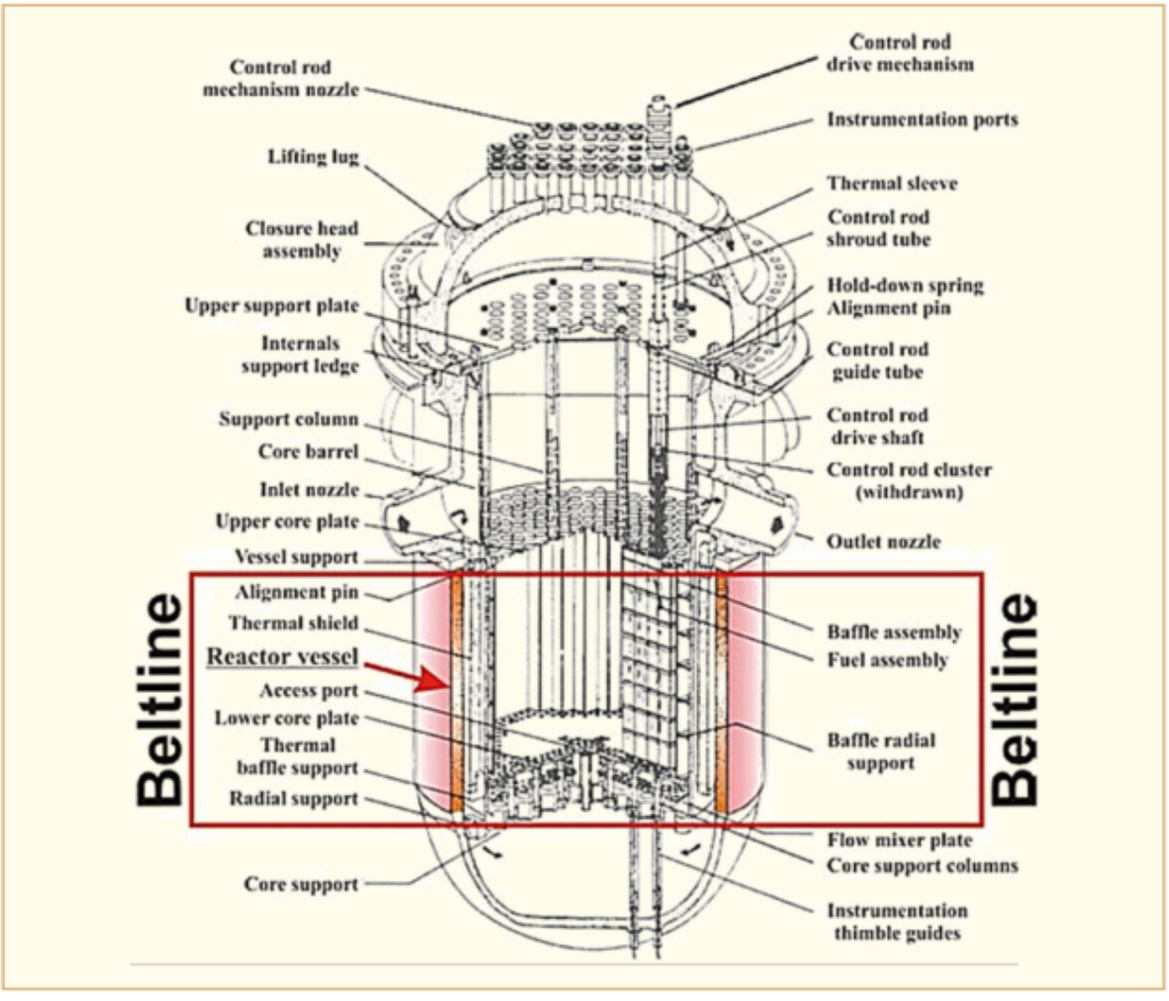

Figure 3-1: Typical PWR Pressure Vessel [Hardin, 2016].

Functions and configuration of the BWR RPV (Figure 3-2):

- Function: to support and contain the core, to direct the coolant flow through the fuel bundles and also, serve as a steam generator, house steam dryer and steam separator assembly;
- Essential characteristics:
  - LAS vessel, clad with SS (except removable top head);
  - Removable top head and nonremovable bottom head;
- Differences from PWR:
  - There are many nozzles penetrations near or in the beltline;
  - There are control rod penetrations in the bottom head.

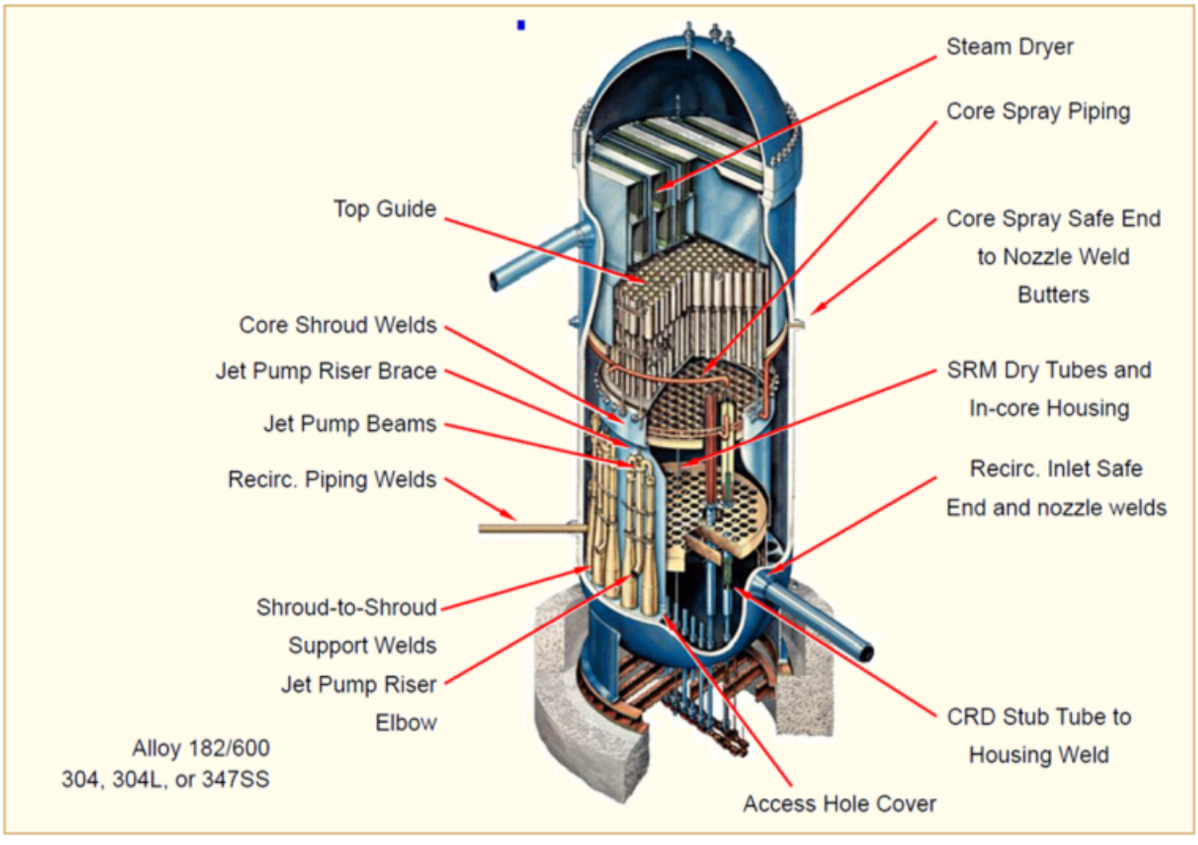

Figure 3-2: Typical BWR Pressure Vessel [Wirtz, 2016].

LAS (plate, forging, welds, and HAZ) is susceptible to thermal aging. Thermal aging is caused by slow diffusion and segregation of impurity elements (e.g., primarily phosphorous) into grain boundaries at operating temperature. The result is an increase in DBTT but not yield strength/hardness; also known as a "non-hardening embrittlement". The degree of embrittlement is largely a function of the P content and temperature.

The LAS components susceptible to thermal ageing are:

- RPV LAS components, e.g., RPV flange, nozzle shell ring, and outlet nozzles, they experience temperatures of up to 315°C;
- Vessel heads of some reactors may be near the hot leg temperature of about 315°C;
- Pressurizers experience highest operating temperature at around 343°C.

The HAZ of pressurizer welds is viewed as the area the most susceptible to thermal ageing.

LAS is also susceptible to hydrogen content. Hydrogen in ferritic steels can cause a loss of ductility and a time dependent failure at stresses considerably less than yield strength (e.g., delayed failure). The effects of hydrogen vary as a function of hydrogen concentration and strength level: high-strength steels are significantly more susceptible than low-strength steels. A catastrophic failure can occur in high-strength steels at 1 ppm H or less, whereas such failure may require > 4 ppm H in lower strength steels.

LAS in BWR environment is susceptible to Stress Corrosion Cracking. Note that it is extremely difficult to initiate or maintain SCC crack growth in LAS under steady state loading in normal BWR environment: in the absence of high loads (K in excess of 50-60 MPa$\sqrt{m}$), abnormal water chemistry including transients or load cycling, it is difficult to produce and maintain SCC extension. Field experience supports the inherent SCC resistance of LAS in the BWR environment:

- Tsuruga shroud support weld cracked but no SCC growth occurred in LAS;
- Hamaoka CRD stub tube to vessel weld cracked but no SCC crack extension was observed into low alloy steel bottom head;
- Cracking had occurred in BWR feedwater nozzles (due to thermal fatigue) but there was no apparent SCC crack extension.

Note that potential SCC might result from cracking in Alloy 182 attachments to RPV and/or from water chemistry transients, particularly associated with chloride concentrations above 3 ppb.

LAS is also susceptible to neutron Irradiation Embrittlement (Figure 3-3). RPV is fabricated of ferritic low alloy steel, which exhibits good combination of strength and ductility. Carbon and low alloy steels behave in ductile manner at high temperatures but brittle at low temperatures – exhibit a ductile-to-brittle transition over temperature. In the ductile domain, crack propagation consumes large amounts of energy and involves plastic deformation. In the brittle domain, crack propagation is rapid with low energy absorption and little plastic deformation; fracture is sudden and catastrophic. Both failure modes are to be avoided, but brittle fracture warrants special attention.

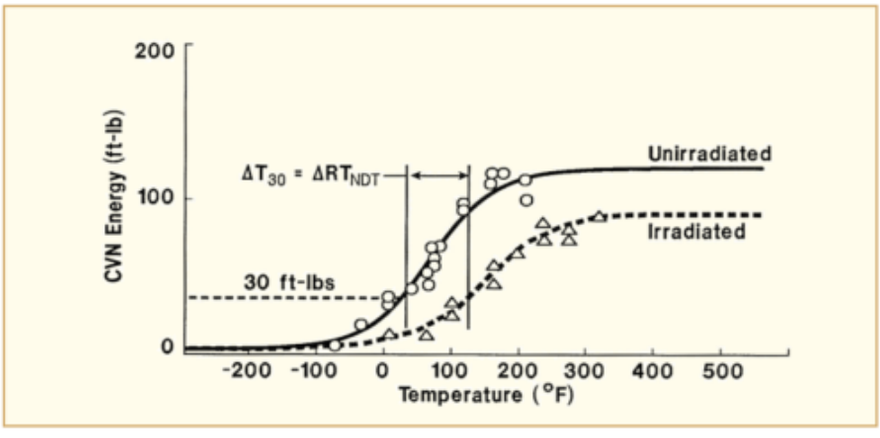

Figure 3-3: Behaviour of carbon steels under neutron irradiation [Hardin, 2016].

Embrittlement is a safety concern as neutron irradiation from the core causes damage to the vessel steel by reducing material toughness: it raises the ductile-brittle transition temperature along with a reduction of the upper shelf energy. A small initial flaw may exist somewhere in the vessel welds or heat-affected-zone just at a critical location. Moreover, high stresses from pressure and thermal loads could cause crack initiation of the small pre-existing flaw. Then, a rapidly growing crack in an embrittled vessel could cause a sudden and catastrophic rupture, either by brittle fracture (if in transition region) or ductile tear (if on upper shelf). Thus, safety margins must be assured to prevent fracture of the vessel as it gradually embrittles over time with increasing neutron exposure.

Neutron irradiation hardens ferritic steel causing an increase in strength and a corresponding decrease in fracture toughness, as a result of several factors:

- Microstructure of bcc (ferritic) RPV steels experiences complex changes when exposed to neutron irradiation, which in turn leads to degradation in mechanical properties as the cumulative exposure increases;
- High energy neutrons interact with atomic nuclei in the steel's crystal lattice structure and create high-energy primary recoil atoms; various features are induced by this process (e.g., solute clusters / copper-enriched clusters);
- These features act as obstacles to movement of dislocations in the crystal matrix (movement of dislocations is necessary for ductile behavior);
- Irradiation conditions (flux, fluence, energy spectrum, and irradiation temperature) strongly influence the process;

4 PWR chemistry

"Western style" PWRs, i.e., those that are based on Westinghouse, Babcock & Wilcox, or Combustion Engineering designs and their licensed derivatives, generally use lithium hydroxide enriched in ^{7}Li for primary side pH_T control. Recently there have been interruptions in the ^{7}Li supply and there is a concern that this may become more common in the coming years[2], thus prompting the evaluation of alternative production sources and an alternative chemical to ^{7}Li for pH_T control. Naturally abundant lithium cannot be used as it would generate an untenable increase in tritium production (a significant radioactive waste concern). Potassium hydroxide, which has been successfully used for pH_T control in VVERs for a number of years, is one alternative to LiOH. The reference [Fruzzetti et al., 2016] summarizes an initial evaluation that highlights technical gaps in industry understanding that must be addressed before KOH can be used as an alternative to LiOH in "Western" PWRs.

There are important differences between VVER and Western PWR experiences:

- Materials: titanium-stabilized SS (VVER) vs nickel-based alloys (PWR);
- Fuel cladding: both zirconium alloy (KOH less corrosive), but low crud and lower boiling (VVER);
- Chemistry: ammonia for hydrogen (VVER) vs dissolved gas (PWR), Li/K new to PWRs;
- Worker dose & radwaste: potassium activation products (VVER).

According to the reference [Fruzzetti et al., 2016], it would take at least 8 years to qualify the use of KOH as alternative to LiOH (Figure 4-1).

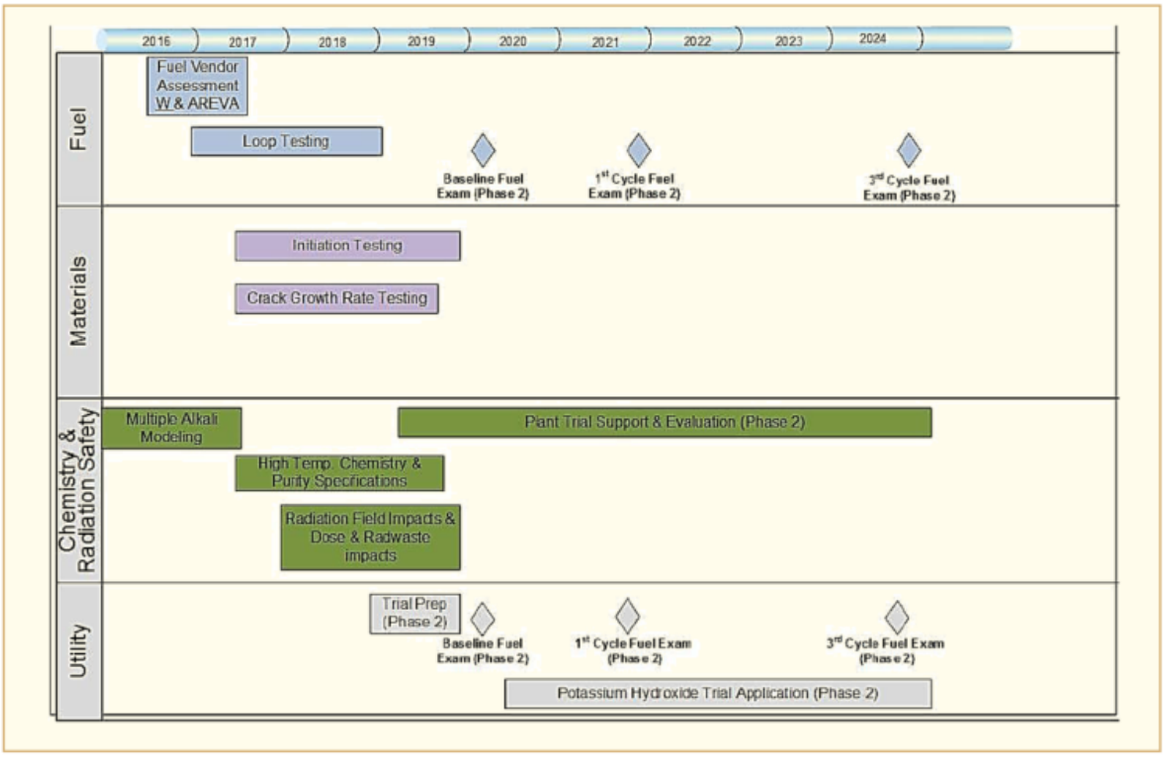

Figure 4-1: KOH use in western PWRs, qualification plan, shortest timeline according to [Fruzzetti et al., 2016].

Studies on the initiation of irradiation assisted stress corrosion cracking of stainless steels in PWR primary water have shown that the susceptibility to cracking increases, and the critical stress level for

[2] Worldwide, there are only 2 plants producing ^{7}Li, one is in Russia and the other in China.

initiation decreases, with dose. The existing database on initiation of IASCC mainly consists of data from tests performed in environments with 1,000 or 1,200 ppm B, 2 ppm Li, and 30 cc/kg H_2. However, many reactors operate or consider operating at a higher Li content at the beginning of the reactor cycle. Limited data indicate that the susceptibility to IASCC increases at 3.5 ppm Li compared to 2.1 ppm (Figure 4-2).

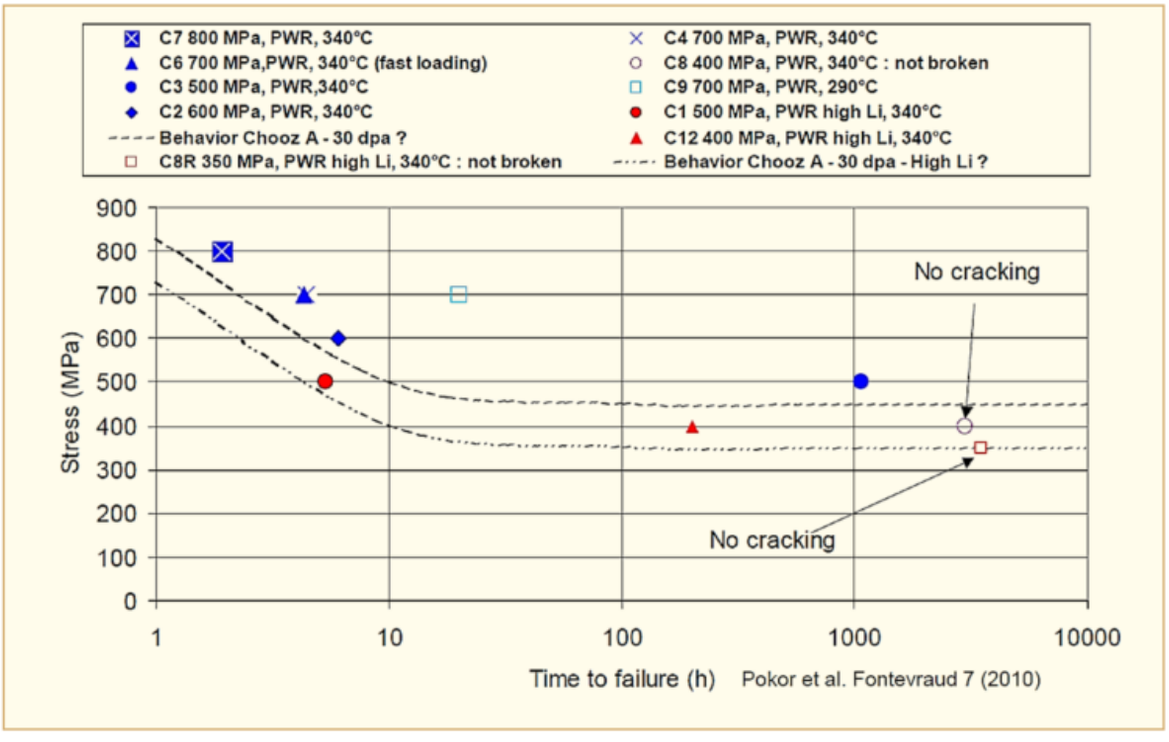

Figure 4-2: Effect of Li on initiation of IASCC [Jenssen and Smith, 2016].

With the objective of investigating the effect of Li content in PWR primary water on the initiation of IASCC in irradiated stainless steel, testing was conducted on specimens fabricated from highly irradiated Type 316 stainless steel. Another objective of the study reported in the reference [Jenssen and Smith, 2016] was to expand the current database for initiation of IASCC to doses relevant for the maximum end-of-life dose for 40 years of operation.

O-ring and uniaxially constant load specimens machined from flux thimble tubes at doses of 60 and 100 dpa were tested in this study. Two tests at different Li contents (2 or 8 ppm of Li, $pH_{300°C}$ = 7.2, 340°C) were conducted, and in each test 12 O-ring and 9 UCL specimens, covering stress levels ranging from 35 to 60% of the irradiated yield strength, were tested. The total testing time for each test was ~4,500 hours.

A larger fraction of the specimens tested at 8 ppm of Li initiated cracking, compared to the test at 2 ppm Li (Figure 4-3). In addition, cracking initiated at a lower stress level in the test with 8 ppm Li.

5 PWR reactor internals and ageing management

The reference [Wilson and Malikowski, 2016] reports Westinghouse operating experience of baffle-former bolts. Westinghouse typical baffle-former bolts design is presented on Figure 5-1.

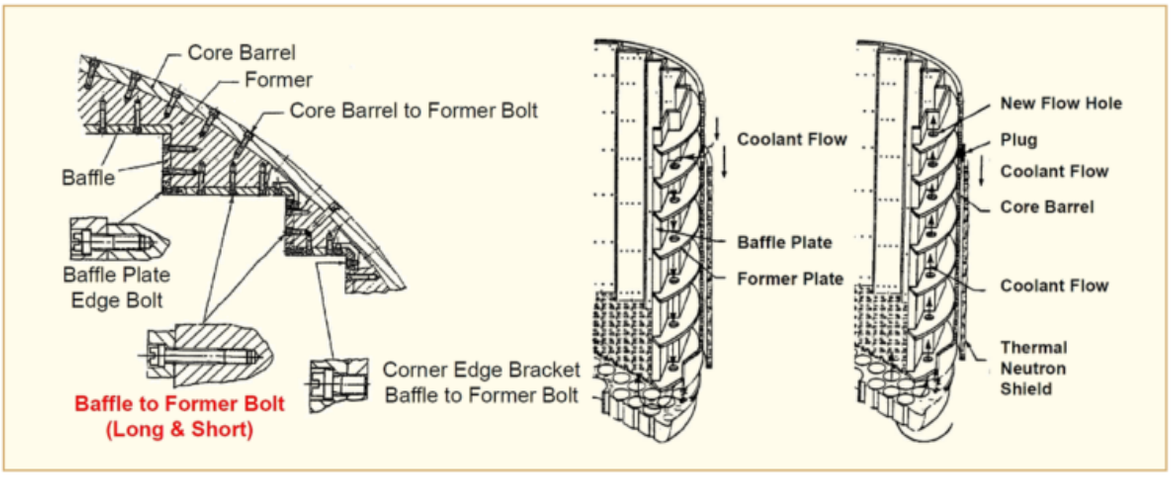

Figure 5-1: Left: baffle-former assembly details, middle: downflow configuration, right: upflow configuration [Wilson and Malikowski, 2016].

The Figure 5-2 shows the timeline of the baffle-former bolts operating experience. One can see that the first cracks were found in 1988 and that 30 years down the road, despite huge research efforts, the only available strategy is inspection and replacement with similar bolts.

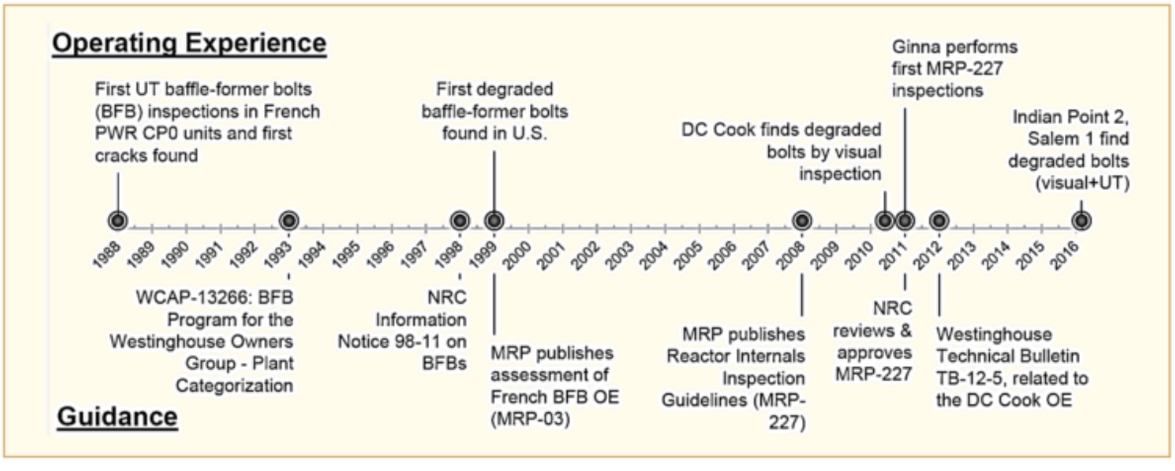

Figure 5-2: Baffle-former bolts operating experience timeline [Wilson and Malikowski, 2016].

As already mentioned at Section 3.2, recent inspections have uncovered a significant number of bolts that are either visually failed or have ultrasonic examination indications. While the topic of baffle-former bolt degradation is not a new topic for the industry, recent quantities and patterns of degradation and/or UT indications suggests that there are additional factors that may be contributing to the susceptibility of a plant to large groupings (clusters) of baffle-former bolt degradation.

The reference [Somville F. et al., 2016] summarizes the experience with baffle to former bolt cracking in the Belgian nuclear units and gives an overview of the ageing management activities implemented in Belgium to follow up or mitigate irradiation assisted stress corrosion cracking of baffle former bolts.

After an operating time of the order of 120,000 hours, some bolts exhibit cracking at the head to shaft radius. Examinations of failed bolts have made it possible to identify the cause of cracking as IASCC (Figure 5-3). Up to now, baffle bolt cracking has been detected in units older than 15 years, where the baffle bolts are not cooled (no holes in the former to allow a water flow on the bolt shaft). In Belgium, the concerned units are Tihange 1 and Doel 1-2.

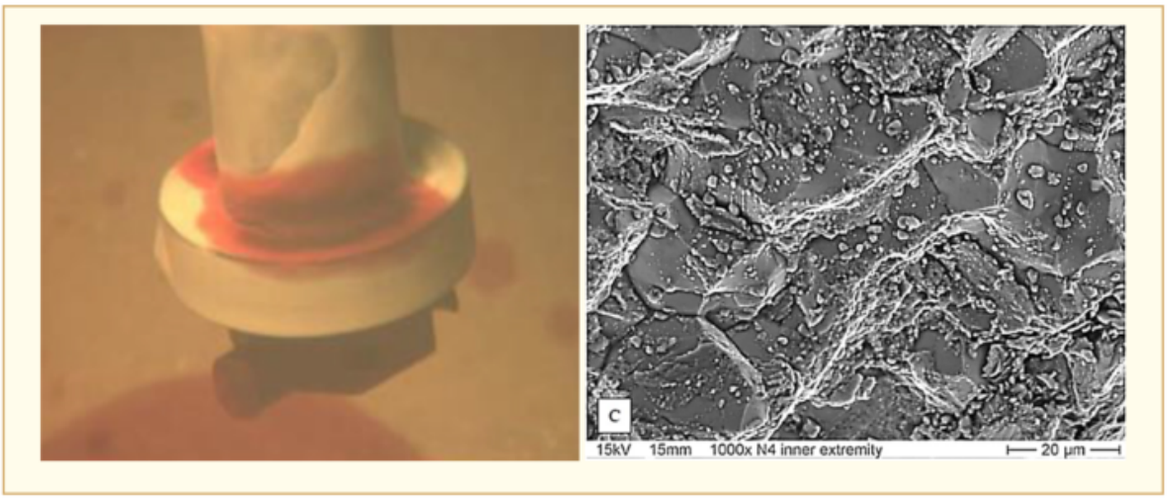

Figure 5-3: Characterization of baffle-former bolts extracted from Doel 1-2 by SCK.CEN (Belgian Nuclear Research Center). Right: the intergranular nature of the cracking is confirmed and view of details of corrosion products on the fracture surface (about 12 dpa at the crack location), [Somville F. et al., 2016].

The baffle bolts situation is now very well characterized in both Tihange 1 and Doel 1-2 since several UT inspections were performed since 1991.

In Doel 1, 10 bolts were replaced in 2005, among which 8 had indications. In Doel 2, 14 bolts were replaced in 2006, among which 6 had indications. In 2006, the Doel 1 withdrawn bolts were shipped to the Belgian Nuclear Research Centre (SCK.CEN) for examination. In the framework of the extended operation of Doel 1-2 beyond the design lifetime, all baffle bolts had to be inspected in 2015.

In 1995, in Tihange 1, 37 bolts were considered as cracked and 53 as uninterpretable; 91 bolts were replaced, including all these cracked and uninterpretable bolts (6 bolts had already been replaced in 1992) (Figure 5-4). In 2002, 5 new cracked bolts (plus 1 uninterpretable) were found, which indicates a kinetic of +/- 1 bolt per cycle. However, an acceleration of the degradation was seen in 2010, when 23 additional cracked or uninterpretable bolts were detected. 42 bolts were replaced in 2011, including additional bolts replaced preventively in order to guarantee the integrity of the baffle-former assembly under all design and accident conditions for 2 cycles (until Fall 2014). The inspection of all baffle bolts that was carried out in 2014 revealed no new cracked bolts and the baffle-former assembly was justified for continued operation for 3 additional cycles.

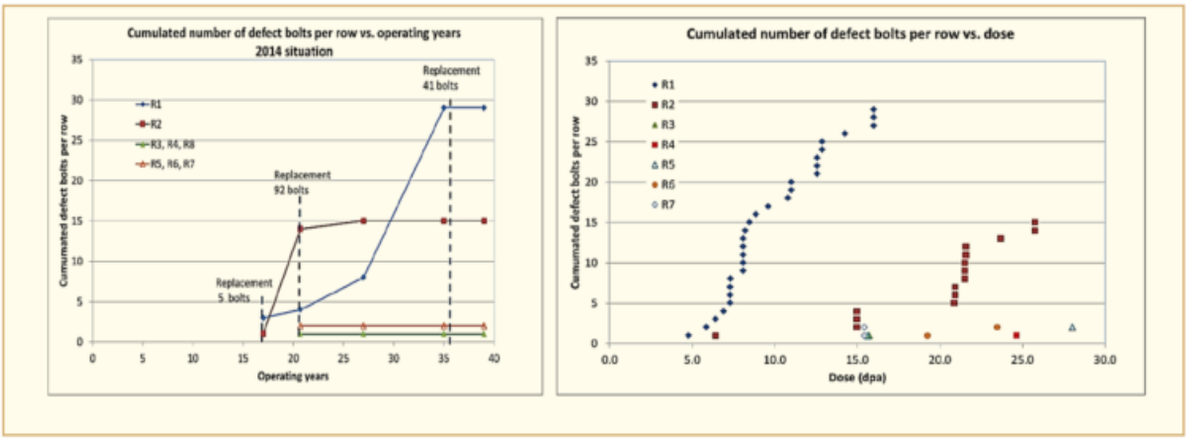

Figure 5-4: Baffle -former bolts status in Tihange 1 (inspections & replacements) [Somville F. et al., 2016].

Of the 65 operating PWRs in the U.S., reactor vessel closure heads at 41 units have been replaced with heads having Alloy 690 nozzles attached using Alloy 52/152 weld metal.

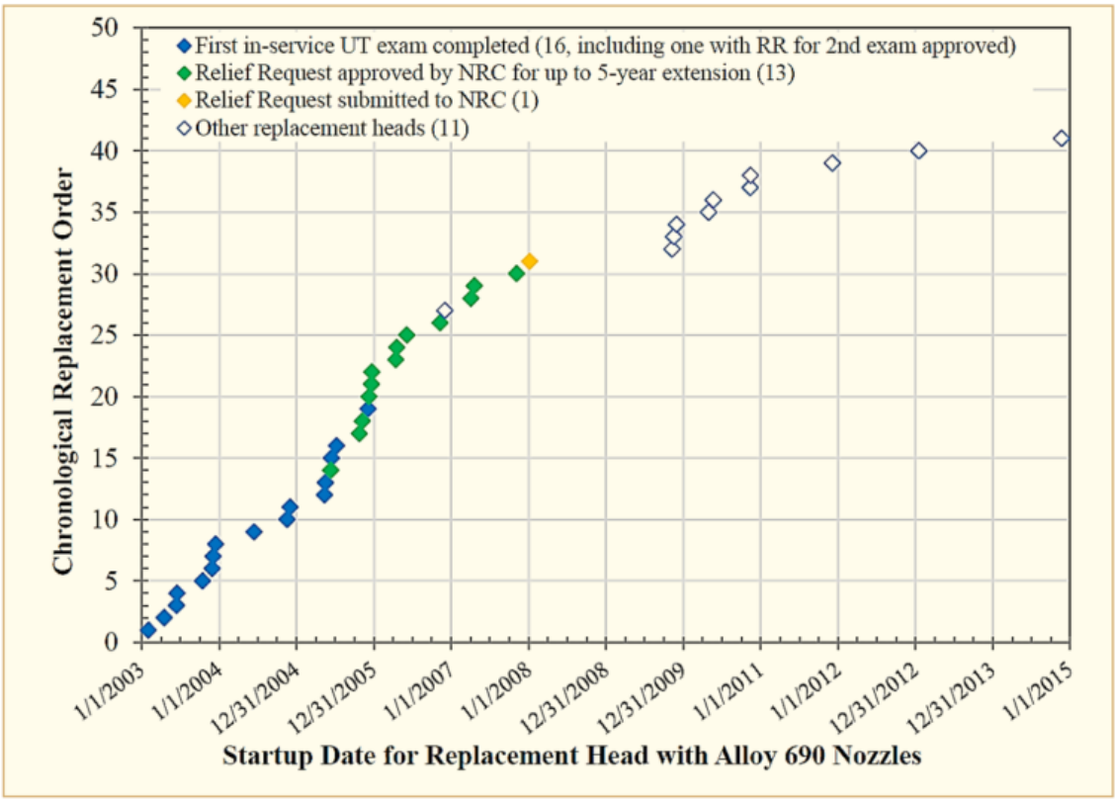

Figure 5-5: Heads replacements in the US as of end of 2015 [White et al., 2016a].

The reference [White et al., 2016a] describes the technical basis for extension of the nominal 10-year interval for periodic volumetric or surface examinations of these components required by ASME Code Case N-729-1 as mandated by U.S. NRC regulations. The technical basis, which was published by EPRI in February 2014 as MRP-375 (EPRI 3002002441), has been cited in licensee submittals requesting extension of the inspection interval for the heads at 15 U.S. PWRs.

Alloys 690, 52, and 152 have a chromium content of approximately 30%. As a result, these replacement alloys are much more resistant to primary water stress corrosion cracking than Alloys

6 PWR nickel-based alloys

SCC studies over the last dozen years have demonstrated that Alloy 690 is not immune to SCC, even in the most optimal microstructures and without cold work. However, the SCC growth rate can vary by many orders of magnitude, in the worst cases with growth rates as fast as Alloy 600, but in most relevant conditions, exhibiting crack growth rates that fall in the low or very low range (Figure 6-1). By contrast, in almost all tests of Alloy 152/52/52i weld metals – including in ~ two dozen specimens involving over 200,000 hours of testing at GE – low or very SCC growth rates have been observed (Figure 6-1). In GE testing, only in a 20% cold worked weld did the growth rates rise into the "high" category, and only one as-welded specimen exhibited a growth rate barely into the medium growth rate range (Figure 6-1). In general, and despite of tests on specimens with various types of weld defects, the weld metals exhibited excellent resistance to SCC, even when there was a high fraction of intergranular cracking.

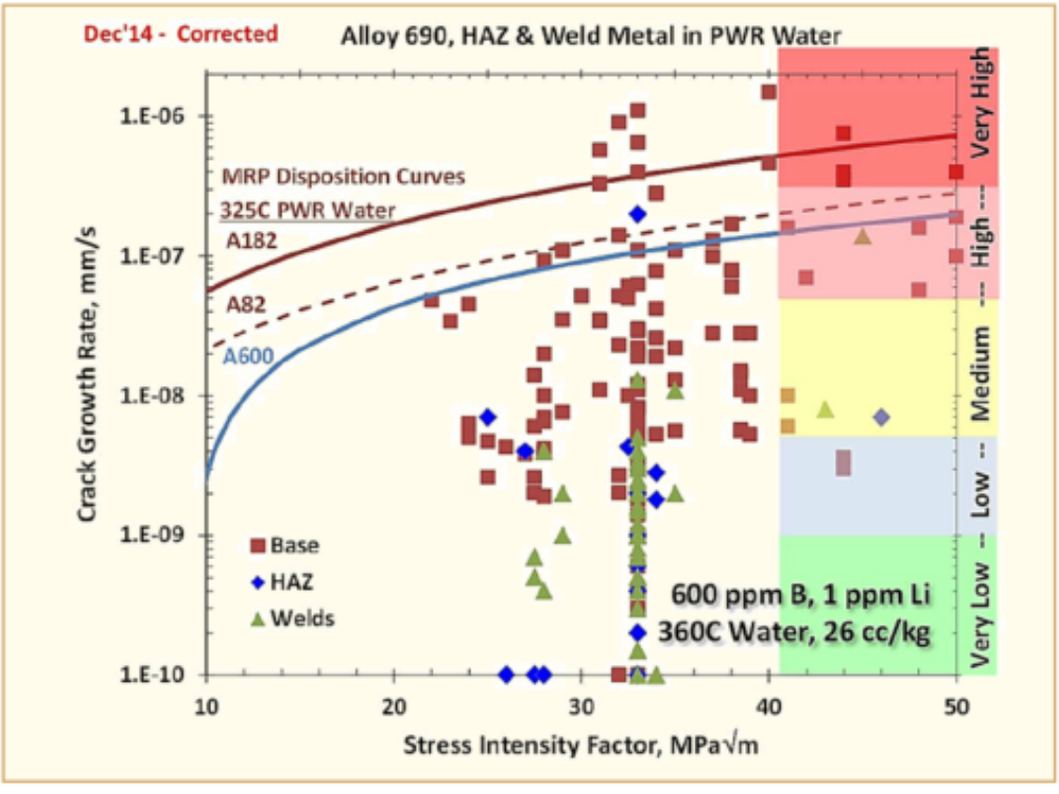

Figure 6-1: Summary of GE data on 690, HAZ & welds. GE CGRs for Alloy 690/152/52 can span a ~20,000× range to values as high as ~2 × 10^{-6} mm/s in PWR primary water [Andresen and Ahluwalia, 2016].

The NRC Issued a Regulatory Issue Summary (RIS 15-10) which was an inquiry to the ASME Code Committee to review the in-service inspection requirements for Alloy 600 full penetration branch connections, see existing configuration Figure 6-2. This NRC request resulted in the initiation of two PWROG projects, PA-MSC-1283 and 1294.

Figure 6-2: Typical branch connection [Waskey, 2016].

PA-MSC-1283 is a Fracture Analysis to evaluate the crack growth rate of the various existing A600 configurations, heat treat conditions and operating loads. The results from this study would provide the technical basis for in-service inspection method and frequency.

PA-MSC-1294 is a project to consider contingency repair techniques and provide a bounding analysis for all nozzle configurations of the selected repair technique. The Figure 6-3, below, represents the selected repair approach to be analysed.

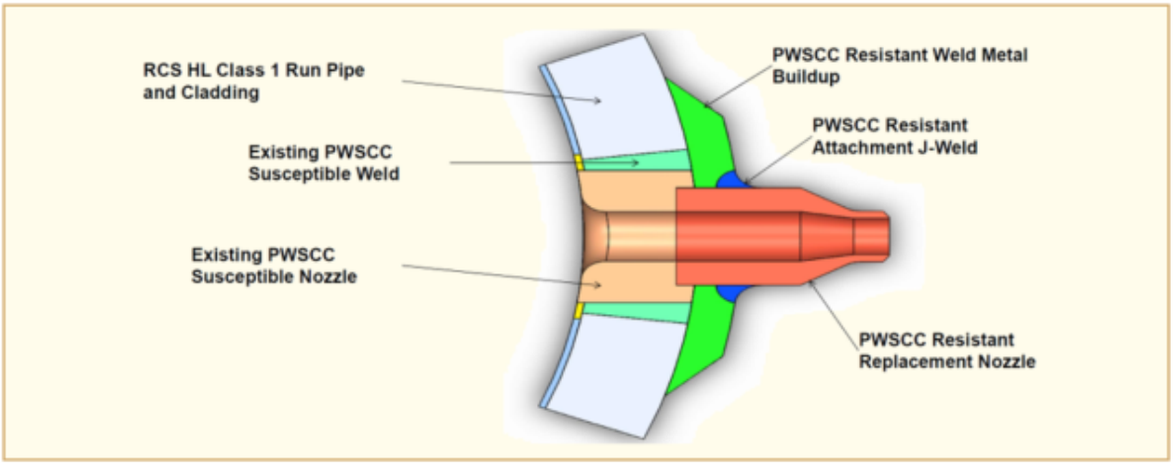

Figure 6-3: PWROG Chosen Repair Design [Waskey, 2016].

Included in this project was a proof-of-principle phase to demonstrate that the repair methodology is implementable and assist in establishing the potential on component repair duration and anticipated dose.

7 PWR stainless steel and modelling

The service experience of austenitic stainless steels in PWR primary chemistry conditions has been good with most of the relatively few failures by stress corrosion cracking which have been observed occurring in occluded locations where the chemistry is less well controlled in than in the main primary circuit such as dead legs, threaded regions and canopy seals (Figure 7-1). These failures have been linked to local elevated oxygen levels and/or anionic contaminants. Nevertheless, a small number of occurrences of SCC have been reported in flowing coolant, almost all of which were associated with high levels of surface and /or bulk cold work (Figure 7-2).

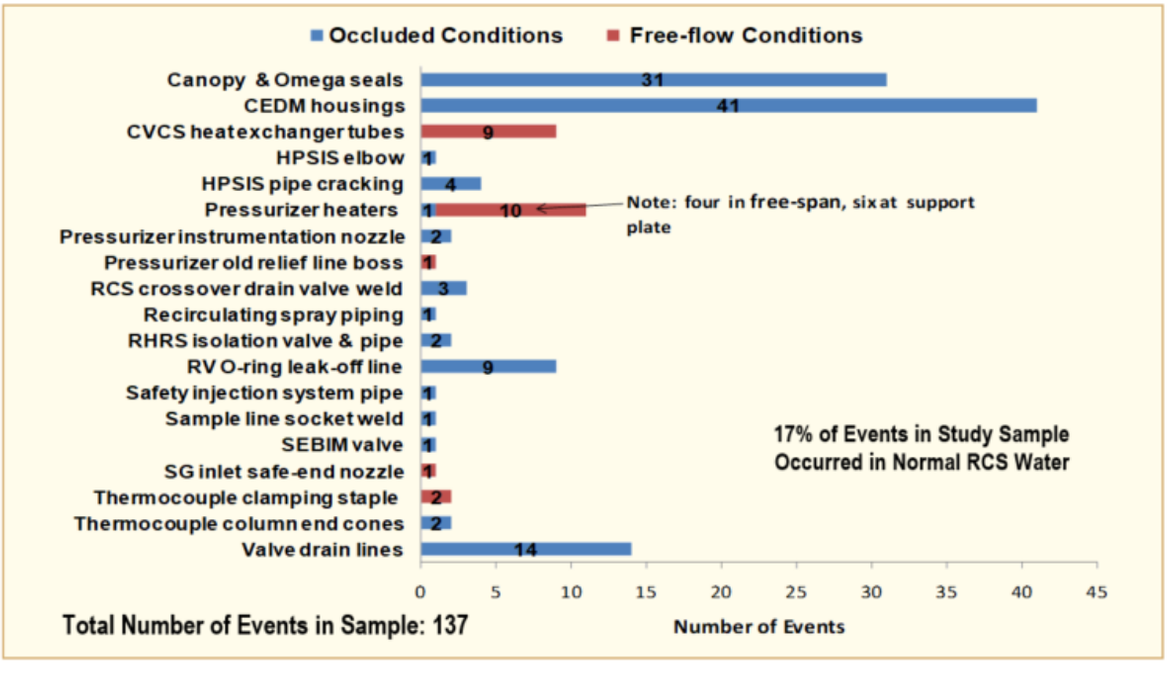

Figure 7-1: Distribution of 137 internally initiated SCC events as a function of affected stainless steel components in PWR primary water under occluded and free-flow conditions [Ilevbare et al., 2010].

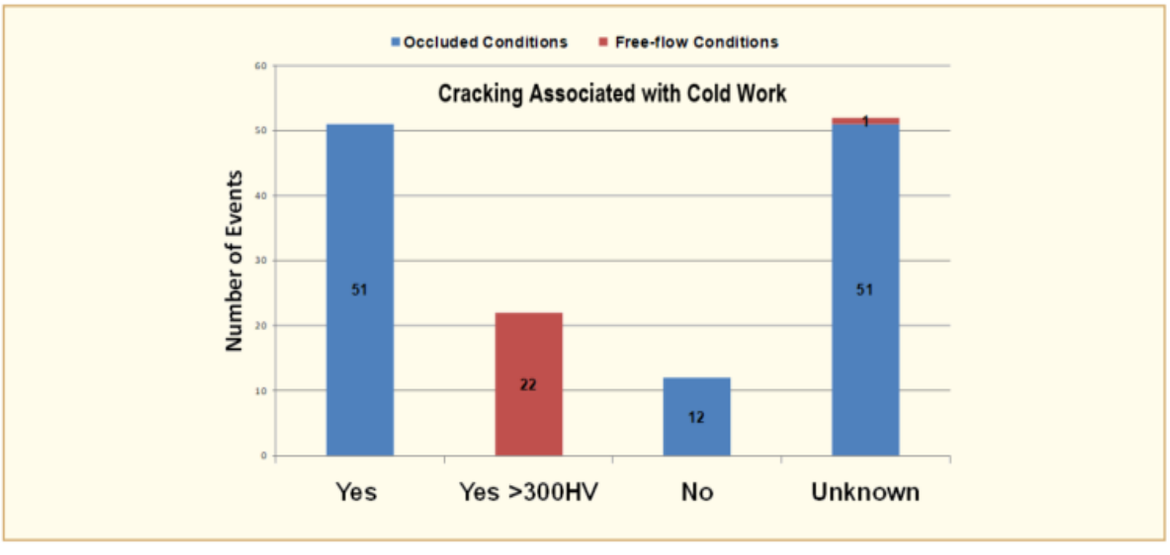

Figure 7-2: Distribution of 137 internally initiated SCC events in stainless steel components showing the proportion of events in which cold work was identified as a contributor to SCC in PWR primary water under occluded and free-flow conditions [Ilevbare et al., 2010].

Cold work can arise from a variety of sources: welding-induced shrinkage (Figure 7-3), machining or grinding (Figure 7-4), deformation during installation, etc.

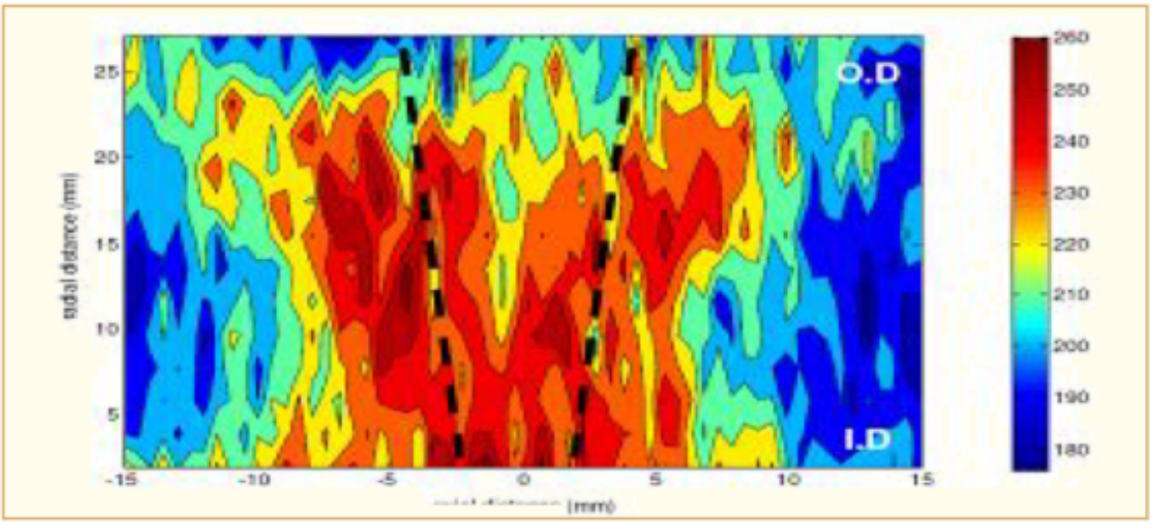

Figure 7-3: Cold work due to weld shrinkage, hardness ~240-260 Hv close to fusion line in a 304L weldment [Tice et al., 2016a].

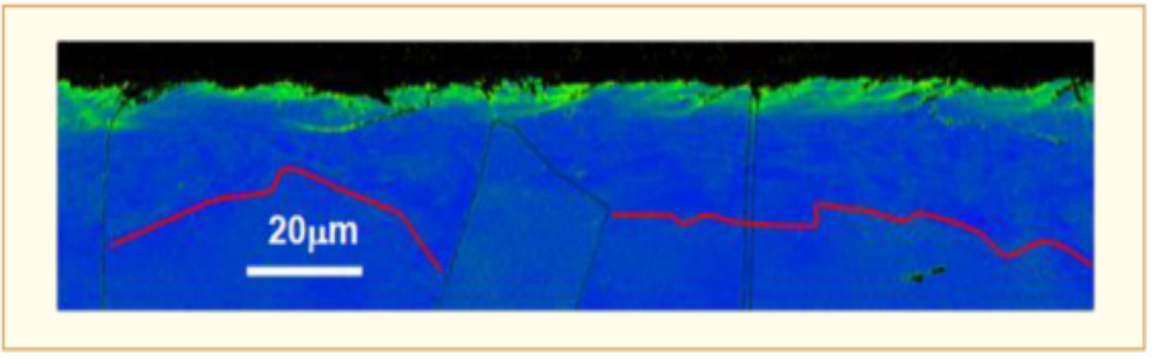

Figure 7-4: Cold work due to grinding, deformed surface layer in 304 stainless steel ground to 0.6 Ra finish [Tice et al., 2016a].

Laboratory testing in simulated primary circuit conditions has demonstrated that propagation of a pre-existing defect by SCC is possible in austenitic stainless steel which has been subjected to a degree of cold work of order 10-15% or greater, even in good quality water (Figure 7-5).

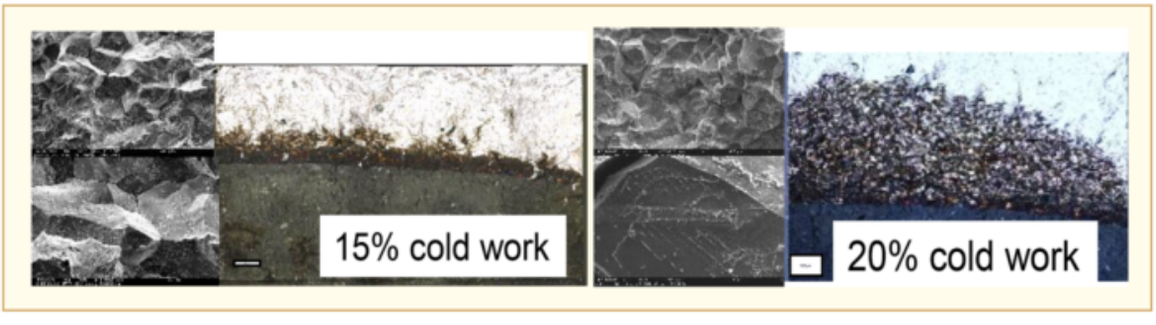

Figure 7-5: Results of laboratory tests indicating that existing cracks can propagate by IGSCC in Types 304 and 316 stainless steel which has been subjected to >~15% cold work [Tice et al., 2016a].

But, based on previous studies, crack initiation, and especially development of a crack large enough to propagate, appears to be difficult, at least under constant load conditions: severe cold working conditions and/or dynamic loading appears to be required for initiation and a highly-deformed layer can increase material susceptibility to SCC initiation.

The purpose of this ongoing study is to determine under what conditions SCC could initiate in austenitic stainless steels in good quality primary coolant, and how small initiated defects could develop into propagating IG stress corrosion cracks.

Two Type 304 stainless steel heats with different microstructures were tested (Figure 7-6). Most tests were performed under slow strain rate loading and the tests were stopped at ≤ 5% plastic strain.

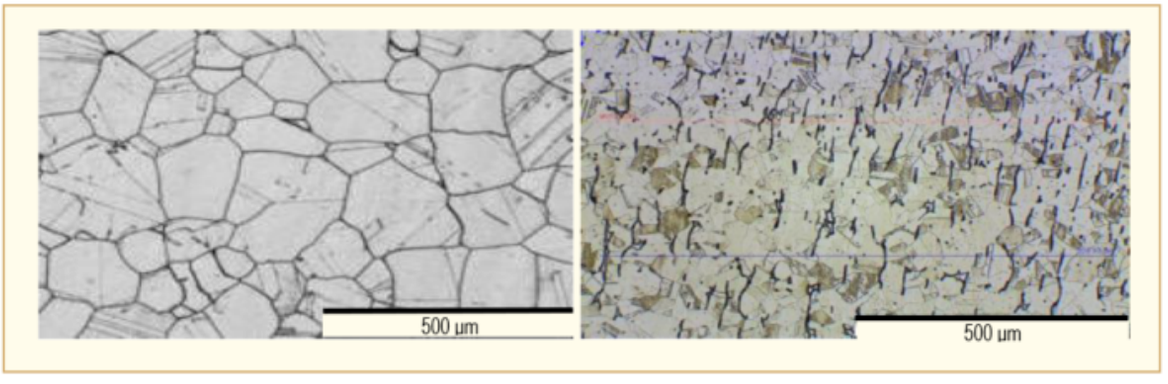

Figure 7-6: Left: Heat A, 133 µm grain size, < 0.5% δ-ferrite. Right: Heat B 35 µm grain size, average 4.5% δ-ferrite (non-uniformly distributed) [Tice et al., 2016a].

For the heat A material, with a low density of inclusions and low δ-ferrite, cracking initiated predominantly on grain boundaries:

- By comparing crack locations with the microstructure characterised pre-test using EBSD, IGSCC initiation was observed to occur preferentially in two locations;
- At high angle grain boundaries separating grains where planar deformation banding was present in one grain but not in the other, especially when these were at a high angle to the loading direction (Figure 7-7);
- At high angle grain boundaries where they were intersected by annealing twins – this appears to be due to enhanced localised deformation (Figure 7-8);
- Annealing twin boundaries were themselves relatively resistant to IGSCC (Figure 7-8);
- In some instances, small transgranular cracks forming under slow strain rate loading at oxidised slip bands appear to propagate to a grain boundary (Figure 7-9).

8 BWR Major Component issues

What is a jet pump (Figure 8-1)? A jet pump is a passive component within the RPV Internals (no moving parts) Jet pumps are used to increase core flow. The flow distribution is about 1/3 drive flow to 2/3 driven flow. The jet pumps have a nuclear safety function to maintain the water level above 2/3 of the core height during a postulated loss of coolant accident.

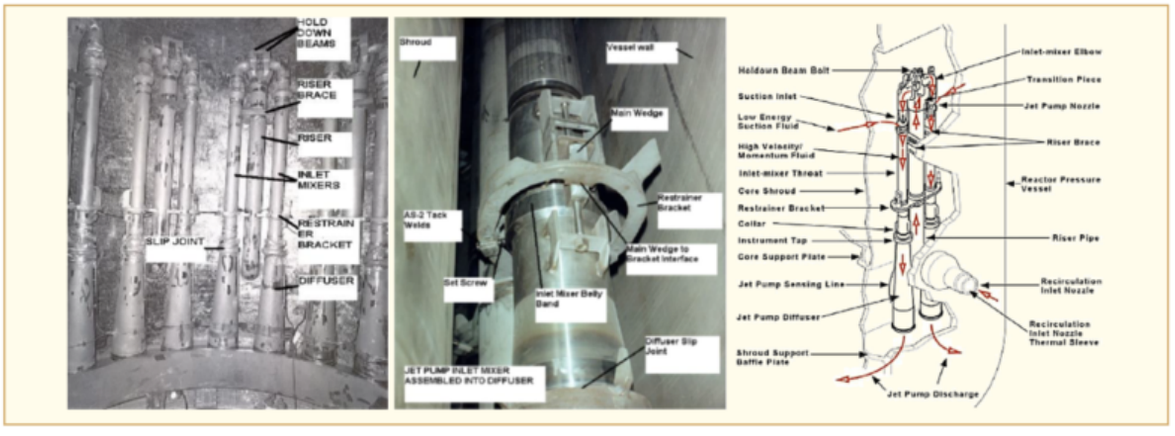

Figure 8-1: Jet pump overview [Wilton, 2016].

Jet pump flow induced vibration is a phenomenon that has been prevalent across the BWR fleet. Leakage in the slip joint between the mixer and diffuser has been defined as a major contributor to the FIV issue that has resulted in many repairs and extended outage durations that have cost utilities millions of dollars per unit to address. Unfortunately, the current repair approaches have not addressed this leakage. AREVA has designed a repair that will address this leakage and stop the major contributor to the damaging FIV. The Figure 8-2 shows the composition of a BWR recirculation system along with the slip join geometry.

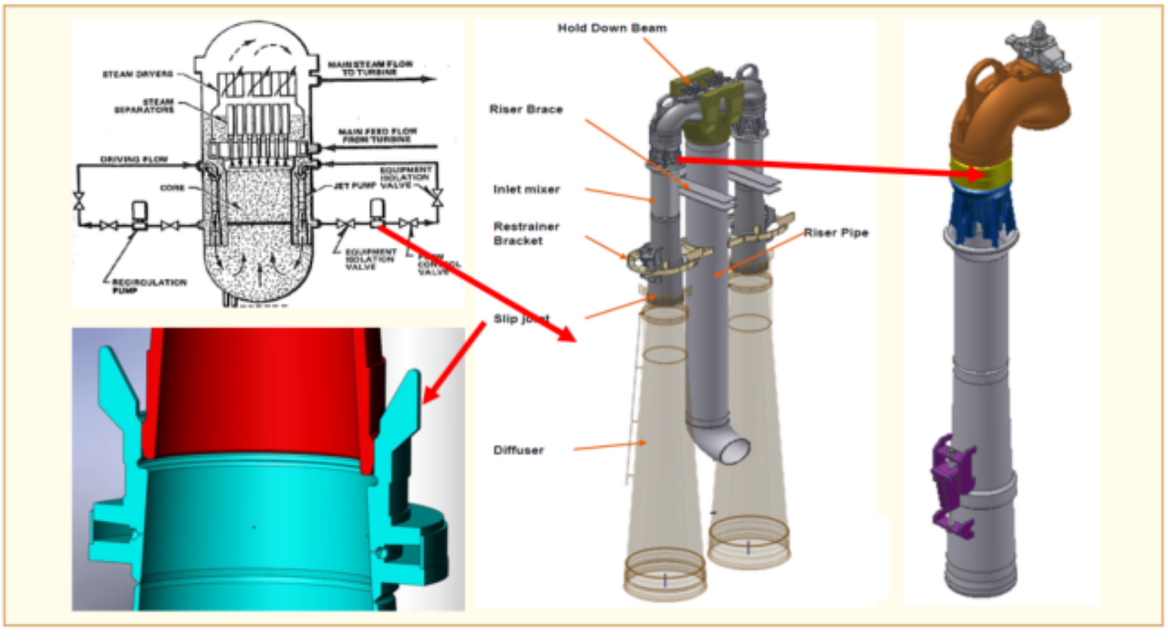

Figure 8-2: Top left: BWR recirculation system. Middle: jet pump assembly. Right: mixer assembly. Bottom left: slip joint section view [Markham, 2016].

The existing configuration has a long annular flow path which makes the slip joint unstable and leaking; this leak path results in negative dampening in the slip joint and damaging flow induced vibrations (Figure 8-3).

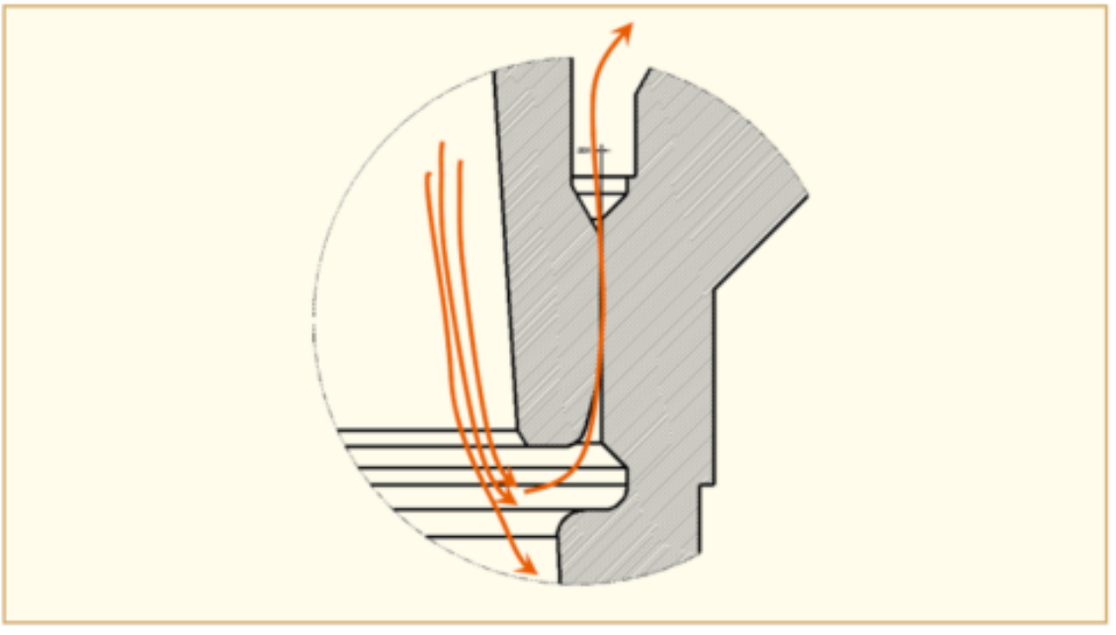

Figure 8-3: Sketch showing the leakage of a slip joint [Markham, 2016].

This leakage is the largest contributor to vibration in the jet pump, it can be outward or inward based on the flow in the jet pump. The vane passing frequencies from the recirculation pumps resonate with the natural frequencies of the jet pump. Moreover, the mixer nozzles generate a turbulent flow.

The labyrinth seal reduces the leakage; however, it does not make the flow path stable. As shown on Figure 8-4, major wear is observed on the labyrinth seal in the slip joint. The slip joint gaps approach 2.5 mm for an original clearance of 0.25 mm.

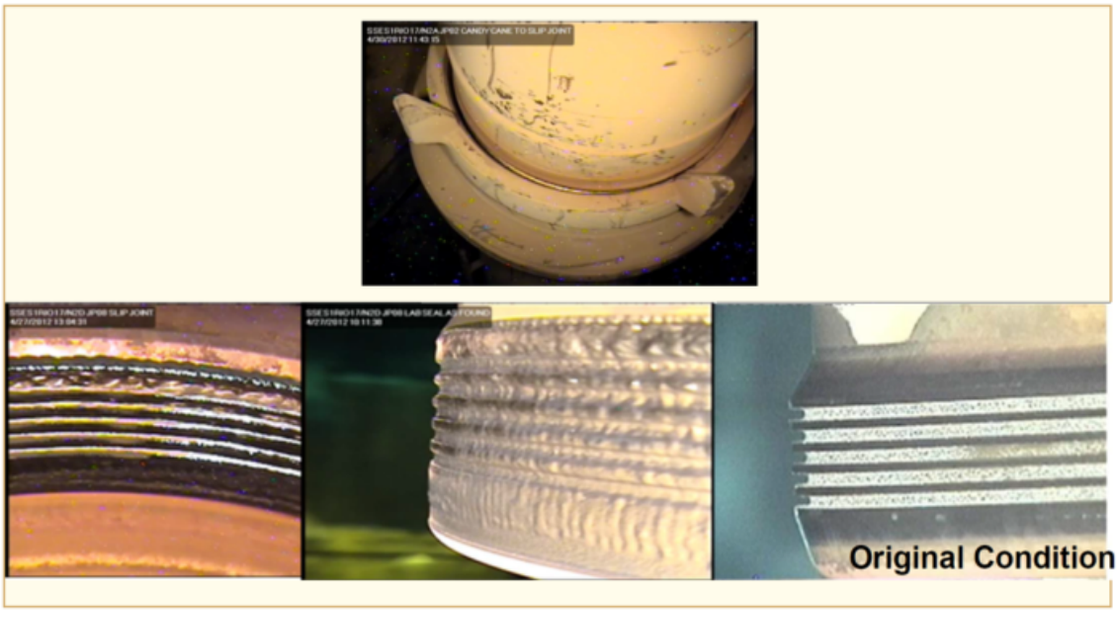

Figure 8-4: View of labyrinth seal wear [Markham, 2016].

9 BWR Water Chemistry and Mitigation

The reference [Andresen, 2016] presents the status of and developments with OnLine NobleChem.

SCC mitigation in BWRs has included eliminating bulk cold worked materials, then crevices, then sensitized SS, then water impurities. This was good, but insufficient mitigation. Corrosion potential mitigation was pursued via hydrogen water chemistry in 1980s, this was most effective in recirculation piping. Then, catalysis conceptualized and initial development done in mid 1980s which was demonstrated with Pt sputtering and electroplated coatings, with noble metals alloys and thermal spray powders and with electroless deposition of Pt in water. NobleChem was first applied at Duane Arnold in 1996. The next step was a continuous improvement as OnLine NobleChem in 2005 which was designed to minimize the critical path time during outages and permit easy, periodic application to address crack flanking. Now, OnLine NobleChem (in yellow on Figure 9-1) is now the dominant process.

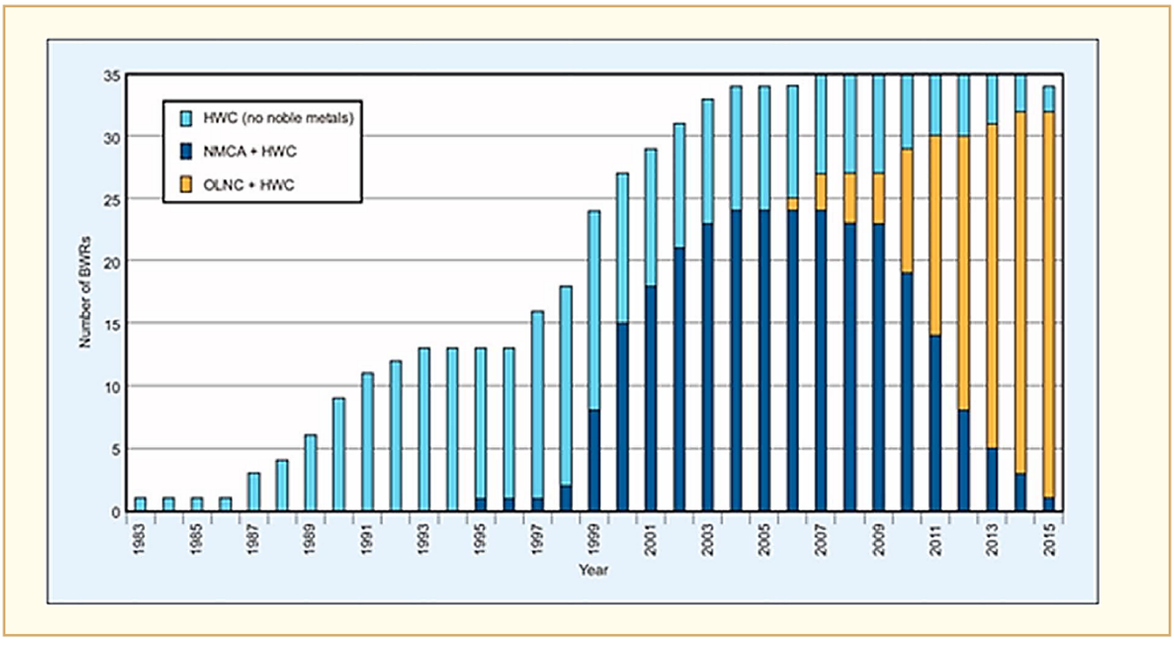

Figure 9-1: Evolution of HWC, NMCA + HWC and OLNC + HWC applications in the US [Andresen, 2016].

In the history of OLNC deployment, there are many positive indications, but negatives must be addressed (Figure 9-2). There are many examples of good news with NobleChem, including low ECP in recirculation flanges, NMP-1 jet pump latch, evidence of component mitigation, reasonable Pt size-distribution on some MMS coupons, etc. But to have confidence, to convince ourselves and the NRC that NobleChem provides mitigation at all plants and all locations of interest, the problem areas must be addressed:

- MMS coupons with little or no Pt, or poor Pt distribution;
- Cases where no Pt is found on plant components (Hatch shroud);
- Evidence that crud exists on many (all?) plant surfaces and associated focus on effective OLNC mitigation;
- Injection tap plugging, and deposition along feed water pipe.

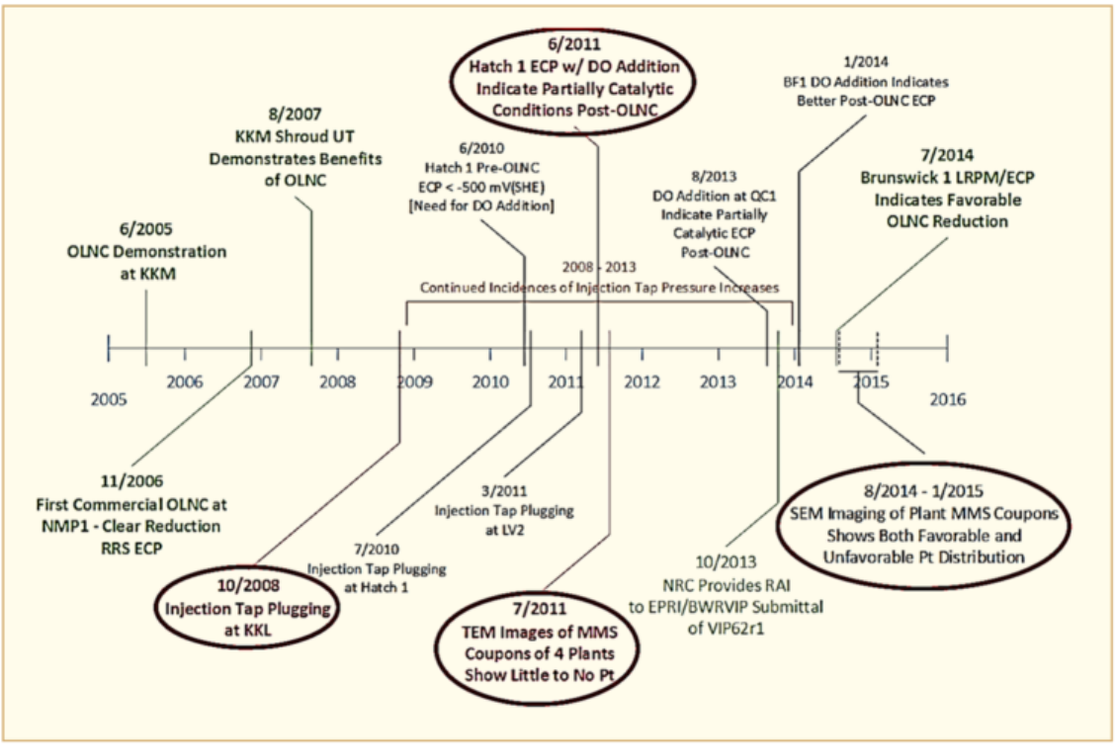

Figure 9-2: History of OLNC deployment [Andresen, 2016].

NMP-1 Alloy X-750 tie rod latch.

This latch was exposed from 2005 – 2013, to 7 OLNC applications. Its location is near the bottom of the annulus, close to recirculation suction nozzle. The average MMS Pt loading, by application was ~0.04 μg/cm^2. The loading range was: 7.1 – 23.8 μg/cm^2. It's unclear why the loading is so high compared to MMS coupons:

- Spread across the wetted surface, this loading is superior to the total Pt injected over 7 applications, so this loading level can't be characteristic of all BWR surfaces;
- Perhaps Pt on accumulated crud (not surface oxide) helps explain this;
- The low Pt on the MMS coupons (Figure 9-3) must also be addressed, as the residence time, flow rate, etc… were expected to yield a similar loading level to other locations in the BWR.

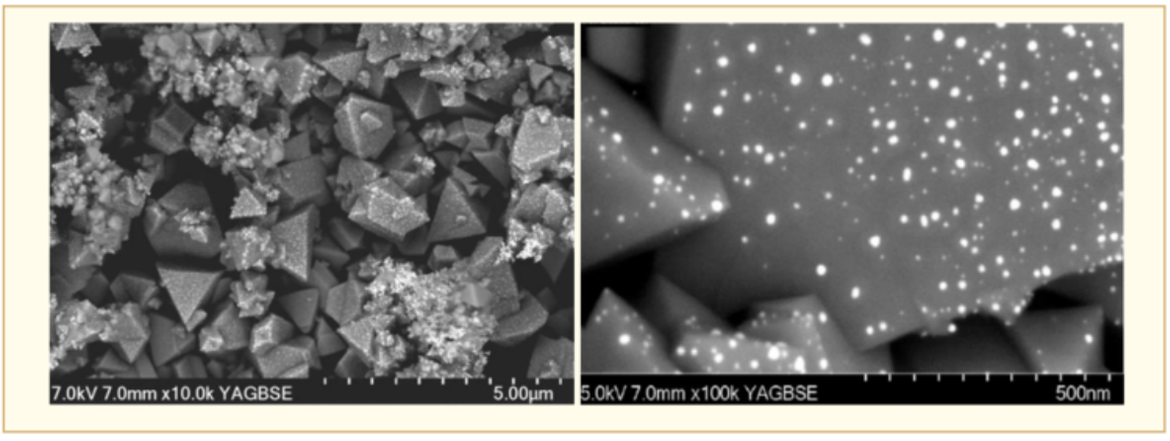

Figure 9-3: NPM1 MMS coupon, Sample F, Position #4, 469 particles/μm2 [Andresen, 2016].

BWR injection tap inspection.

In the example of Figure 9-4, the blockage was limited the last ~ 40 mm of the injection line. Provided information regarding the extent to that deposits spreads within the feedwater line. Images supported theory of platinum depositing at the interface with the feedwater flow, then being slowly pushed up the injection line as it accumulates. In a 19-mm injection tap, 82 mm of solid Pt is ~500 g. If only 75% is plugged, 88 mm of Pt is also ~500 g.

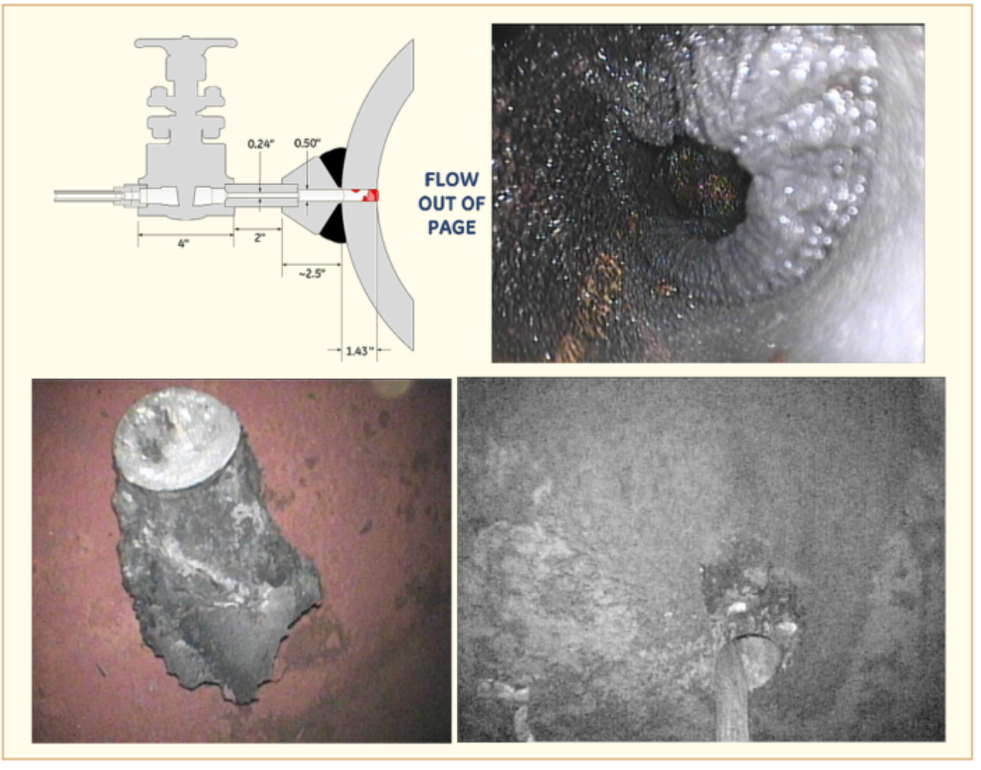

Figure 9-4: BWR injection tap inspection. Dimensions in inches [Andresen, 2016].

Injection tap inspection conclusively shows that blockage can occur at the injection point (Figure 9-5). Originally it was thought to be a plant specific issue due to unusual elements of the injection design.

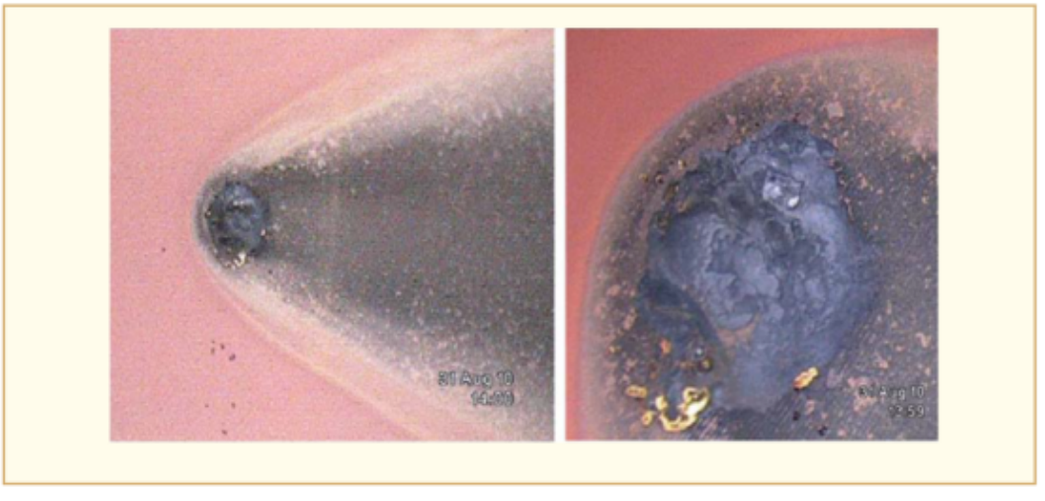

Figure 9-5: Tap injection plugging. The tap is flush hole; the Pt solution flows along the pipe wall; there is a Pt 'plume' deposit on the pipe wall [Andresen, 2016].

10 BWR Assessment

The reference [Leber, 2016] reports the history of KKM core shroud cracking over the 1990 – 2000 period:

- 1972: commercial start-up of KKM (BKW owner), GE BWR 4, MK 1 containment, core shroud made of AISI 304.
- 1990: KKM's initiative: inspection of welds: first (worldwide) indications of circumferential cracks in the HAZ of the H4 weld, detected by VT inspection, at the level of core centre at the ID. This was confirmed by first UT inspections.
- 1991/1992: four areas with crack indications were re-inspected, visually and by UT (the latter in 1992 only).
- 1992: a plug sample, 50 mm in diameter was removed. The crack was identified as SCC, its depth varied from 2 to 4.6 mm.
- Since 1993, KKM performs systematic detailed UT inspections.
- In 1996, BKW took the decision to preventively install 4 axial tie rods.

The water chemistry during the 2000 – 2015 period had to take into account this past experience. Hydrogen injection (180 µg/kg to feedwater loops A & B) is in place since 2000, changing the environment from oxidizing to reducing and reducing the electrochemical corrosion potential from less than -230 mV to -500 mV. In addition, Noble Metal Chemical Addition was launched with 185 g of noble metal.

In 2005, KKM proceeded with the worldwide first noble metal application with the new method:

- On-Line NobleChem™ with about 37 g of Pt injected; the goal was to prove the feasibility of the feed in during power operation.
- The chemical was a Pt complex ($Na_2Pt(OH)_6$) in 1% in deionized water: Na^+ and OH^-, Pt segregates elementally as nanoparticles on metal surface.

At the end of 2013, the feed-in strategy was optimized with 2 applications with a Pt injection rate of 0.3 g/h: 1) 80-90 days after the start-up of the reactor, 100 g of Pt was injected during 330 h, 2) in the subsequent springtime, 80 g of Pt was injected during about 260 h (Table 10-1). Since Na^+ completely dissolved in the reactor water, and does not deposit on the metal surfaces, it can be used as a tracer for monitoring the application (Figure 10-1). Table 10-2 compares NMCA chemistry with OLNC™ chemistry.

Table 10-1: OLNC™ applications at KKM [Leber, 2016].

Campaign	Start	Duration [h]	Appl. amount Pt [g]	Comment
2005	2005.06.15	270+188	36.7	First Appl. OLNC, MSLR Response
2006	2006.01.28	201	98.6	Fuel Behaviour
2007	2007.01.18	226	197.7	Standard Appl.
2008	2008.01.15	254	216	Standard Appl. / Inhomogeneous Solution
2009	2009.01.20	244	183.5	Average 2008/2009 200 g
2010	2010.01.19	248	199.2	Standard Appl.
2011	2011.01.18	245	199.2	Standard Appl.
2012	2012.01.17	244	199.1	Standard Appl.
2013_1	2013.01.29	240	199.5	Standard Appl.
2013_2	2013.11.28	296	99.6	Strategy Change, 0.3 g/h Pt
2014_1	2014.04.22	261	79.5	Strategy Change, 0.3 g/h Pt
2014_2	2014.11.27	359	99.9	Strategy Change, 0.3 g/h Pt
2015_1	2015.04.20	260	78.1	Strategy Change, 0.3 g/h Pt
2016_1	2016.01.11	332	100.0	Strategy Change, 0.3 g/h Pt
				© ANT International 2017

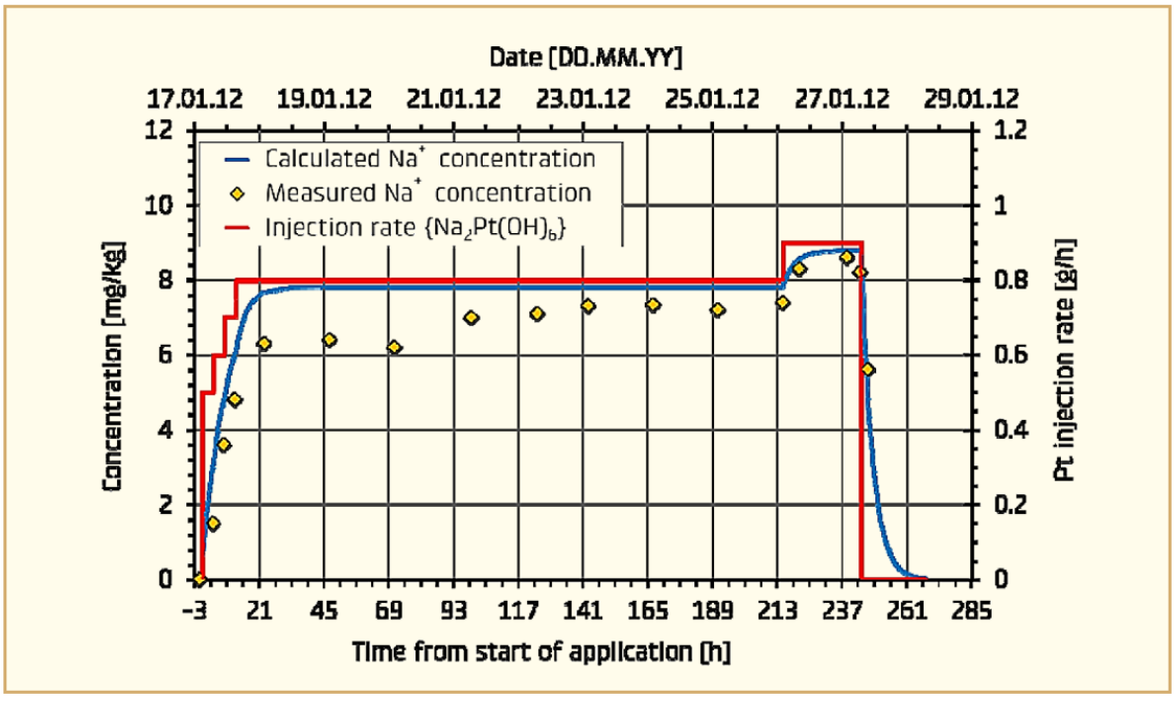

Figure 10-1: Monitoring Pt injection rate by Na^+ calculation via its measured concentration in reactor water during OLNC™ application in 2012 [Leber, 2016].

11 BWR Inspection/Operating Experience/NDE

In recent years evidence of core shroud indications exhibiting atypical orientations has been reported by utilities following in-vessel visual inspections of the core shroud assembly. Inspection data exhibiting reportable indications that cross weld material and appear to propagate outside of the expected extent of the core shroud weld heat affected zone has generated questions regarding the possible cause and characteristics of the observed indications. One concern is that the indications occur in regions of high fluence on the core shroud such that it is considered possible that the cracking is irradiation assisted stress corrosion cracking. If this is the case then there are potentially significant implications for the manner in which the Boiling Water Reactor utilities must manage degradation of the core shroud and other reactor internal components. Current inspection, flaw evaluation, and repair guidelines are inherently based on the expectation that cracking will occur in the vicinity of the core shroud welds; therefore, if IASCC is beginning to occur in the operating fleet then there exists the possibility that inspection volumes and associated tooling, procedures, and qualifications must change. The Boiling Water Reactor Vessel and Internals Project has completed a project to extract a sample of a 304 stainless steel core shroud, irradiated to approximately 2×10^{21} n/cm^2 (E > 1MeV), in one of the plants that has reported indications extending across weld material and out into the base material. Metallurgical testing has been performed on the boat sample to investigate the cracking mechanism(s) that may have contributed to the indications reported in the core shroud. The overall objectives of the sample examinations are to determine whether the cracking is due to IASCC or to some other mechanism such as cold work. The reference [Sommerville et al., 2016] summarizes the testing and conclusions drawn from the experimental program performed with the boat sample material.

The cracking in the HAZ and in the base metal is essentially entirely intergranular (Figure 11-1) whereas the cracking in the weld is interdendritic (Figure 11-2).

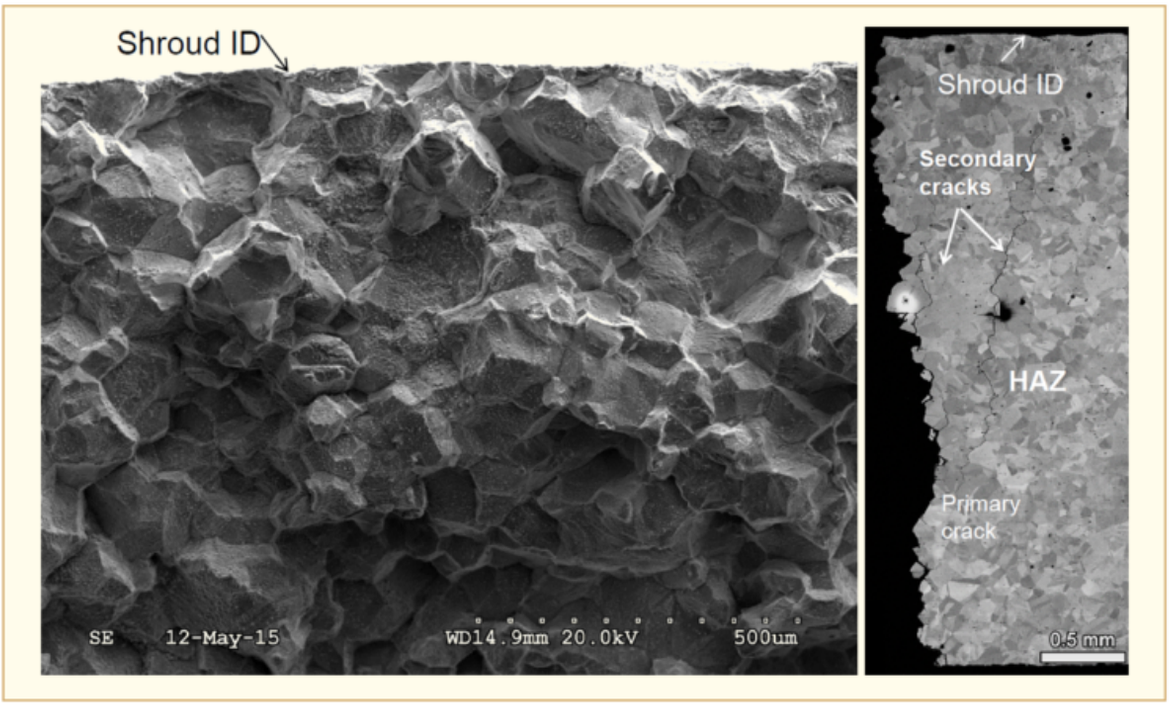

Figure 11-1: Hatch, core shroud, base metal open crack surface [Sommerville et al., 2016].

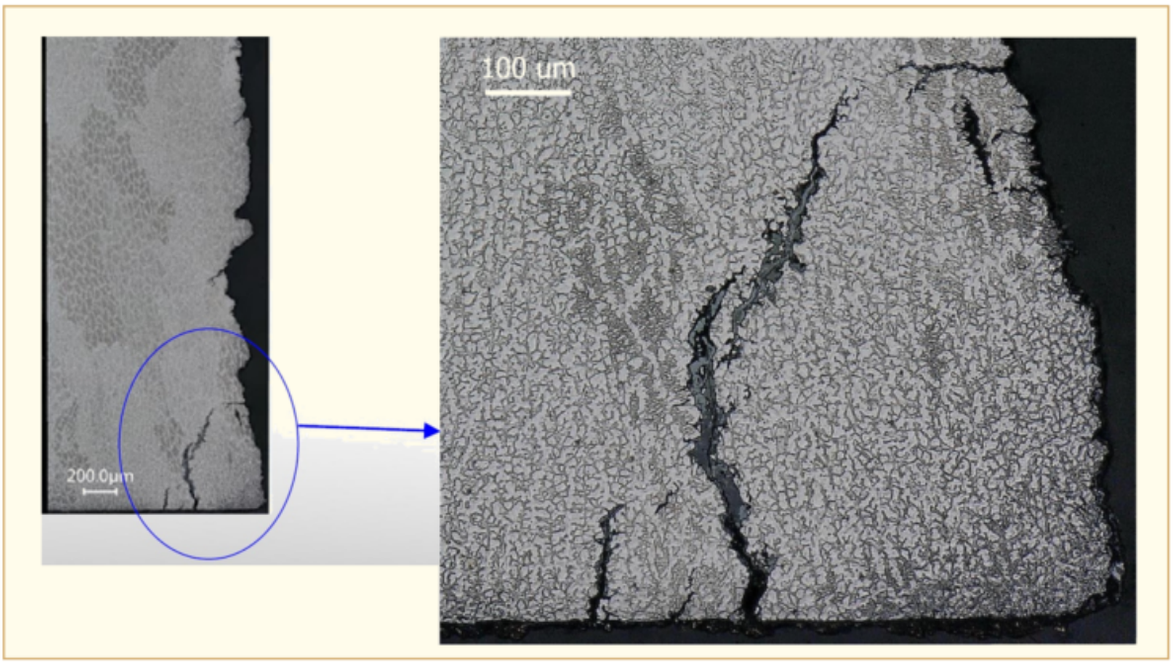

Figure 11-2: Hatch, core shroud, cracking in the weld [Sommerville et al., 2016].

The boat sample exhibited elevated strength (YS: 553 to 577 MPa and UTS: 587 to 608 MPa at 288°C) and hardness (bulk: 300 HV) due to both irradiation hardening and fabrication-induced cold work. The strength properties are consistent with expected values for this fluence level (at ID: 3.2 to 3.4 dpa, bulk: 2.6to 2.8 dpa). The hardness observed through the entire sample thickness is above the threshold value known to promote SCC (270 HV).

EDS compositional profiles across a high-angle grain boundary in the base metal (also seen in HAZ) show RIS within ≈ 5 nm of the grain boundary (Figure 11-3):

- Cr depletion as low as 12-14% versus 18% in the bulk,
- Fe depletion,
- Ni enrichment,
- Very slight enrichment in Si and P along with Mn depletion.

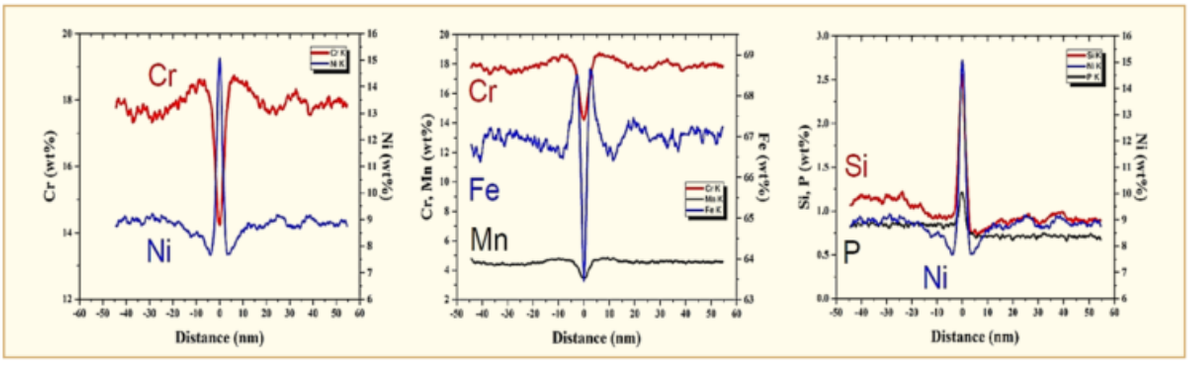

Figure 11-3: Grain boundary composition [Sommerville et al., 2016].

ATEM of crack tips shows (Figure 11-4) :

- The appearance of the gap in the oxide layer of a primary crack tip may indicate that the reactor coolant has access to the crack tip;
- A Ni enrichment is observed ahead of crack tip for all cracks, however, perhaps not as highly enriched for primary crack tip;
- In previous examinations of BWR shroud and top guide samples, oxide-filled crack tips and Ni enrichment ahead of crack tips were features associated with inactive cracks.

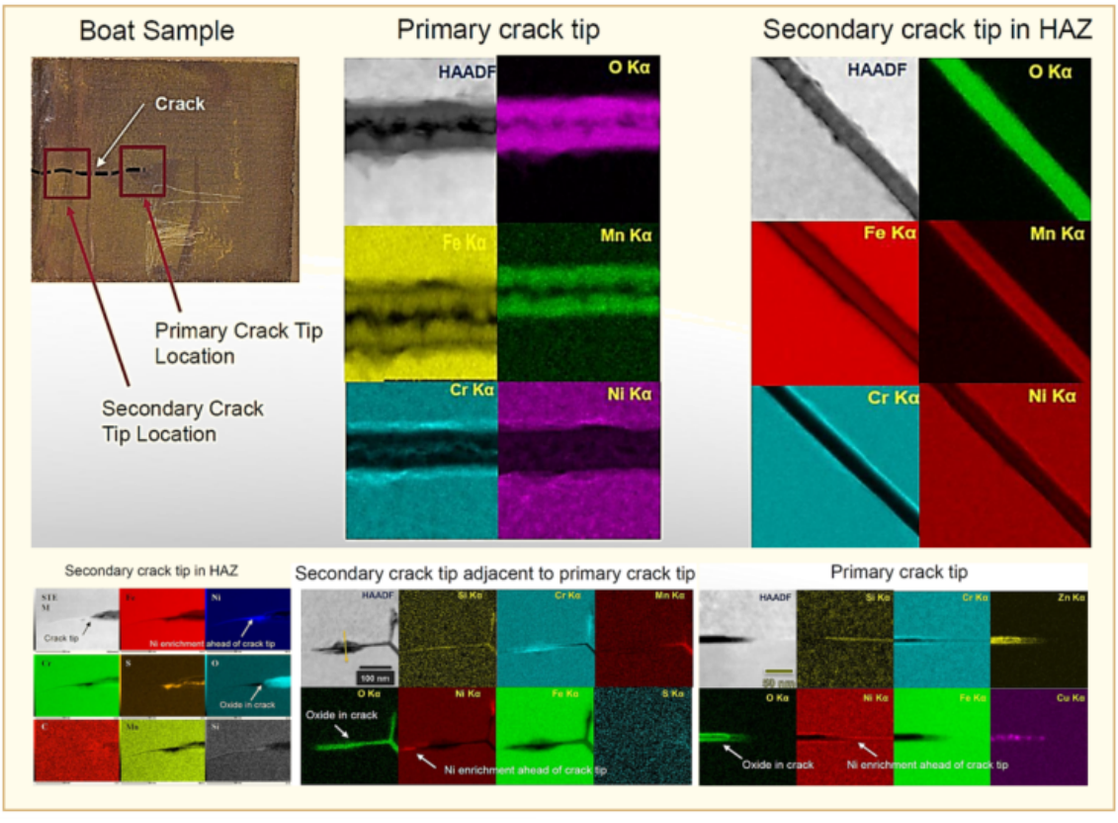

Figure 11-4: ATEM examination of crack tips [Sommerville et al., 2016].

The implications of this boat sample results are the following:

- The changes in the boat sample material properties are typical for this fluence range, based on previous material testing for the fleet;
- The irradiation has increased the material susceptibility to SCC:
  - RIS and radiation hardened microstucture are consistent with a fluence of ≈ 2×10^{21} n/cm^2 (≈3 dpa);
  - There is no evidence of weld-induced sensitization;
  - The through-sample hardness is sufficiently high to make the material susceptible to SCC;
- Non-irradiation factors were also present that may contribute to IGSCC:
  - Significant fabrication-induced cold work;
  - Potentially aggressive species are observed in the crack environment: S, Cu and Pb;
- The examination of crack tips suggests:

  - Secondary crack tip is likely dormant;
  - Primary crack tip may exhibit reactor coolant present at crack tip which could indicate an active crack;

- These results do not change the perspective that off-axis cracking does not represent a challenge to long-term shroud integrity.

In recent years, BWR core shroud indications exhibiting "off-axis" orientations have been reported by several U.S. Boiling Water Reactors following in-vessel visual inspections (IVVI) of the core shroud. These indications have some characteristics that are not typical of intergranular stress corrosion cracking. Specifically, the indications are observed to propagate outside of the weld HAZ and are generally oriented perpendicular to the associated weld. Indications may emanate directly from the weld toe or may occur as perpendicular branching components of IGSCC flaws. Although such off-axis indications have been generally known to exist within the U.S. fleet of BWRs, these indications were generally dispositioned as minor due to their short length and insignificant impact on structural margins. However, observation of more significant off-axis indications in the high fluence region of a BWR/4 plant, with some indications reported to be thru-wall by specialized UT measurements, has resulted in a desire to improve industry understanding of the extent and significance of off-axis indications. The reference [Lunceford et al., 2016] documents a survey of the U.S. fleet operating experience and evaluates these data with regard to extent of cracking and observable trends.

First of all, what is core shroud "off-axis" cracking?

IGSCC is a commonly observed phenomenon in BWR core shrouds. Typically, the cracking propagates parallel to the weld and is contained in the HAZ, and also, this cracking is promoted by the weld sensitization, weld residual stresses and cold work.

In contrast, off-axis cracking is SCC which is oriented generally perpendicular to the associated shroud weld (Figure 11-5):

- The cracking extends outside of the HAZ;
- In most cases, cracking terminates at the weld toe;
- In a few cases, the cracking appears to propagate into or even across a weld;
- Often, IGSCC branching with a significant off-axis component is also reported as off-axis cracking, especially if the cracking propagates outside of the HAZ.

12 Probabilistic Fracture Mechanics/xLPR

As the US Nuclear Regulatory Commission moves toward a more risk-informed regulatory structure, probabilistic fracture mechanics methodologies have been developed to determine initiating even frequencies for probabilistic risk assessment. PFM is an analysis technique that allows greater insight into the structural integrity of components than similar deterministic analyses, by estimating the entire range of possible variations in behaviour of a component, instead of aiming to estimate only a bounding behaviour. PFM allows the direct representation of important uncertainties through the use of best-estimate models and distributed inputs, and allows the determination of the direct impact of uncertainties on the results, which gives the user the ability to determine and control the specific drivers to the problem. However, PFM analyses can be more complicated and difficult to conduct than deterministic analyses. Determining validated best-estimate models, developing input distributions with limited data, characterizing and propagating input and model uncertainty, and understanding the impacts of problem assumptions on the adequacy of the results, can make PFM analyses difficult to conduct and difficult to approve in a regulatory application. The reference [Rudland et al., 2016] provides some thoughts on how to improve confidence in structural analyses performed using PFM, by focusing on topics such as solution convergence, input distribution determination, uncertainty analyses, sensitivity analyses (to determine impact of uncertainties on result) and sensitivity studies (to determine impact of mean values on the results). By determining the main drivers to the probabilistic results and investigating the impacts of the assumption made to develop those drivers, the confidence in the overall results can be greatly improved.

For several years, the NRC and EPRI have been jointly funding an effort to develop the Extremely Low Probability of Rupture V2.0 computational code. The objective of this code is to evaluate the likelihood of piping failure compared with other more likely outcomes such as crack arrest, crack detection during inspection, or the formation and detection of a leaking crack. The initial effort is focusing on the evaluation of dissimilar metal welds in pressurized water reactors subjected to primary water stress corrosion cracking and fatigue, with and without the effect of various mitigation methods, to determine if the rupture probability is sufficiently low to justify continued regulatory credit for leak-before-break in applicable piping systems. The reference [Tregoning et al., 2016] provides an overview of the organization and structure used to develop xLPR V2.0; summarize the probabilistic framework and modules that make up the code; discuss the quality assurance and reporting provisions; describe internal and external peer review activities, discuss code verification and validation; provide a status of ongoing activities to complete V2.0; describe the planned use of the code to assess LBB of DMWs; and present the plan for supporting continued development and evolution of the code.

The reference [Schmitt et al., 2016a] presents the results of a generalized statistical framework for the integration of laboratory and field data in the development of a probabilistic model for the prediction of the PWSCC initiation time. The fidelity of such a model is critical to the probabilistic prediction of leakage and instability risks associated with PWSCC susceptible components. The statistical framework described in this reference applies a laboratory data set for refinement of underlying model dependencies and a field data set for regression of the initiation (failure) time model. Having established the modelling methodology in a previously published paper, this reference focuses on the development of input distributions from plant data, parameter regression, generation of predictive results for PWSCC initiation time, and validation of the underlying model.

The computer code FAVOR performs probabilistic fracture mechanics simulations that are used to assess the effects of normal and accident loading on the shell region of nuclear reactor pressure vessels. FAVOR was first developed in the mid-1990s, and was used extensively in the calculations that supported the NRC's pressurized thermal shock re-evaluation effort. More recently (late 2000s and onward) the capabilities of FAVOR have been augmented to enable the modelling of both boiling-water and pressurized-water reactors.

The reference [Kirk et al., 2016] focusses on current efforts to further augment the FAVOR code, and to bring its computational routines up to date. This reference focusses on options for modelling the probability of fracture beginning from shallow surface breaking flaws, where the depth of the flaw is slightly greater than the thickness of the austenitic stainless steel cladding deposited on the inner diameter surface of the vessel for purposes of corrosion control.

13 Long Term Operations (LTO)

The reference [Iyengar et al., 2016] provides an overview of the various activities undertaken by the Nuclear Regulatory Commission in support of subsequent license renewal. Although the NRC staff can accept subsequent license renewal applications now, the review would be based on guidance provided in NUREG-1800, Revision 2, "Standard Review Plan for Review of License Renewal Applications for Nuclear Power Plants" and NUREG-1801, Revision 2, "Generic Aging Lessons Learned Report – Final Report." Because this guidance applies to plants operating from 40-60 years, additional review would be needed to ensure that the applicant addressed issues anticipated during 60-80 years of plant operation for SLR. Such reviews would be longer and more resource-intensive. To improve the efficiency of SLR application reviews, the NRC staff has undertaken several activities to revise the guidance documents. These activities include reviews of aging management practices, plant audits, technical information exchanges with industry and Department of Energy, and confirmatory research.

In cooperation with the DOE Light Water Reactor Sustainability Program, the NRC completed NUREG/CR-7153, "Expanded Materials Degradation Assessment, Vol. 1-5" (ADAMS Accession Nos. ML14279A321, ML14279A331, ML14279A349, ML14279A430, ML14279A461) to identify the most significant technical issues for nuclear power reactor operation beyond 60 years. The EMDA ranked the significance, current knowledge, and uncertainty associated with aging-related degradation phenomena that could affect systems, structures, and components (SSCs) over 80 years of operation. As outlined in the staff requirements memorandum on SECY 14-0016, the major technical issue areas are:

- Reactor pressure vessel neutron embrittlement at high fluence;
- Irradiation-assisted stress corrosion cracking of reactor internals and primary system components;
- Concrete and containment degradation; and
- Electrical cable qualification and condition assessment.

The NRC staff conducted several audits to investigate the effectiveness of aging management programs. The findings are documented in the publicly-available Technical Letter Report, "Review of Aging Management Programs: Compendium of Insights from License Renewal Applications and from AMP Effectiveness Audits Conducted to Inform Subsequent License Renewal Guidance Documents," (ML16167A076).

The development of SLR guidance was based on NUREG-1800 and NUREG-1801, the understanding gained from the audits, NUREG/CR-7153, an evaluation of domestic and international operating experience of nuclear plants, lessons learned from staff review of previous license renewal applications, and assessment of recent research findings. Draft SLR guidance documents were issued in December 2015, as draft "Generic Aging Lessons Learned for Subsequent License Renewal Report," (NUREG-2191, Volumes 1 and 2) and draft "Standard Review Plan for Review of Subsequent License Renewal Applications for Nuclear Power Plants" (NUREG-2192).

Since the draft guidance documents were issued, the staff has held several public meetings with stakeholders and the public to discuss the proposed revisions and bases for the revisions. The NRC staff will continue to lead outreach activities to stakeholders and the public in order to provide information on the proposed changes to the guidance documents, solicit feedback on the documents, and revise the documents, as appropriate, to reflect stakeholder and public feedback. The final guidance documents are expected to be issued in mid-2017.

United States and International utilities are actively engaged in assessing the economic and societal benefits of operating nuclear plants beyond their initial license periods. Nuclear plant generated electricity is still the largest contributor to non-carbon dioxide emitting generation. In the US, a majority of operating plants has already received approval for an additional 20 years of operation, and soon it is expected that utilities will begin the process to seek a second 20-year renewal. The keys to successful renewal are to maintain safe and reliable operations by building a sound technical case through the following activities:

- Develop comprehensive understanding of aging degradation issues for systems, structures and components;
- Implement specific plant aging management programs to address aging degradation;
- Confirm behaviour of degradation mechanisms for the entire period of operation.

The reference [Tilley et al., 2016] steps through these above elements to illustrate how a strong technical case may be created for safe and reliable long-term operation. Examples or case studies will be provided to clearly link the fundamental science of materials degradation to the inspection, testing and evaluation efforts implemented at a plant and to the confirmatory data that is provided by both actual operating experience and the extensive research and development projects pursued by industry, governments, and the academic community.

The RAMA Fluence Methodology is a system of software components that include a three-dimensional Method of Characteristics-based transport code, parts model builder code, state-point model builder code, fluence calculator, and nuclear data library. Sponsored by the Electric Power Research Institute and maintained by TransWare Enterprises Inc., RAMA is used to determine neutron fluence in BWR components in compliance with the requirements and guidelines provided in U.S. Nuclear Regulatory Commission Regulatory Guide 1.190.

Sponsored by the Nuclear Regulatory Commission and maintained by Oak Ridge National Laboratory, the Scale code package provides radiation transport, depletion, and uncertainty analysis solvers with an interconnected framework suitable for a broad spectrum on nuclear analyses. Specifically, COUPLE and ORIGEN-S provide a direct approach to activation and depletion calculations.

The reference [Jones et al., 2016] presents the RAMA Fluence Methodology and Scale code package coupled. Using appropriate tooling, this package allows for a wide class of materials reliability and light water reactor sustainability analyses to be performed. Previous use of the coupled system allowed for the determination of helium concentration within reactor materials. The coupled methodology has the potential to be applied to more sophisticated calculations in and around the reactor such as:

- Long-term management of activation of reactor internals;
- RPV and component activation for dose estimates;
- Final decommissioning strategies for reactor component segmentation.

Coupling is performed through a detailed processing script and uses the RAMA calculated fluxes and fluences to accurately collapse an ORIGEN library for any given region. Material compositions are also pulled from the RAMA model and utilized in the activation and depletion calculation.

Corrosion is a major service life limiting mechanism for both pressurized water reactors and boiling water reactors. While most of the ongoing corrosion research emphasis in the nuclear corrosion community has been focused on environmentally-assisted cracking of austenitic stainless steels and nickel-base alloys and its weld metals, in particular stress corrosion cracking under its various labels such as intergranular stress corrosion cracking in BWRs, primary water stress corrosion cracking in PWRs and irradiation assisted stress corrosion cracking in both reactor systems, there are other somewhat less sophisticated corrosion phenomena that can also seriously and detrimentally affect plant life extension that should be not ignored. The reference [Gordon, 2016] discusses three of these other important corrosion areas, i.e., general corrosion of the light water reactor containments, flow-accelerated corrosion of carbon steel and the corrosion of buried piping.

Some containment corrosion history:

- 1980, Oyster Creek. This plant is a Mark I BWR (Figure 13-1) which started up in 1969. During a refuelling outage, some water was noted around various containment penetrations and floors. Intrusion of water was observed into the annular space between the carbon steel drywell shell and the concrete shield wall (Figure 13-2 and Figure 13-3). The presence of water in the sand bed (Figure 13-4) indicates possible corrosion of drywell (Figure 13-5). A radiological analysis indicated an activity level similar to primary water. It was suggested that

the source of the water was the reactor cavity located immediately above the drywell (Figure 13-2).

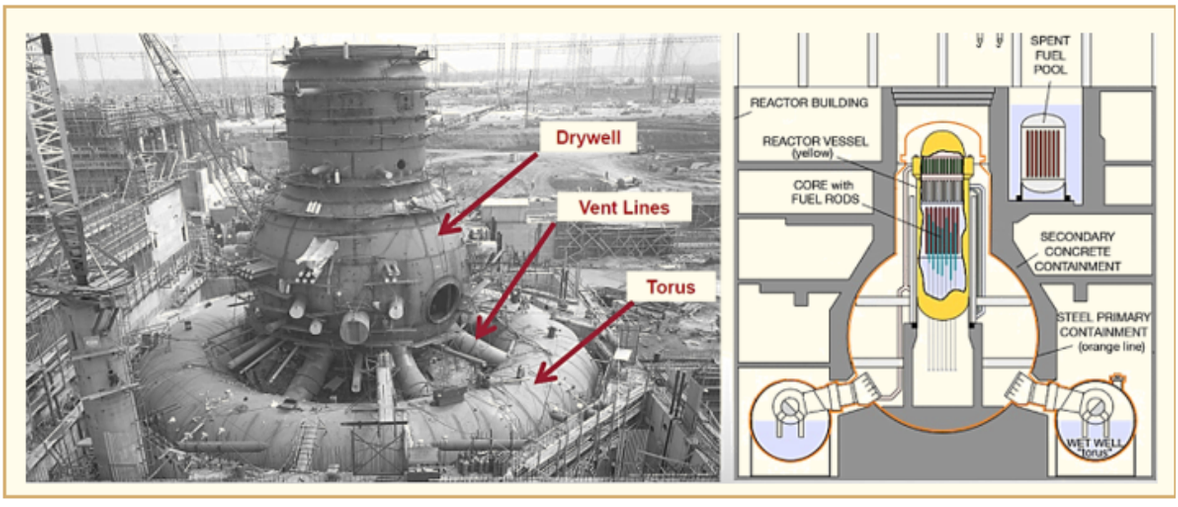

Figure 13-1: Example of Mark I containment (here: Browns Ferry 1 in 1973) [Gordon, 2016].

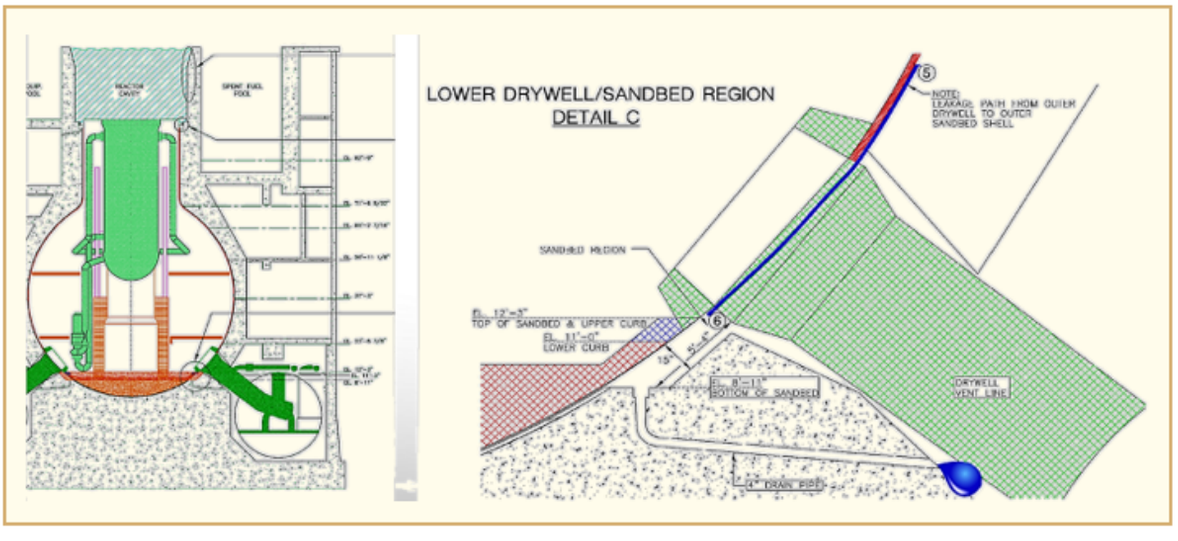

Figure 13-2: Oyster Creek, leak path [Gordon, 2016].

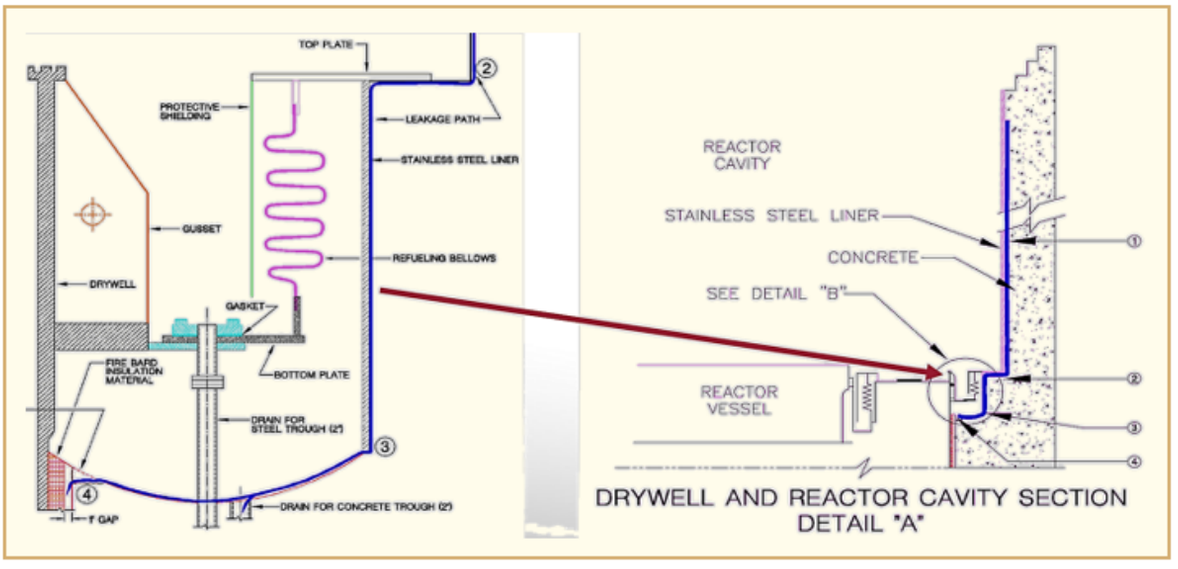

Figure 13-3: Oyster Creek, detail of leak path [Gordon, 2016].

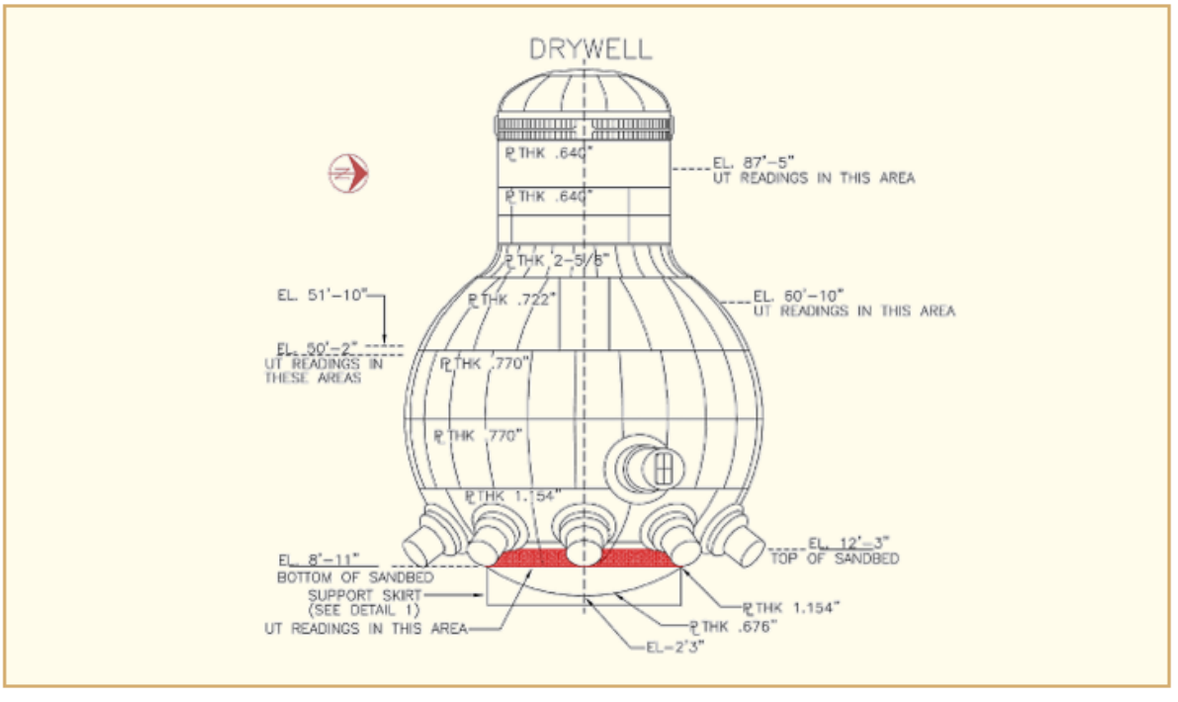

Figure 13-4: Oyster Creek drywell [Gordon, 2016].

14 Non-destructive Examination Techniques

Void swelling of PWR internals constructed from 304 and 316 austenitic stainless steels is a subject of possible concern, especially for extended life-times beyond 40 years. Swelling of these steels is known to be primarily sensitive to the dpa level, dpa rate and local temperature. The latter is determined by the adjacent coolant temperatures, the local gamma heating rate, and the thickness of the component. Therefore, the temperature distribution within a plate or bolt can be elevated above the coolant temperature, producing non-uniform internal swelling distributions that are in excess of that which would be produced at the local coolant temperature. Variations in dpa rate and gamma heating across the component will also contribute to spatial variations in swelling (Figure 14-1).

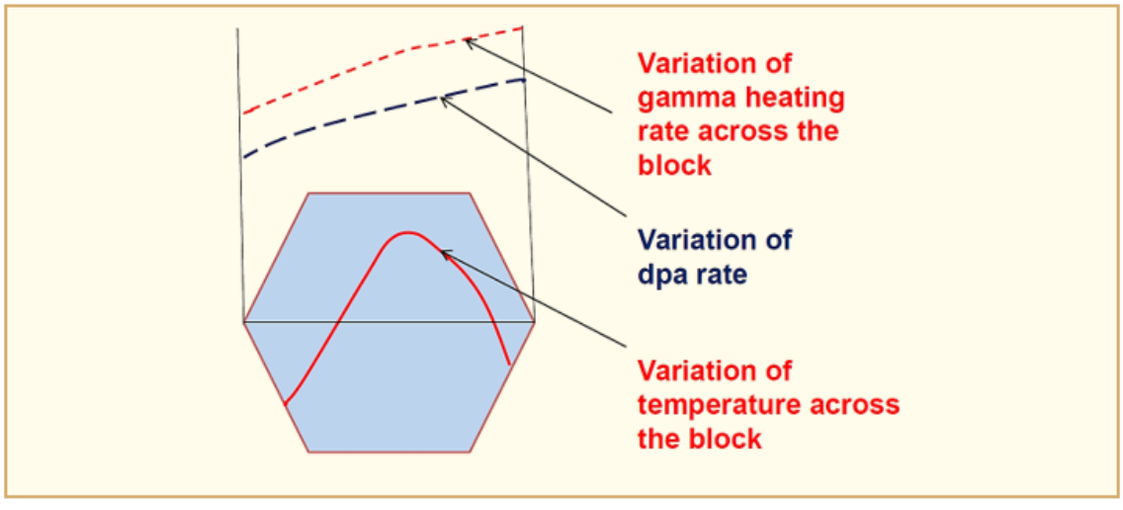

Figure 14-1: Temperature distribution inside of the block selected by Westinghouse for this study, arising from gradient in gamma heating. Local temperature is determined by 1) coolant temperature at block surface, 2) gamma heating distribution and 3) distance from block surfaces [Garner et al., 2016].

The average swelling across a baffle plate or other thick components can be determined using changes in ultrasonic velocity caused by voids and concurrent formation of carbide precipitates, both of which cause changes in elastic moduli but not in the same direction. In the reference [Garner et al., 2016], results are shown of a comprehensive experiment that separates the separate contributions of swelling and carbide precipitation, and demonstrating that ultrasonic time-of-flight measurements can indeed measure the average swelling level and in some cases the spatial distribution of void swelling within thick 304 stainless blocks. These findings provide optimism that a sensor can be developed to non-destructively measure the swelling of baffle plates from the inside surface of the baffle-former assembly. Additionally, it is shown that after some minimal preparation the swelling along the axis of a baffle bolt can be determined by coupled time-of-flight measurements and a new non-destructive surface imaging technique involving backscatter electrons.

The reference [Spanner, 2016b] describes improvements to the ultrasonic procedures to be used for the detection of thermal fatigue in nuclear power plants in accordance with the requirements of the Electric Power Research Institute Material Reliability Program inspection and evaluation guidelines. These examinations have been performed at nuclear plants in the USA since the 1980s with very few detections of degradation. However, since 2013 there have been three unplanned outages to repair leaks caused by thermal fatigue. The MRP formed a thermal fatigue focus group to analyse these leaks and seven additional plant issues related to thermal fatigue inspection programs. Then the group developed recommendations to address these recent operational experiences. The MRP has been developing improvements to the ultrasonic procedures and this reference shares these. A computer based training program for the ultrasonic personnel has been developed that is described. And finally, the MRP has fabricated a variety of thermal fatigue mockups that are loaned to member utilities prior to an outage so the ultrasonic personnel can practice detecting thermal fatigue just prior to the examinations. Implementation of these mockups are also described.

15 Reactor Pressure Vessel Integrity

Chemical composition of materials and irradiation conditions are usually taken into account to evaluate and/or predict irradiation embrittlement of RPV steels. However there in an increasing interest in effect of an initial property on the embrittlement which might be caused by a superposition effect of pre-existing microstructures and irradiation defects in irradiated materials. In the reference [Nomoto et al., 2016], initial properties such as yield stress of unirradiated materials on amount of embrittlement of RPV steels in experimental data is investigated (Figure 15-1).

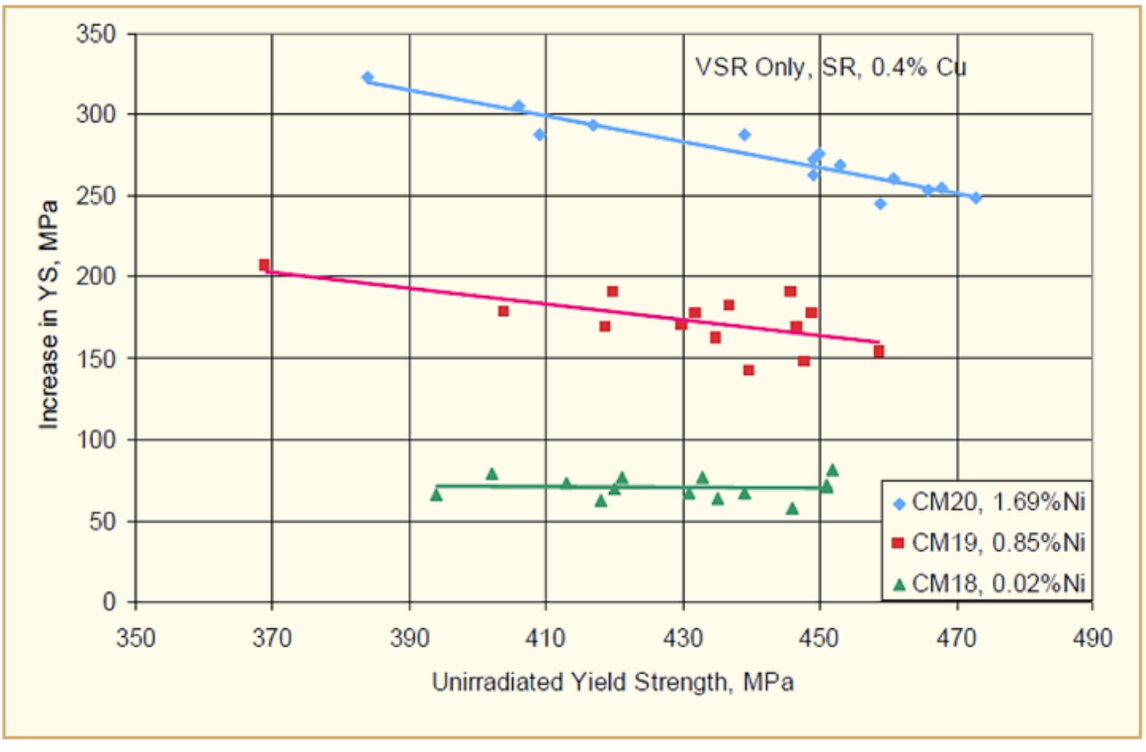

Figure 15-1: Effect of initial yield stress on hardening. Materials having higher initial (= unirradiated) yield stress show lower irradiation hardening [Nomoto et al., 2016].

Chemically–tailored reactor pressure vessel steels were irradiated at 290°C to different neutron fluence levels to investigate the effect of Cu and P on one hand, and Mn an Ni on the other hand. The aim is to investigate individual effects as well as combined effects such as Cu/P and Ni/Mn elements on the tensile properties. The reference material composition is typical of an A533B and the composition of the chemically-tailored steels was then varied by changing only one variable at once and keeping all others similar. Typically, three content levels corresponding to low, medium and high concentration were considered.

The reference [Chaouadi et al., 2016a] describes the irradiation program together with the test results. The effect of individual composition variables and the combined Cu/P and Ni/Mn effects are assessed and discussed.

Within the limits of the experimental data (composition variables, irradiation conditions), Cu is clearly and by far the most radiation-sensitive element (Figure 15-2 and Figure 15-3). As concerns P, its effect is relatively small (Figure 15-2). At the irradiation temperature of this study, no synergy between Cu and P has been observed (Figure 15-4).

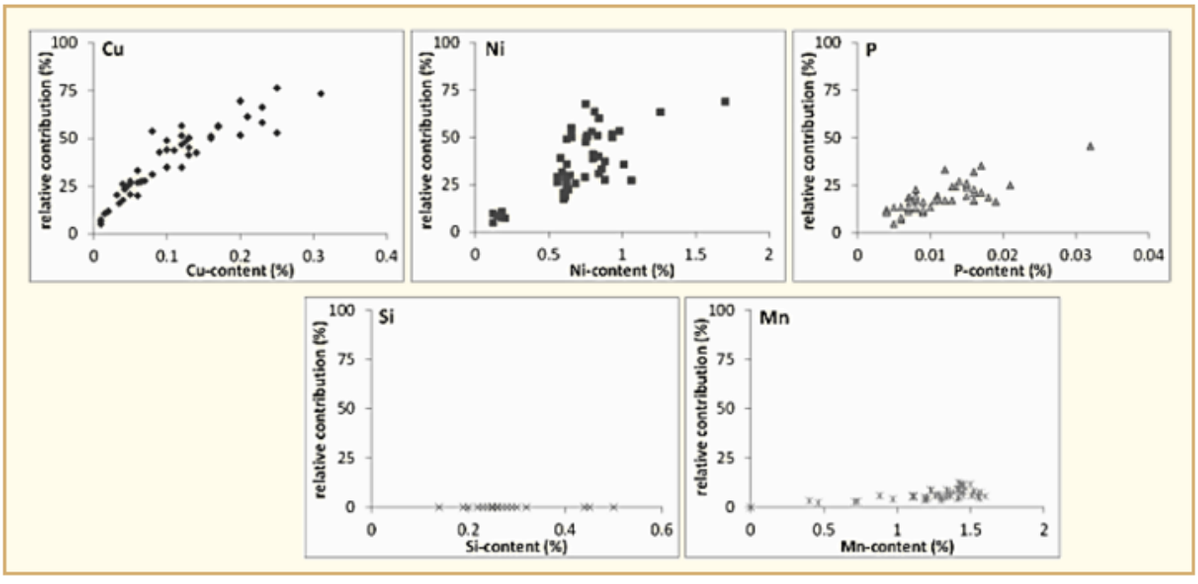

Figure 15-2: Relative contribution of Cu, Ni, P, Si and Mn to radiation embrittlement (72 data points, fluence = 11.4×10^{19} n/cm^2) [Chaouadi et al., 2016a].

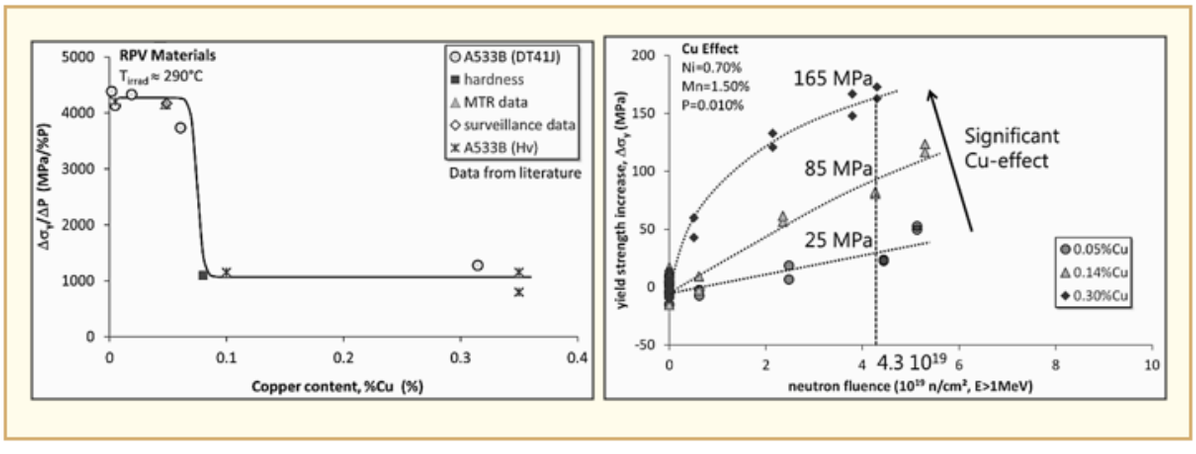

Figure 15-3: Role of Cu in irradiation hardening and embrittlement [Chaouadi et al., 2016a].

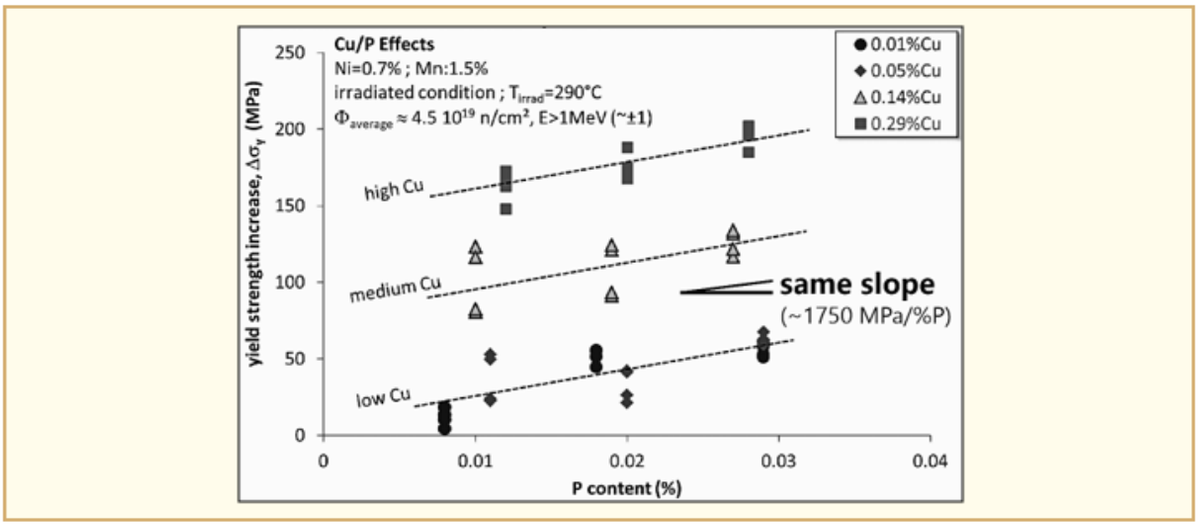

Figure 15-4: Cu/P effects on irradiation hardening. There is a constant slope at all Cu levels, which means there is no synergy between P and Cu (at 290°C PWR relevant, however, this might not hold for other irradiation temperatures) [Chaouadi et al., 2016a].

Ni and Mn effects are significantly lower in comparison to Cu effect. No synergy between Ni and Mn is observed except for the high Ni/high Mn steel (1.7% Ni/1.8% Mn) (Figure 15-5).

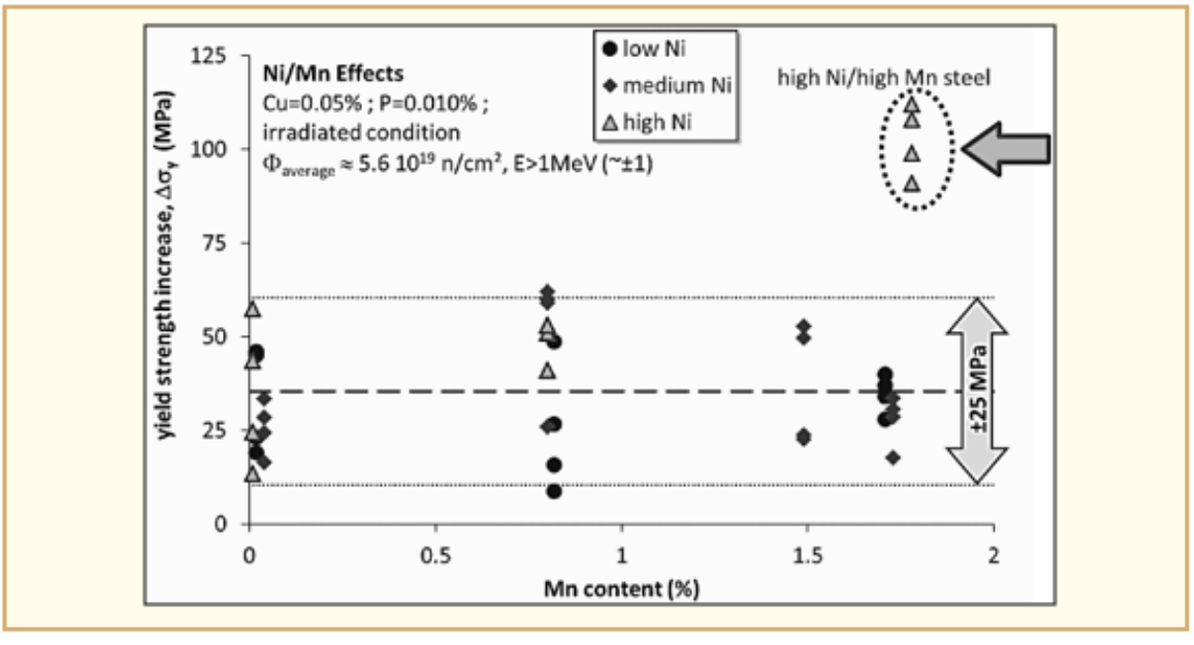

Figure 15-5: Clear Mn effect at high Mn content (1.7%) [Chaouadi et al., 2016a].

TEM examination revealed the presence of a second phase (NiMn-rich phase). 1.7% Ni/1.8% Mn steel has a significantly higher work hardening capacity. This behaviour is attributed to martensitic transformation during deformation (twins).

The EPRI MRP and BWRVIP compiled a team to evaluate potential non-conservatisms in NUREG-0800 Branch Technical Position 5-3 (BTP 5-3) guidance for estimating weak direction properties from strong direction test data (Figure 15-6). A plant survey was conducted to assess the extent of use of BTP 5-3 in the PWR and BWR fleets in the USA. Then, the effect of current and continued use of the BTP 5-3 methods on RPV integrity was assessed.

16 Peening and Surface Mitigation

The reference [Alley, 2016] provides a current status regarding the NRC's evaluation of Materials Reliability Program Topical Report MRP 335 regarding peening of dissimilar metal butt welds and reactor pressure vessel head penetrations and their associated J-Groove welds. The limits of the NRC's review of the topical report and the relationship between the topical report and plant specific relief requests is discussed. A discussion of the NRC's use of probabilistic and deterministic information in evaluating MRP-335 is provided as well as a discussion for longer term approaches to industry submission and NRC evaluation of probabilistic fracture mechanics information.

Laser peening and water jet (i.e., cavitation) peening are surface stress improvement methods that are available to mitigate primary water stress corrosion cracking of Alloy 600/82/182 nickel-base alloy components in nuclear power pressurized water reactors (Figure 16-1). These peening methods generate compressive residual stresses at the wetted surface, preventing future initiation of PWSCC. PWSCC of pressure boundary components made using Alloy 600 and its weld metals Alloys 82 and 182 has been a major materials degradation concern affecting PWRs. PWSCC cracking and leakage concerns have necessitated costly inspections, repairs, replacements, and lost power production.

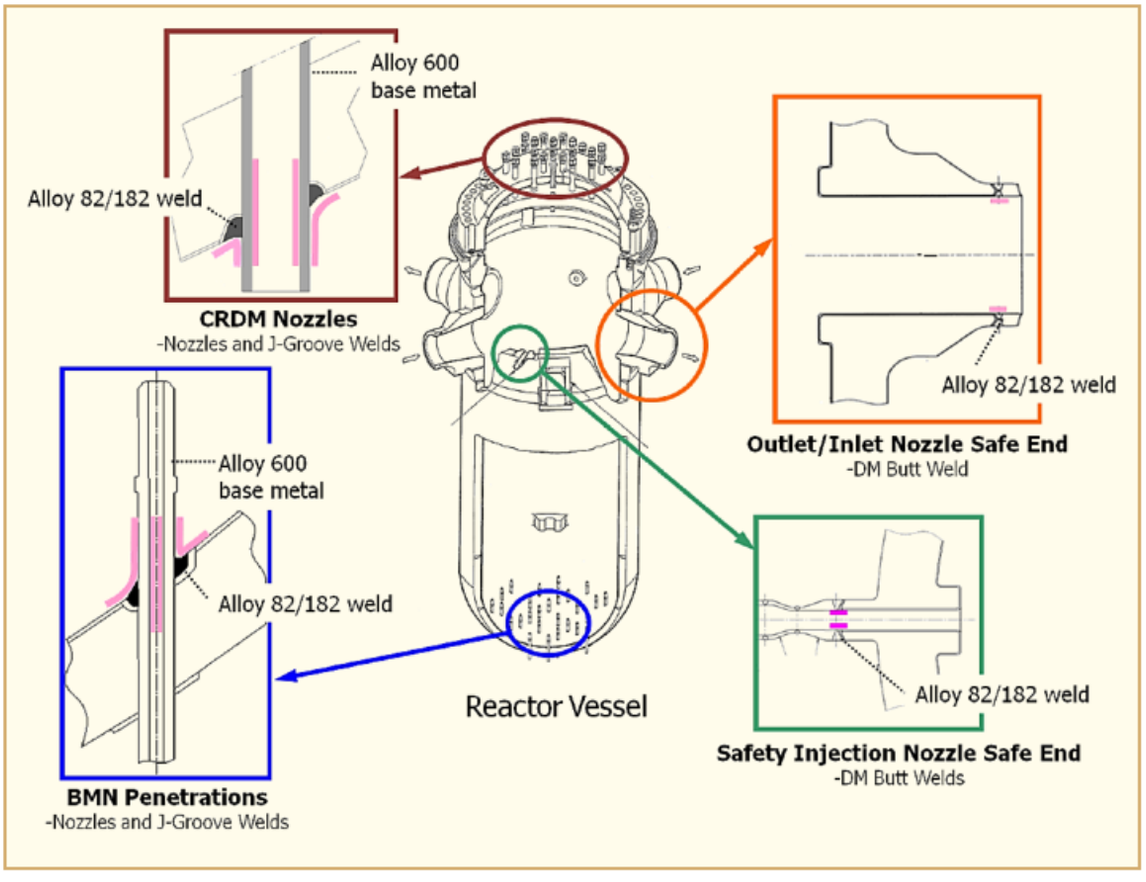

Figure 16-1: Candidate areas for SCC peening mitigation [White et al., 2016b].

Beginning in 1999, in-service peening has been extensively applied in Japanese boiling water reactors and PWRs to mitigate stress corrosion cracking (Table 16-1).

Table 16-1: Experience with peening in the nuclear power industry [White et al., 2016b].

PWRs	BWRs
Japan (starting in 2001): • At least 23 out of 24 PWR units have applied water jet peening or laser peening to BMNs and/or reactor vessel inlet/outlet nozzle DMWs; • WJP and LP have also been applied to reactor vessel safety injection nozzles; • USP has been applied to steam generator inlet or outlet nozzles at more than 10 PWRs and for pre-service peening of 9 replacement reactor vessel heads with A690 nozzles.	Japan (starting in 1999): • WJP and LP have extensively been applied to core shrouds and bottom head penetrations (i.e., CRD stub tubes); • Applying to new ABWR units during the fabrication and construction phases.
The AWJ conditioning process has been widely used in the US for more than a decade in PWR nozzle repair applications.	
Several hundred thousand steam generator tubes have been shot peened over the past 30 years, extending their useful life.	
Successful application of shot peening on Alloy 600 pressurizer heater sheaths installed in 1990 at one PWR.	

The first peening mitigation applications in the U.S. are planned for 2016 and 2017. EPRI has developed a detailed technical basis demonstrating the effectiveness of peening to mitigate PWSCC without adverse effects. The technical basis, which includes extensive data generated by peening vendors as well as confirmatory testing sponsored by EPRI, is now being used to support acceptance by the ASME Boiler & Pressure Vessel Code and U.S. regulator of appropriate relaxation of inspection intervals for peened components. In this approach, performance criteria define the requirements for the peening stress effect (compressive residual stress magnitude, depth, and coverage), while also requiring that the effect be sustained for at least the service life of the component and that there are no unacceptable adverse effects. The technical basis work includes stress measurements of representative test specimens, corrosion testing including with simulated PWR primary coolant, and testing and analyses to consider thermal stress relaxation and stress shakedown due to load cycling. The recommended inspection intervals for use with peening are based on the benefit of peening to prevent future PWSCC initiations. Deterministic and probabilistic modelling of assumed pre-existing PWSCC flaws supports the detailed inspection requirements, which include pre-peening, follow-up, and long-term periodic in-service examinations.

The first two US applications of Mitsubishi's Water Jet Peening process on the Alloy 600 susceptible areas of a reactor vessel will take place in the Fall of 2016 and 2017 at the Wolf Creek and Callaway plants respectively. The reference [Martin, 2016] summarizes the WJP experience base from Japan on reactor vessel nozzles, bottom mounted nozzles, and safety injection nozzles and most importantly, how Mitsubishi has taken that base of experience and evolved the WJP technology for present day US applications. The primary focus of the presentation is on the efforts, preparations, and milestones achieved since the contract was signed in mid-2013 to address the US utility specific differences that need to be taken into account for a series of successful US Water Jet Peening projects.

Mitsubishi had, in 2016, 15 years of experience in WJP, with a total of 21 Japanese plants mitigated. The 45 WJP projects breakdown is the following:

- BMN projects = 21;
- RVN projects = 18;
- Safety injection nozzles projects = 6.

US plants have also needs regarding potential WJP applications (Figure 16-2). Thus, Mitsubishi has developed tools for the US market (Figure 16-3). Two tools for BMNs WJP and two tools also for RVNs WJP have been fabricated. A WJP training centre has been built with BMN and RVN mock-ups (Figure 16-4) and a full size WJP equipment (Figure 16-5).

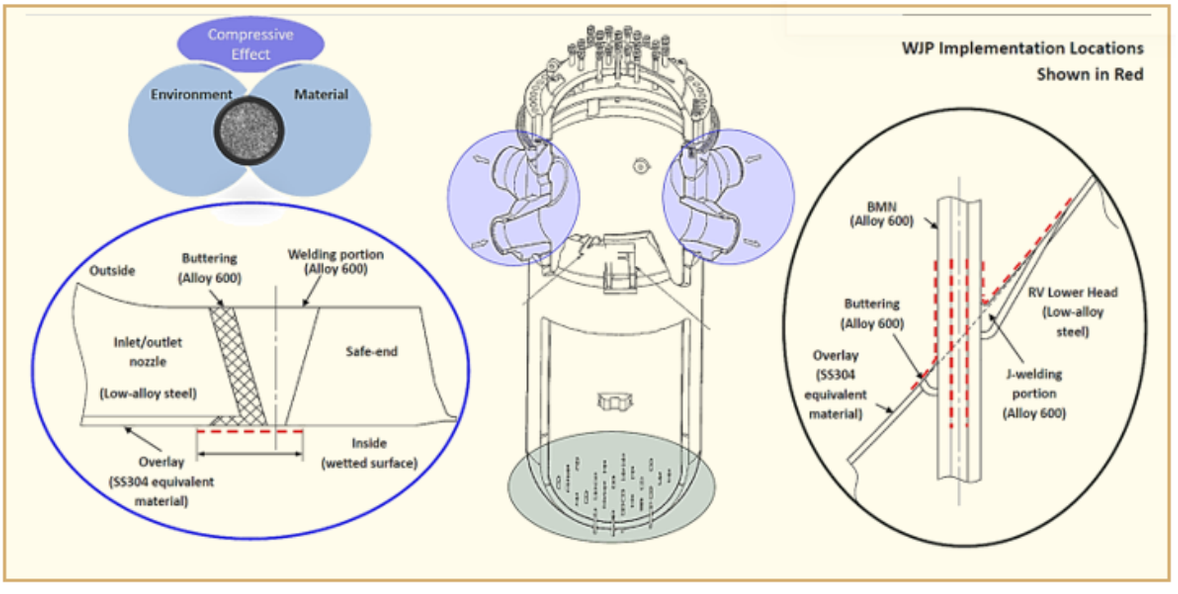

Figure 16-2: US needs for WPJ implementation [Martin, 2016].

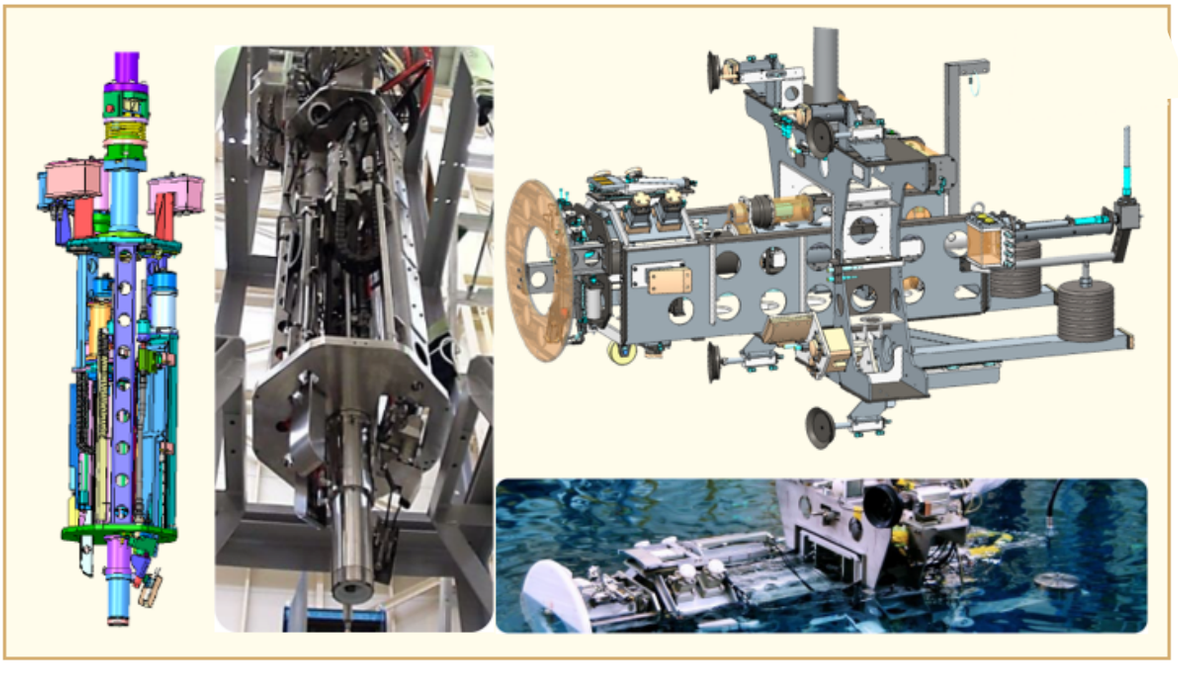

Figure 16-3: WJP tools developed for the US market. Left, vertical: BMN tool. Right, horizontal: RVN tool [Martin, 2016].

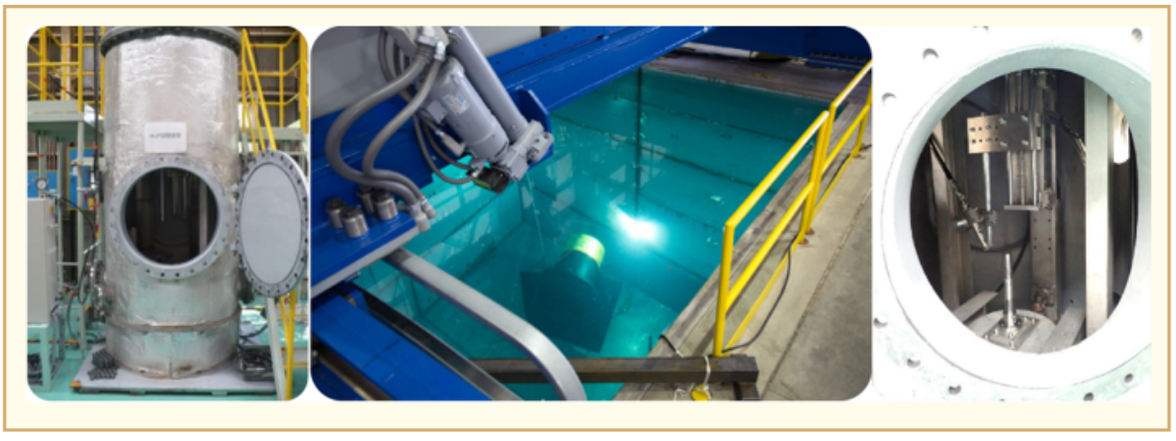

Figure 16-4: WJP training centre. Mock-ups of BMNs (left and right) and of RVN (centre) [Martin, 2016].

Figure 16-5: WJP equipment at the training centre [Martin, 2016].

The reference [Poling and Lanka, 2016] summarizes the process and tooling development AREVA has completed to apply the Ultra High Pressure Cavitation Peening process to Alloy 600 Reactor Vessel Head Penetration Nozzles, susceptible to PWSCC. Applying the UHP Cavitation Peening process to Alloy 600 components will stop PWSCC initiation and prevent future expensive repairs.

AREVA has completed an extensive corrosion testing, process parameter development and tooling qualification program for validation of the UHP Cavitation Peening Process. Results have demonstrated successful mitigation of PWSCC on target areas in simulated nuclear environments. Endurance testing has proven that the process can be applied in a cost-effective manner to prevent PWSCC, eliminate future repairs, reduce maintenance costs, and provide more effective on-time for the reactor.

Braidwood and Byron RPV heads are T-cold heads with the RPV head penetration nozzles fabricated using B&W tubular products. Inspections to date have identified the following flaws:

- Byron 2: two nozzles (spring 2007, fall 2014);
- Byron 1: four nozzles (spring 2011);
- Braidwood 1: one nozzle (spring 2012).

Each flaw has been repaired using an NRC approved embedded flaw overlay. To date, the inspection program has not detected cracking indications on the Braidwood 2 RPV head.

Before presenting the Byron 2 experience, let's have a look to the UHP cavitation peening technology.

Ultra-High Pressure Cavitation Peening, uses an ultra-high velocity jet which creates pressure below that of vapor pressure in water (Figure 16-6). Vapor bubbles form in water, it's cavitation. Then, shock waves occur from bubble collapse at surface generating high pressure on the material. These shock waves generate compressive stresses in the surface layer of material. The surface roughness is slightly increased by the UHP cavitation peening (Figure 16-7).

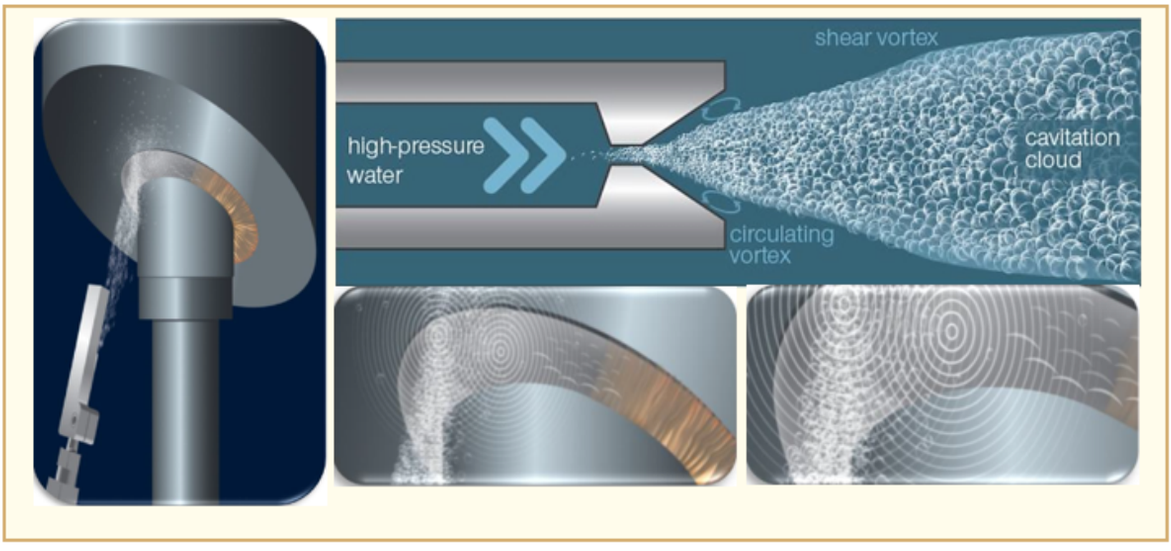

Figure 16-6: UHP cavitation peening technology [Poling and Lanka, 2016].

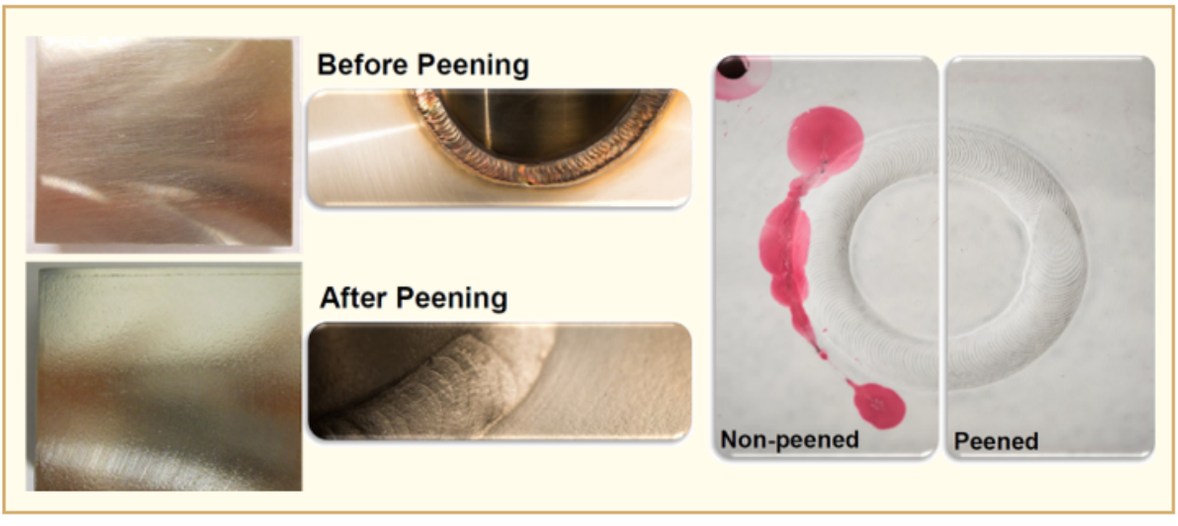

Figure 16-7: Impact of the UHP cavitation peening on the surface state [Poling and Lanka, 2016].

The Figure 16-8 shows the tools for the RV head peening of all OD surfaces. The OD peening tool has a "kickstand" to address vertical loads and opposing nozzle brackets to address horizontal loads. The Figure 16-9 shows the tool for the RV head peening of open penetrations IDs: nozzles without thermal sleeves (such as thermocouples, spare nozzles). There is a seal around the open penetration and flood up system. The Figure 16-10 shows the tool for RV head peening the ID annulus with thermal sleeves: the ID annulus is peened without removing or modifying the thermal sleeves.

17 Cast Austenitic Stainless Steel

The CF-grade cast austenitic stainless steels are used extensively in light water reactors for components with complex shapes because of their excellent mechanical properties and corrosion resistance. In contrast to a fully austenitic microstructure of wrought stainless steel, CASS alloys consist of a dual-phase microstructure of delta ferrite and austenite (Figure 17-1). The delta ferrite is critical for the soundness of castings, and can improve the strength and corrosion resistance of CASS alloys. However, the delta ferrite is also susceptible to thermal aging embrittlement due to its inherent instability at elevated temperatures. Consequently, the fracture resistance of CASS alloys can be reduced considerably after long-term exposure to reactor service temperatures.

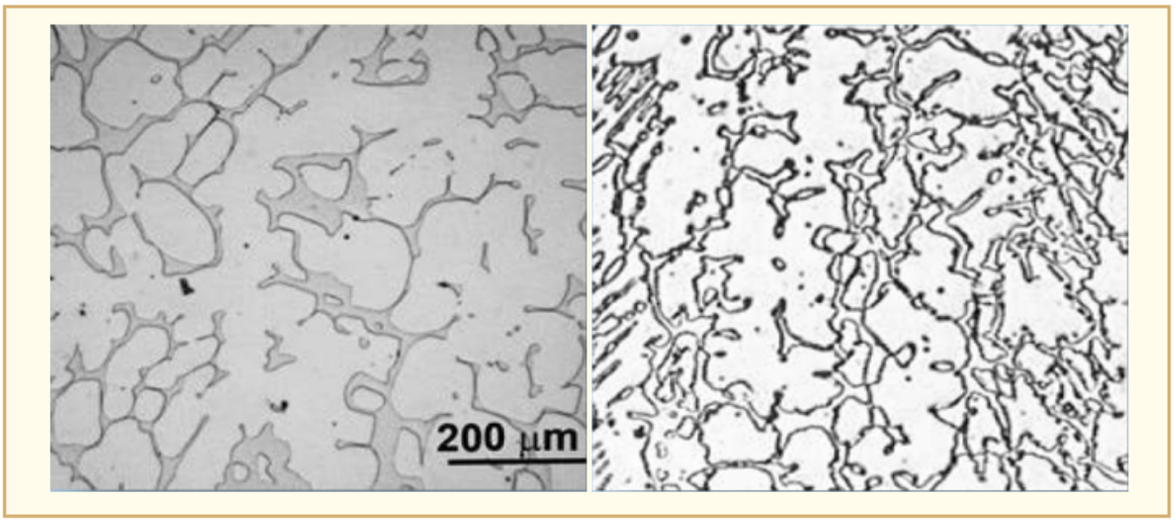

Figure 17-1: Left: CASS CF8 structure, right: weld structure [Rao et al., 2016].

To evaluate the cracking behaviour of CASS alloys used in reactor core internals, neutron-irradiated CASS specimens were tested in simulated light water reactor environments. While crack growth rate tests showed no strong effect on the stress corrosion cracking in low-corrosion-potential environments, fracture toughness J-R curve tests showed significant reductions in fracture toughness resulting from both thermal aging and neutron irradiation (Figure 17-2). The loss of fracture toughness due to neutron irradiation seemed more evident in the samples without prior thermal aging.

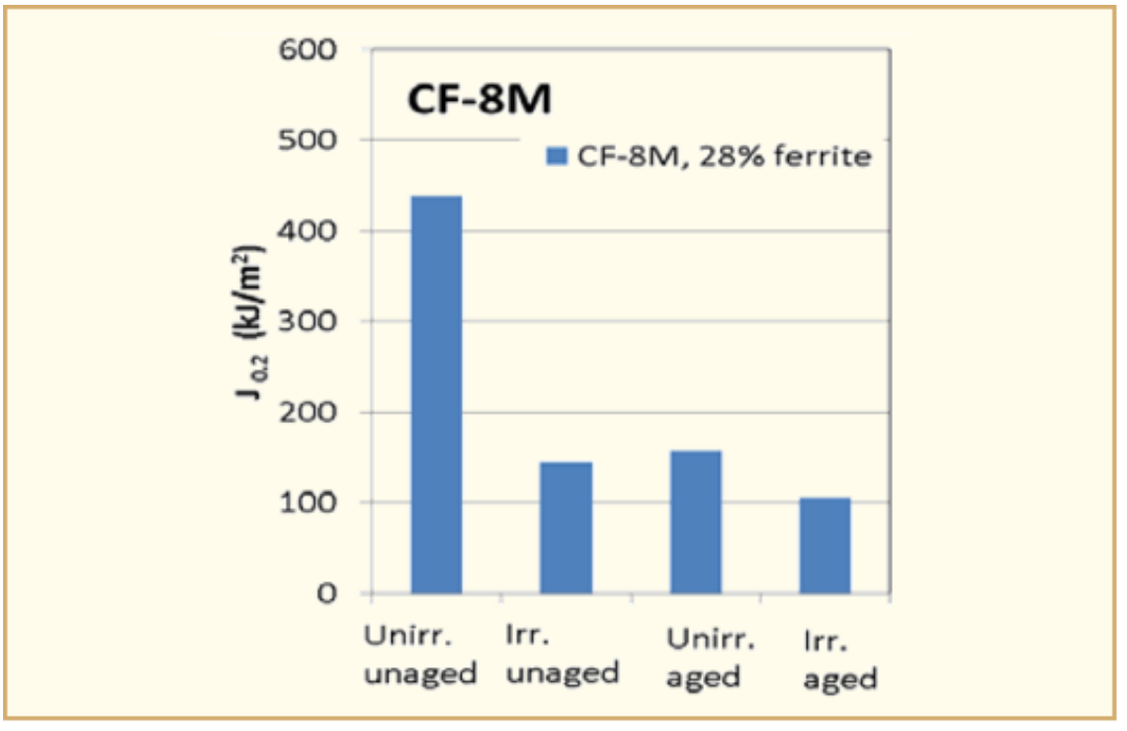

Figure 17-2: CF8-M fracture toughness. Both thermal aging and neutron irradiation can reduce the fracture toughness. The combination of thermal aging and irradiation reduces the fracture resistance further. The extent of irradiation-induced embrittlement is greater in the unaged specimens compared to the aged specimens [Rao et al., 2016].

Embrittlement of duplex stainless steels by thermal aging shortens the service life of structural components in light water reactors. This is an important issue when life extension programs are aiming at 60–80 years in service, as ductile failure is a design prerequisite. Aging is mainly attributed to two types of phase transformations occurring within the minor ferritic phase. Demixing of the ferrite by spinodal decomposition into Cr-rich α' and Fe-rich α regions as well as precipitation of secondary phases. At temperatures below 300°C the reduction of mechanical properties is significant, but the decomposition is limited, hence quantification and analysis of interaction between phenomena is difficult.

Materials studied here are from the PWR Ringhals 2 steam generator and exposed to primary circuit water for 70,000 at 291°C and 325°C, respectively, followed by 22,000 h at a reduced service temperature.

Charpy impact testing between -196°C and +400°C was made on the castings and connecting welds of 308 type (Figure 17-3). Large microstructural heterogeneity and anisotropy caused scatter in cast material and less in welds. A large effect of aging temperature was seen for cast material with 75°C drop in DBTT while welds showed only limited aging.

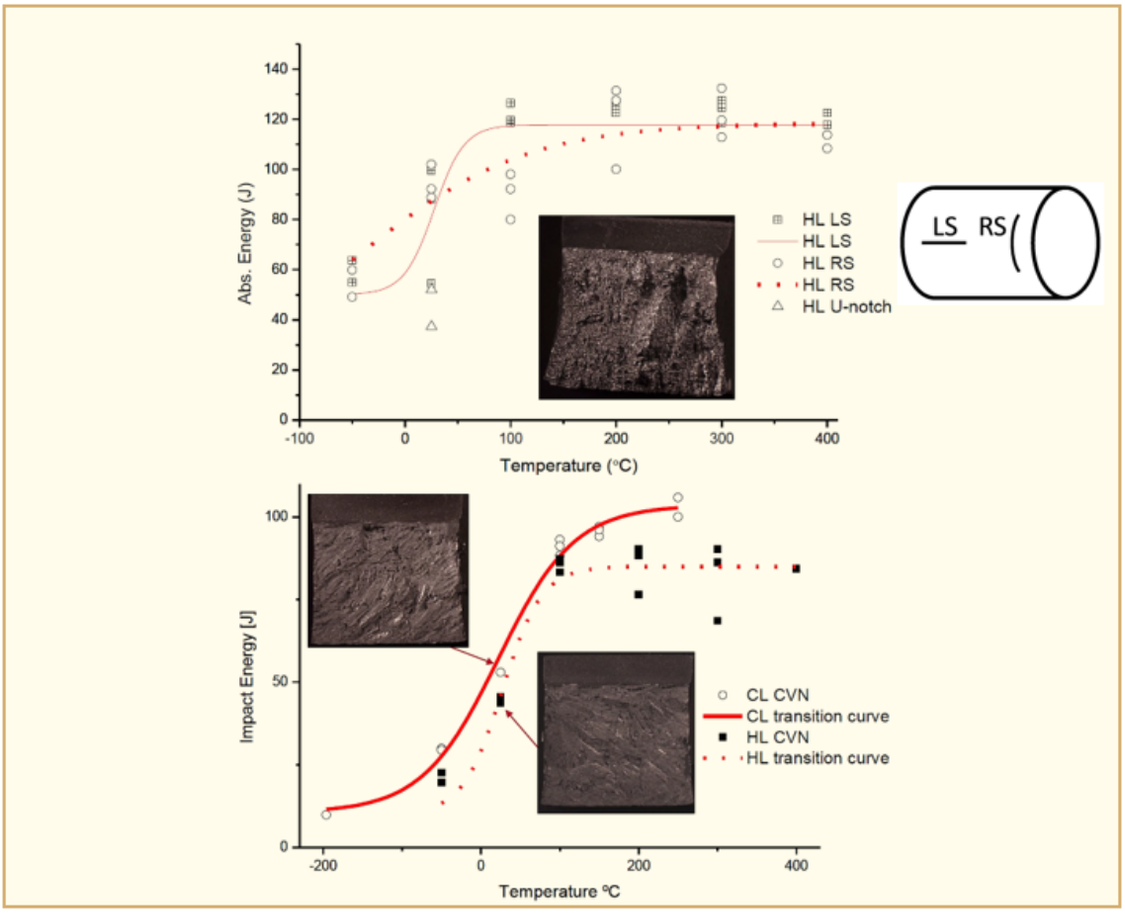

Figure 17-3: Results of impact testing Charpy-V. Top: hot leg elbow; bottom: weld. The hot leg elbow exhibits a large reduction in impact toughness from CL-state. There is a large scatter, especially in the RS direction. Note also the lower energies for U-notch specimens. The weld exhibits less scatter compared to cast material and a significant reduction in USE. There is only a small aging effect on the transition temperature [Bjurman et al., 2016].

TEM- and APT-analysis are made on in-service aged pipe bend castings of stainless steel quality CF8M. Using APT, spinodal decomposition and G-phase formation are measured in significant amounts in the 325°C and to a limited degree for the 291°C state. From analysis in TEM, no spinodal decomposition, G-phase or nano-size phase boundary or dislocation precipitates were found.

The reference [Ickes et al., 2016] lists all the reactor internals components made of CASS (see next page).

18 Thermal and Environmentally Assisted Fatigue

The current MRP Thermal Fatigue Guidelines (MRP-146 and MRP-192) require examinations to look for and report instances of craze cracking. Craze cracking is typically found as a semi-random pattern of shallow cracks that initiate on a component surface when that surface is exposed to repeated thermal shocks from relatively large changes in internal fluid temperatures. Craze cracking is also known in various industries as “mosaic cracking,” “elephant hide,” or “alligator hide”. Craze cracking is a generally tell-tale sign of thermal fatigue. Typically, craze cracks are not large enough to characterize using qualified examination methods, and seldom challenge component integrity. The component’s functional capability may not be significantly compromised until a primary crack emerges and grows. In cases where cyclic stresses resulting from thermal shocks may never penetrate the component material deeply enough to form a primary crack, component replacement may not be an appropriate response.

The Figure 18-1 shows one example of craze cracking observed in reactor vessel head control rod drive mechanism nozzles. This type of cracking has been identified at numerous units in U.S. and Europe. It was attributed to PWSCC. The flaws remained shallow (typically < 2 mm) and it was not associated with any known through-wall flaws that caused leakage.

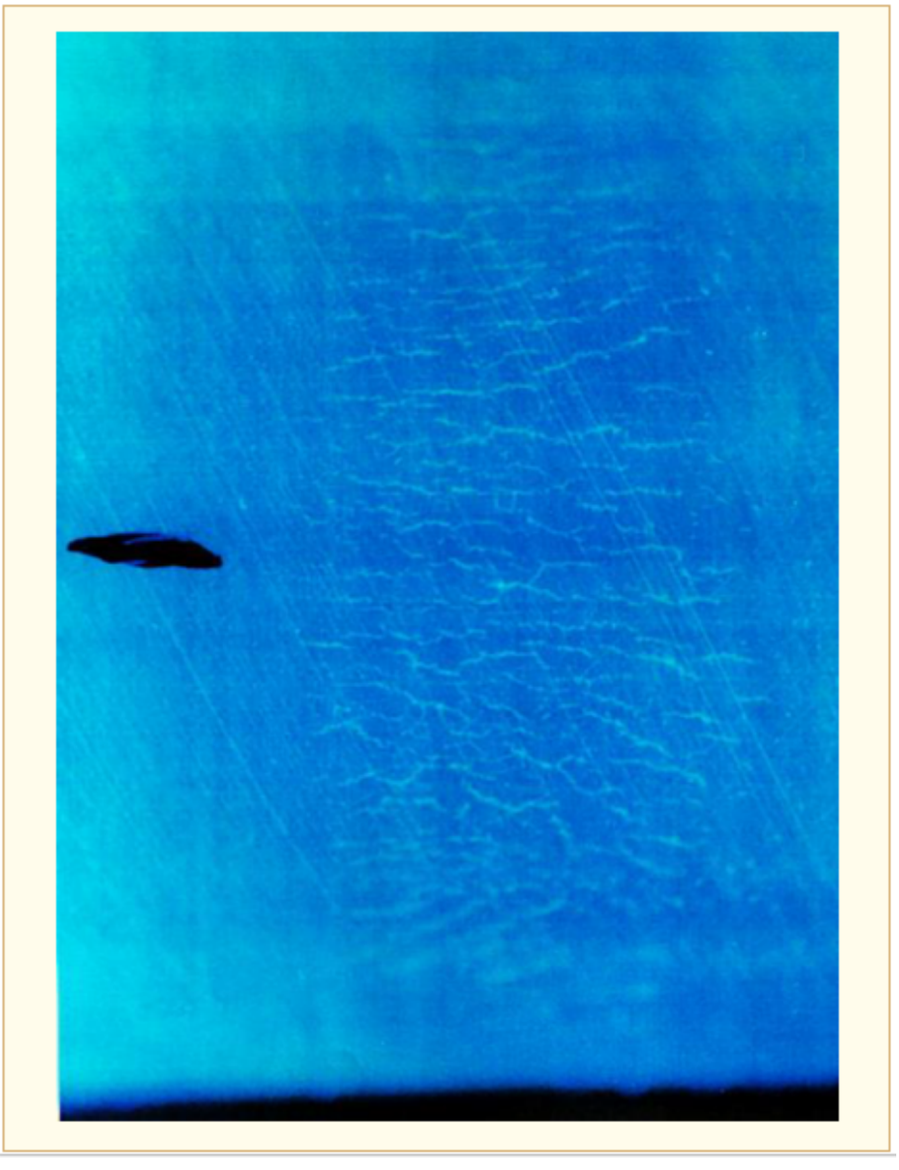

Figure 18-1: Fluorescent dye penetrant results of Ringhals Unit 2 CRDM Nozzle [Fyfitch et al., 2016].

S. Taheri and others evaluated thermal fatigue craze cracking observed in residual heat removal systems of French 900 and 1300 MWe units. They also provide explanation of differences between high cycle thermomechanical and mechanical fatigue which are related to difference between spatial stress gradients:

- Stress gradients are higher near inner surface and negligible farther away for high frequency thermal loading whereas
- Craze crack arrest is explained as a result of a decreasing stress intensity factor reaching a threshold level.

The Figure 18-2 presents a craze cracking example observed in French RHR system piping. The operating temperature ranges between 20 and 300°C and the temperature variation was around 140°C. A qualitative determination of fatigue life lead to crack arrest at 2.5 mm deep for RHR piping in French 1300 MWe units. One interesting finding is that the crack arrest depth is deeper for a thin tube than for a thick tube.

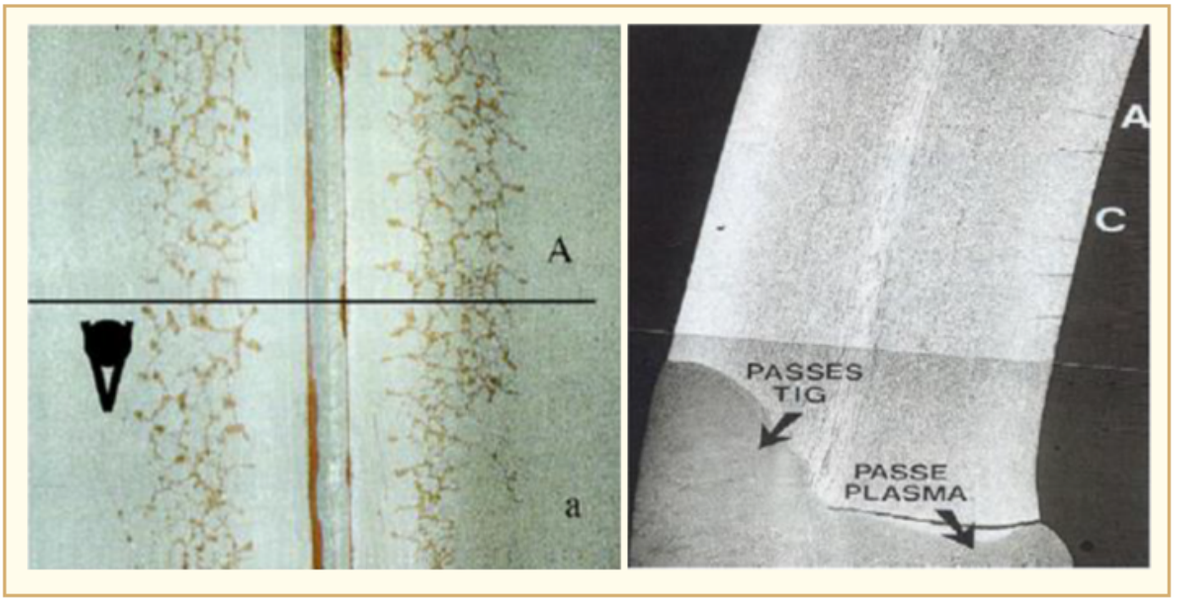

Figure 18-2: Left: craze cracking on a French residual heat removal pipe inner surface. Right: crack depth observed in the crazing at (a) [Fyfitch et al., 2016].

Evaluations performed by Japanese, in response to thermal fatigue operating experience, observed that if relatively high frequency fluid temperature fluctuation sinusoidal waveform exists, the possibility of crack arrest occurs at less than 10 Hz (Figure 18-3). On contrary though, for cases where cracking propagates through-wall, the waveform deduced to be trapezoidal shape and the crack arrest frequency is found relatively low. Results show that crack could initiate at fluid temperature range of more than 120 K (i.e., 120C°) regardless of the magnitude of the membrane constraint. Also, growth of initiated crack would be difficult to stop.

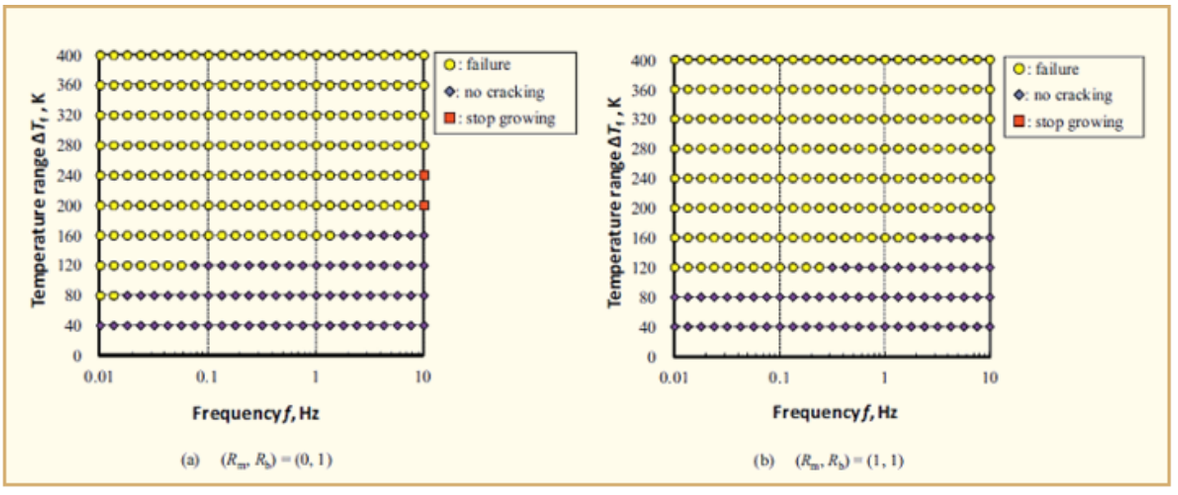

Figure 18-3: Calculated fluid temperature and frequency conditions for failure, crack arrest, and no cracking (trapezoidal temperature fluctuation) [Fyfitch et al., 2016].

The Figure 18-4 shows the test sample used by Jones et al to perform thermal fatigue testing and analyses of stainless steel pipes. The purpose was to provide data for improvements in analytical methods and ASME Code fatigue curves. The water chemistry was controlled to very low dissolved oxygen content, consistent with PWR specifications. At periodic intervals, the testing was interrupted to ultrasonically inspect for the presence of cracking.

Thermal cycling tests were performed as follows:

- Pipes pressurized to 17.2 MPa and temperature cycled between 38°C and 343°C in three seconds;
- Followed by holding at 343°C for 237 seconds and then quenching to 38°C in three seconds and then
- Followed by another 237 second hold time.

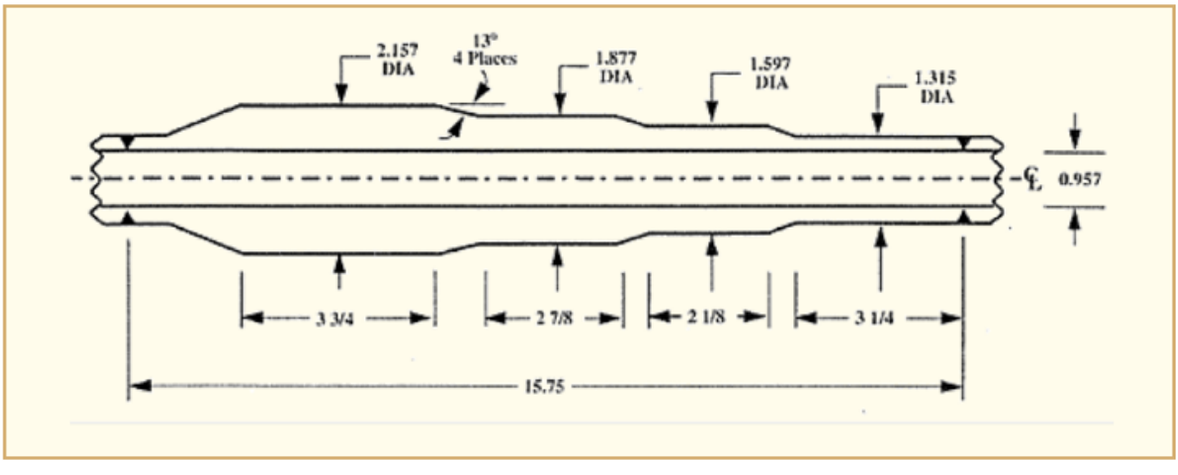

Figure 18-4: ASME code fatigue study; type 304 stainless steel test sample (dimensions in inches) [Fyfitch et al., 2016].

The results show the presence of craze cracking at all the circumferential locations in two thickest sections with no preferred orientation (Figure 18-5). No cracking was observed in the two thinner sections. This cracking supports the assumption that the initial cracking was due to local peak thermal stress on the pipe inner wall.

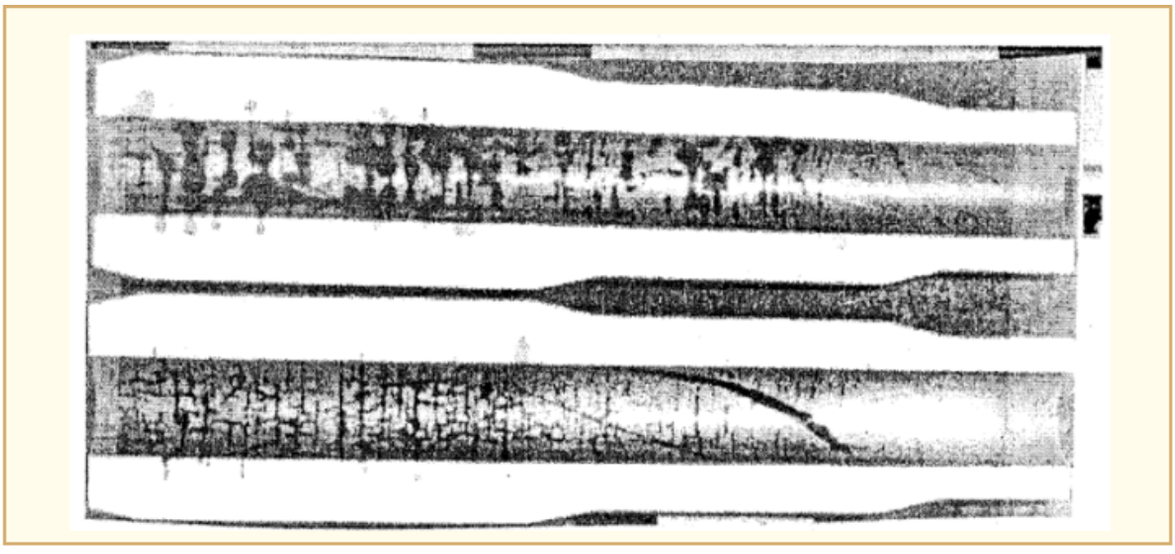

Figure 18-5: ASME code fatigue study: liquid penetrant inspections for the type 304 stainless steel pipe test specimens [Fyfitch et al., 2016].

The report MRP-23, Revision 1 (Figure 18-6) provides guidance for thermal fatigue inspections to support the implementation of NEI 03-08 requirements.

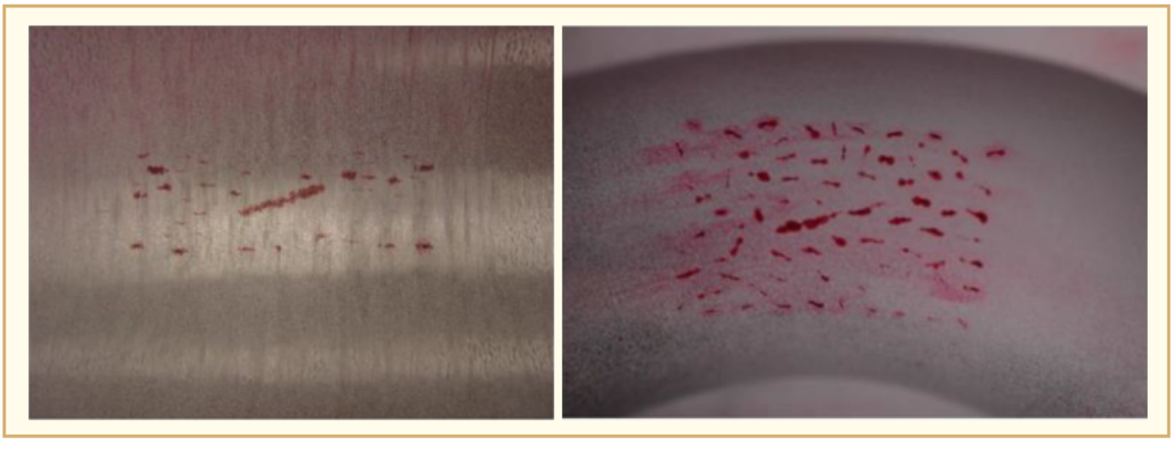

Figure 18-6: Left: dye penetrant photograph of typical pipe crazing and crack patch. Right: dye penetrant photograph of typical elbow crazing and crack patch [Fyfitch et al., 2016].

In summary, the key drivers for craze cracking are:

- The material surface characteristics: surface finish (roughness) and cold-work (e.g., resulting from grinding, damage from a loose part, or shot peening);
- Metallurgical features (e.g., grain size tends to influence cyclic plasticity and fatigue crack initiation);
- Material cracking susceptibility (e.g., Alloy 600 is susceptible to PWSCC);
- Mixing of hot and cold fluids;
- Stratification of fluids with sufficiently high temperature changes (ΔT) capable of exceeding the yield strength of the material;
- Thermal cycles exceeding the fatigue endurance limit of the material in the environment of concern (i.e., PWR water conditions);

19 Welding Techniques & Residual Stress Modelling

EPRI and NRC recently concluded a collaborative research program, conducted under a Memorandum of Understanding, on weld residual stress prediction (Figure 19-1).

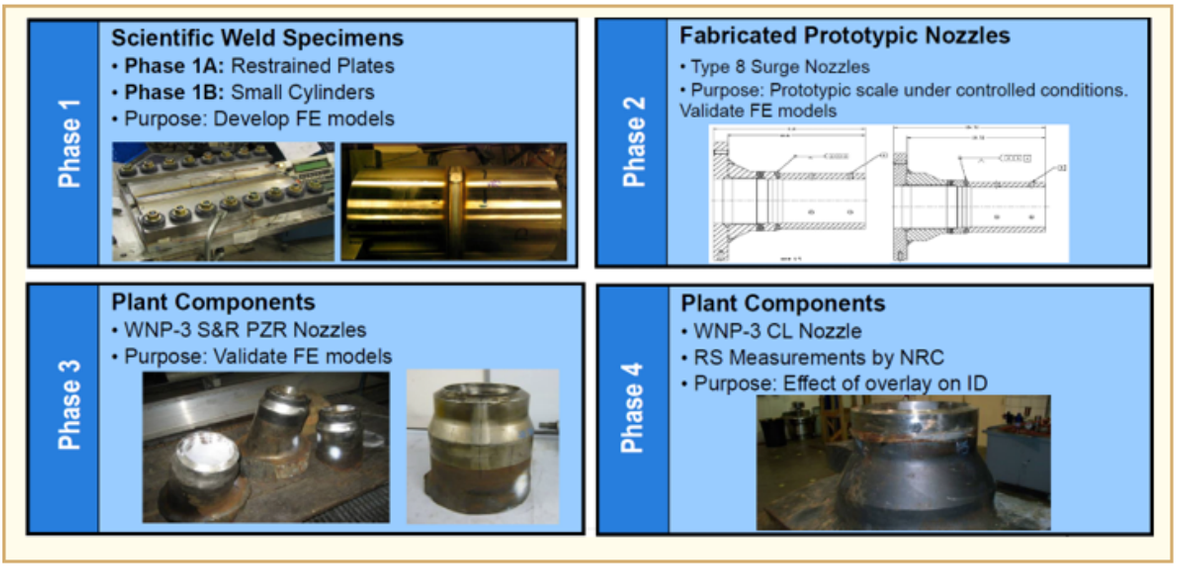

Figure 19-1: Four phases of the 4-year program under MoU with EPRI which ended in December 2015 [Benson and Homiack, 2016].

here was a reasonable agreement on average between measurements and models (Figure 19-2). There was a significant scatter about the average. However, there was a need for a future work: improving, characterizing and understanding the prediction uncertainty.

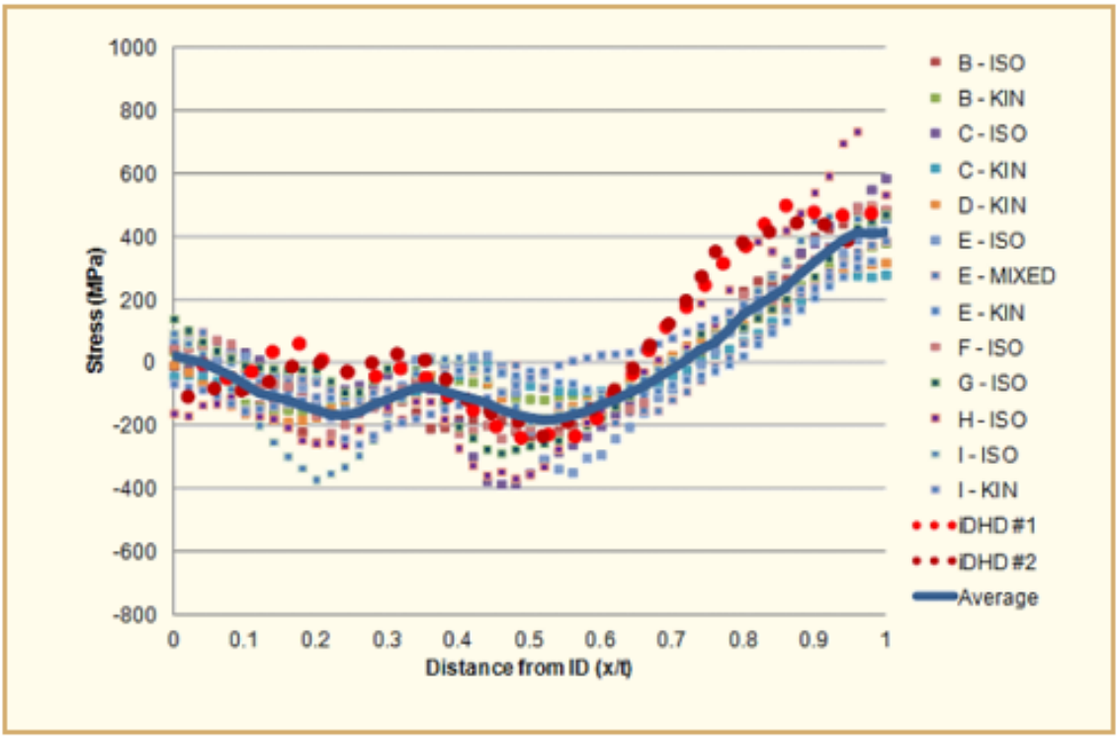

Figure 19-2: WRS phase 2a results [Benson and Homiack, 2016].

The latest data set from the program consisted of measurement and modelling data from a round robin study on a full-scale pressurizer surge nozzle mock-up (Figure 19-3). Characterizing and quantifying uncertainty in this data set has proven challenging, with only simplistic procedures employed to date. In the reference [Benson and Homiack, 2016], the NRC presents a more robust method to quantifying uncertainty in both the measurement and modelling data. This reference provides an overview of the mathematical approach to uncertainty characterization and discuss results of the analysis, if available.

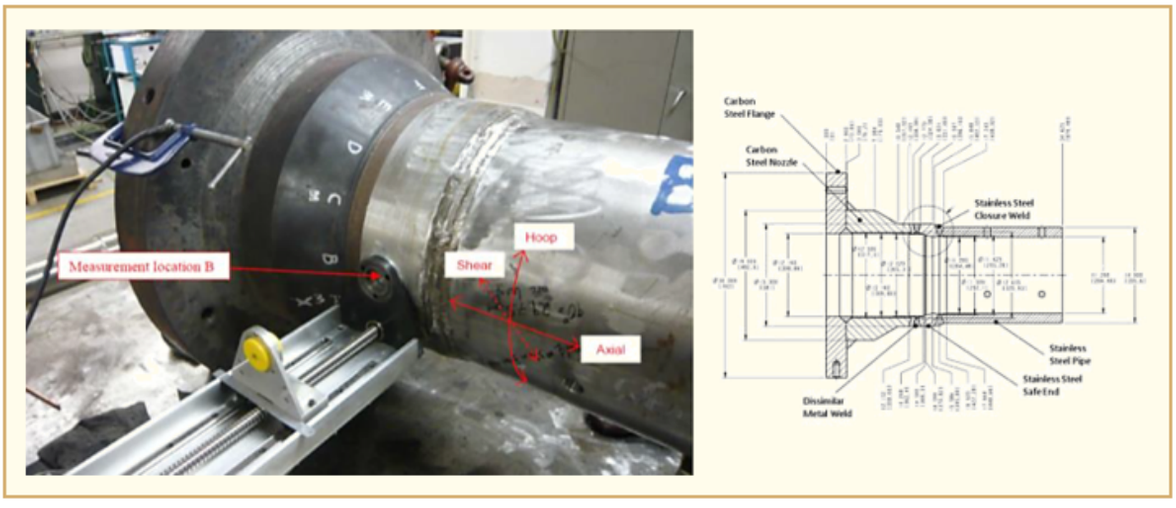

Figure 19-3: Hole drilling and contour measurements in the second pressurizer surge line mock-up [Benson and Homiack, 2016].

Material degradation mechanisms place a significant burden on nuclear power plants, and they are typically managed in a "reactive" manner through chemistry control, targeted inspection frequency, and ultimately repair/replacement. EPRI has developed a methodology for proactively managing material degradation through the manipulation and control of residual stresses in the material [Stover, 2016]. This approach highlights the highest-risk locations and provides guidance on available mitigation technologies to facilitate the procurement and fabrication of components with significantly reduced risk of long-term degradation. This methodology can be used as a strategic tool during the construction of new nuclear plants to assess when and where stress mitigation techniques will provide significant value for long term asset management over the life of an advanced light water reactor. Additionally, EPRI has initiated a project to add to and develop existing WRS knowledge with the fabrication, numerical modelling, and WRS measurement of a SMR, nozzle mock-up (Figure 19-4).

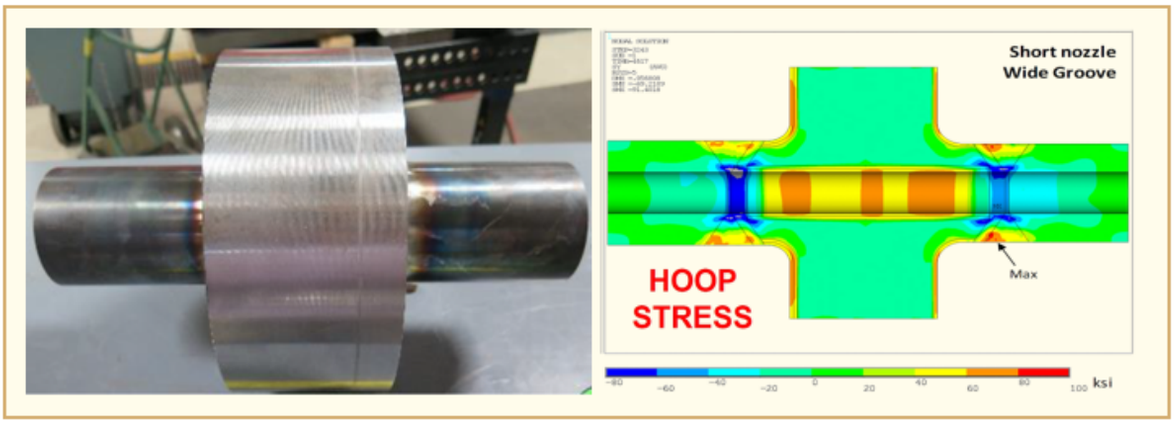

Figure 19-4: SMR nozzle mock-up [Stover, 2016].

Residual stresses imparted by the welding process are a principal factor in the primary water stress corrosion cracking of Alloy 82/182 nickel-alloy dissimilar metal piping butt welds in pressurized water reactors. Numerical methods by finite element analyses are frequently used to simulate the welding

process in order to predict the residual stress distribution in the weld and base material as an input to crack growth calculations. The crack growth calculations, in turn, have demonstrated a high sensitivity to the welding residual stress distribution inputs. As part of the industry's proactive approach to addressing materials degradation, a project has been implemented to validate the analytical models used to perform welding residual stress analysis against measured residual stresses. This project addresses the lack of stress measurements for prototypical PWR nozzle dissimilar metal weld configurations to validate the stress models routinely applied in the analysis of PWSCC of PWR Alloy 82/182 piping butt welds.

The reference [Broussard and Crooker, 2016] summarizes work that has been performed to further develop methods that improve confidence in welding residual stress analysis results. Multiple tasks were performed in support of this objective, including residual stress modelling, laboratory experiments, residual stress measurement technology development, and data analysis. This reference also summarizes welding residual stress analysis and modelling guidance that has been developed over the course of these efforts. The results of these tasks have been issued as MRP-316, Rev. 1 (EPRI 3002005498) and MRP-317, Rev. 1 (EPRI 3002005499).

In the reference [Yonezawa et al., 2016], hot cracking susceptibility on 18 laboratory heats of 30% Cr - Ni based alloys was studied by longi-Varestraint test (Figure 19-5), on-heating (Figure 19-6) and on-cooling (Figure 19-7) hot ductility test, and fissure-bent test (Figure 19-8). Hot cracking susceptibility of the 18 laboratory heats based on the longi-Varestraint and on-heating and on-cooling hot ductility test did not correspond to that of fissure-bent test. Hot cracking susceptibility based on the longi-Varestraint test and on-heating and on-cooling hot ductility test was improved by degreasing of C, P, S, Si, Nb, Ti, Al contents (Figure 19-9). The hot cracking susceptibility based on the fissure-bent test was not improved by degreasing of C, P, S, Si, Nb, Ti, Al contents, and improved by the addition of C and Nb content.

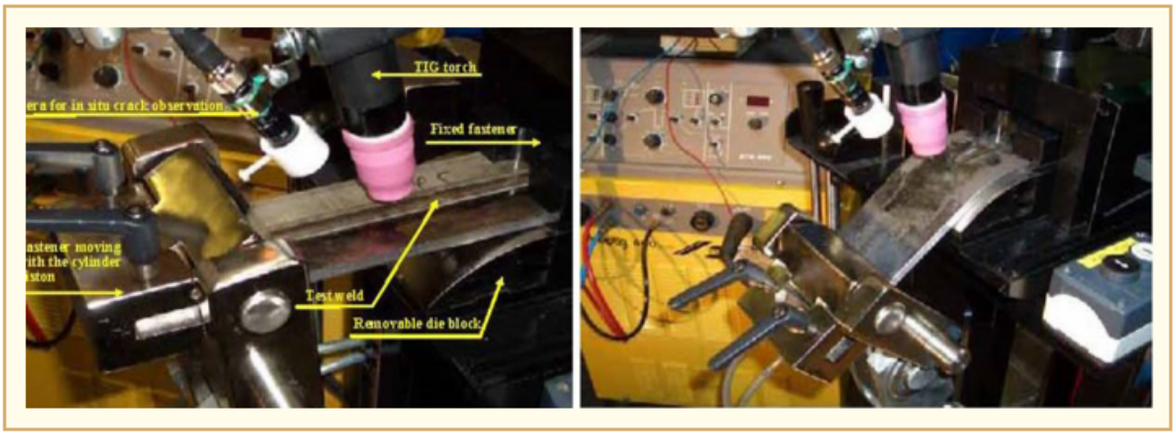

Figure 19-5: Longi-Varestraint test [Yonezawa et al., 2016].

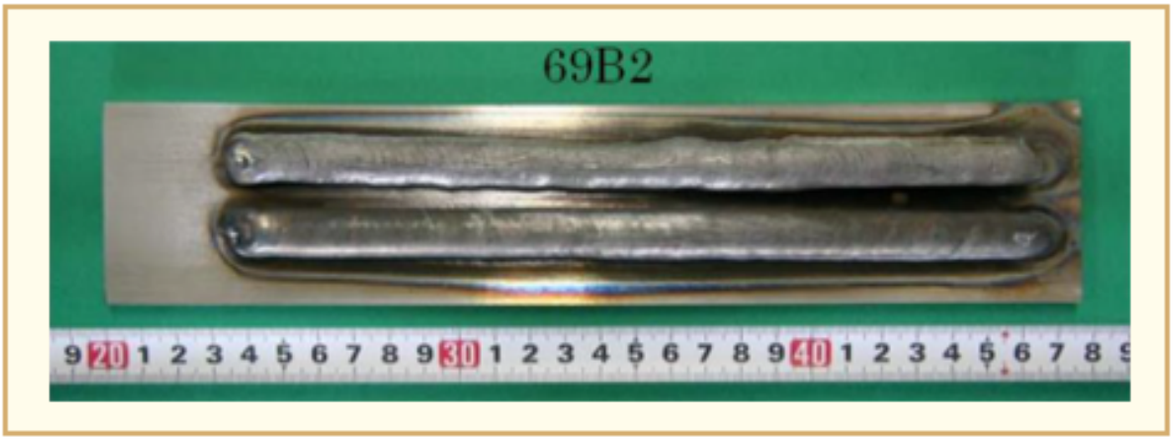

Figure 19-6: On-heating hot ductility test: 1) in vacuum or Ar gas, 2) heating up to target temp. by 110°C/sec, 3) hold temp. during 10 min, 4) tensile test under 5 mm/sec, 5) measure the rupture load & reduction of area [Yonezawa et al., 2016].

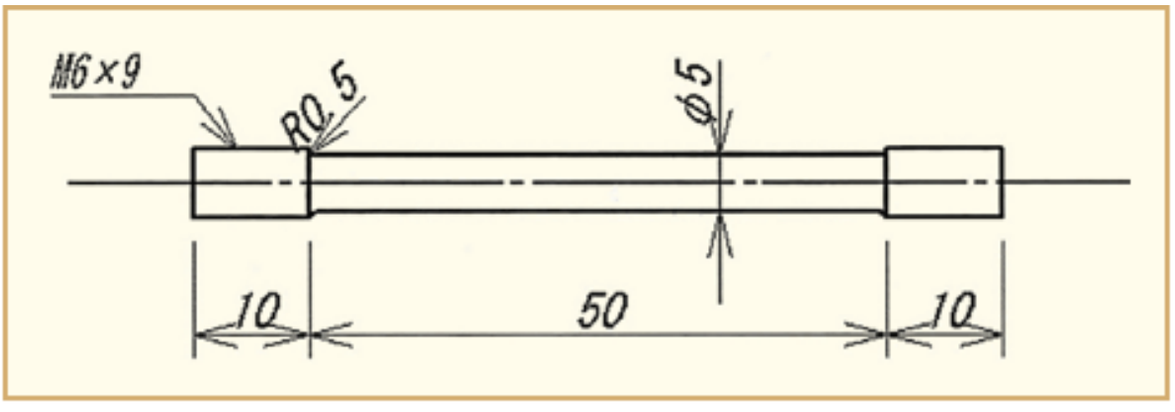

Figure 19-7: On-cooling hot ductility test: 1) in vacuum or Ar gas, 3) heating up to 1300°C by 110°C/sec, 3) hold temp. during 10 min, 4) cooling to target temp. by 50°C/sec, 5) hold temp. during 60 sec, 6) tensile test under 5 mm/sec, 7) measure the rupture load & reduction of area [Yonezawa et al., 2016].

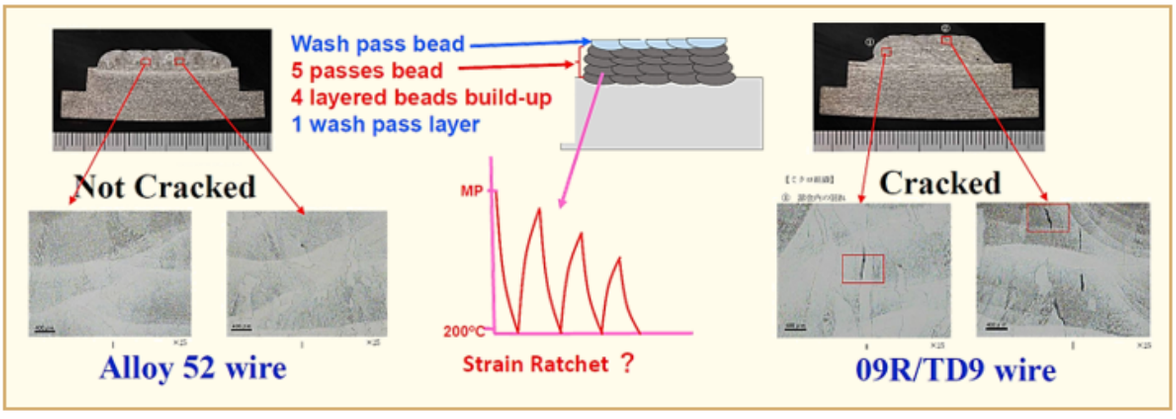

Figure 19-8: Microscopy of the cross-sections for five passes four layered beads build-up & wash bead (FPFLB) test specimens using commercial Alloy 52 and lab. melt 09R/TD9 wires [Yonezawa et al., 2016].

20 Operational Experience & Plant Component Research

Austenitic stainless steels are extensively used in reactor component technology. Although well characterized from many aspects, their irradiation behaviour is not fully represented neither understood, in particular fracture toughness. The number of variables including material and irradiation ones are multiple and do not allow investigations focused on individual effects.

Therefore, we irradiated 316L in the high flux BR2 reactor at about 290°C to different neutron dose levels with the aim to measure fracture toughness and tensile properties in order to investigate the irradiation hardening-to-embrittlement correlation. In other words, the objective is to determine whether the measured embrittlement is due to the irradiation hardening alone or not. Moreover, the experimental results obtained in the reference [Chaouadi et al., 2016b] are compared to other existing data to rationalize all the observations and improve radiation damage understanding.

The damage rate increases significantly in the low neutron dose range (<1 dpa) (Figure 20-1).

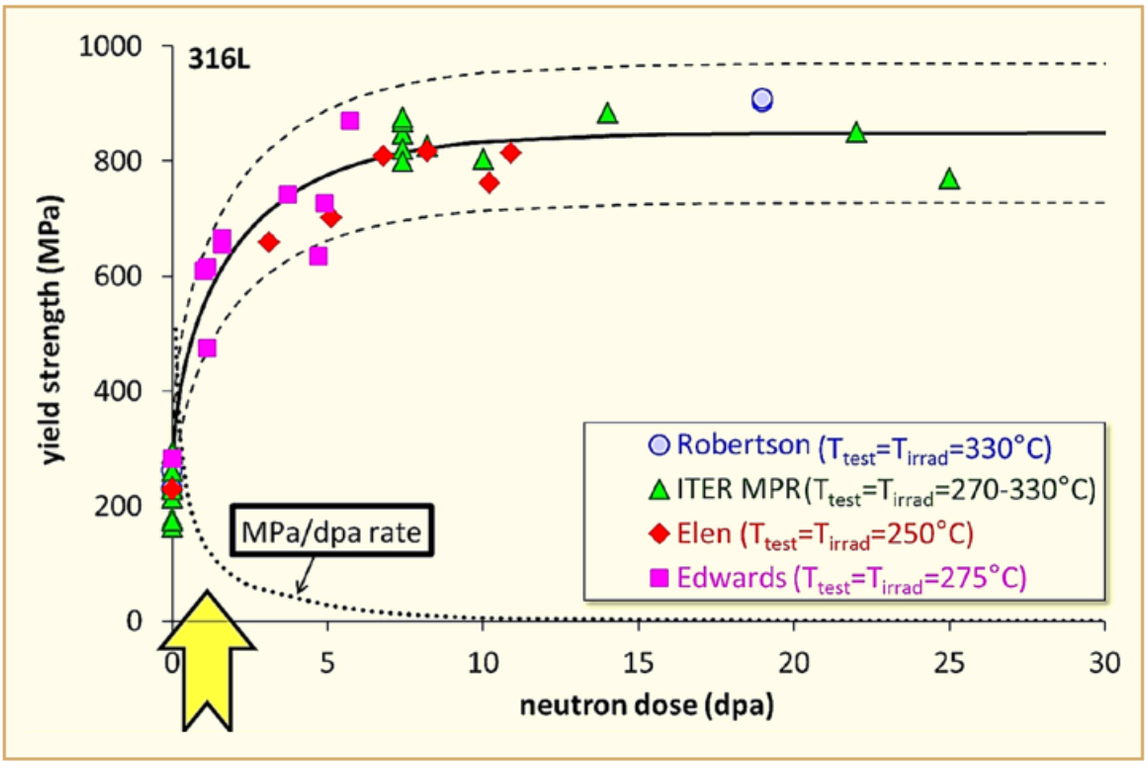

Figure 20-1: Irradiation hardening of 316L. More significant effects observed in the low dpa range, in particular 0 – 1 dpa [Chaouadi et al., 2016b].

Despite the significant changes of the tensile properties (strength (Figure 20-2) and ductility (Figure 20-3)) in the low dpa range, fracture behaviour remains almost unaffected (Figure 20-4).

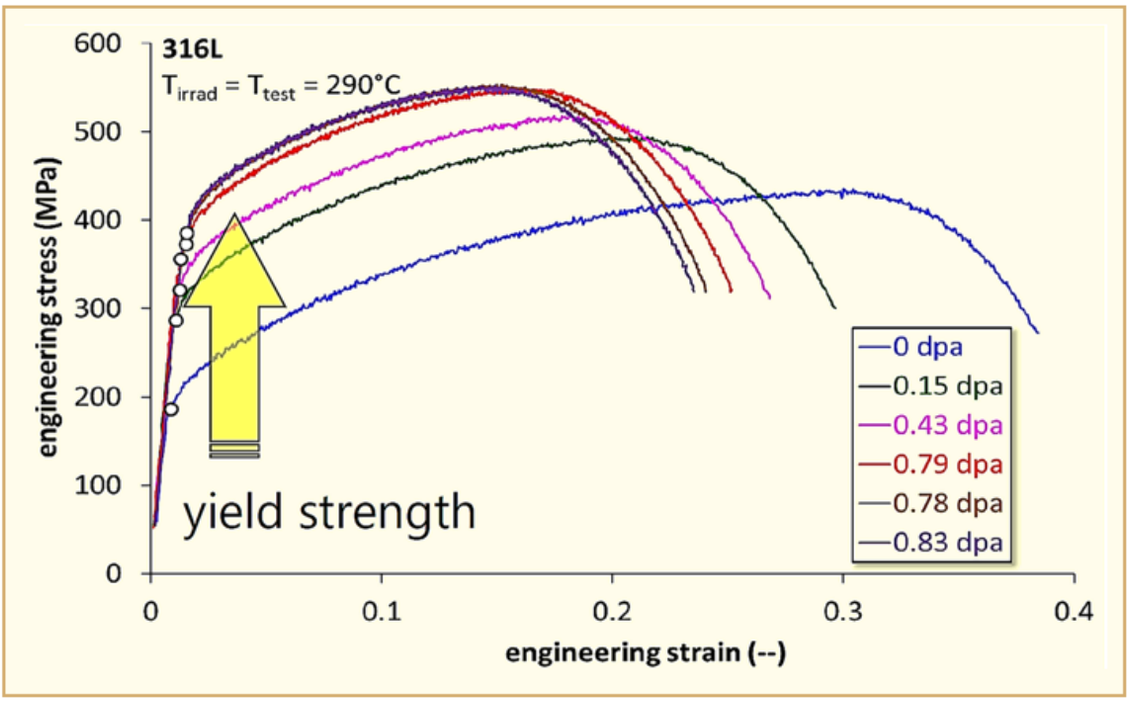

Figure 20-2: Tensile test results. Irradiation has a significant effect on the tensile curve [Chaouadi et al., 2016b].

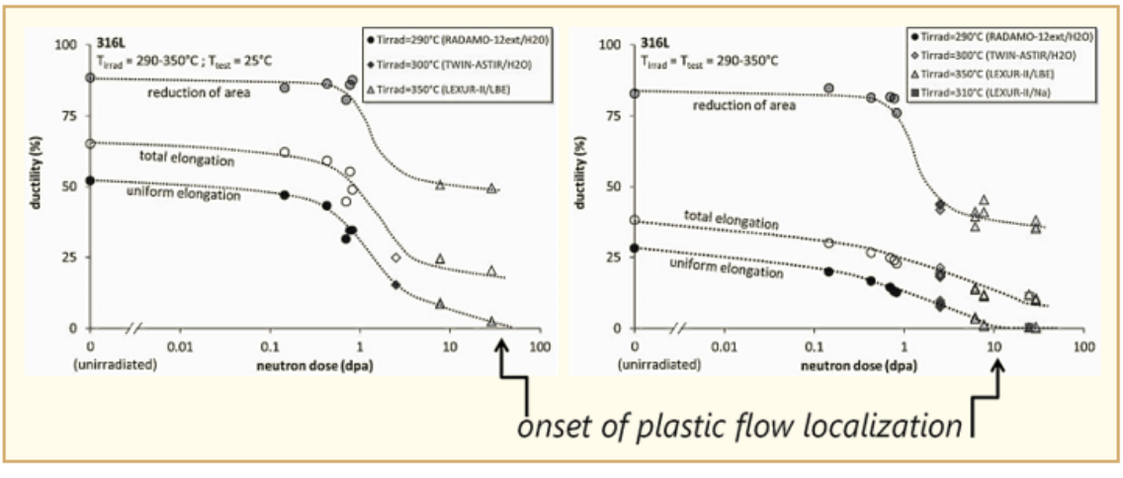

Figure 20-3: Tensile test results. Ductility [Chaouadi et al., 2016b].

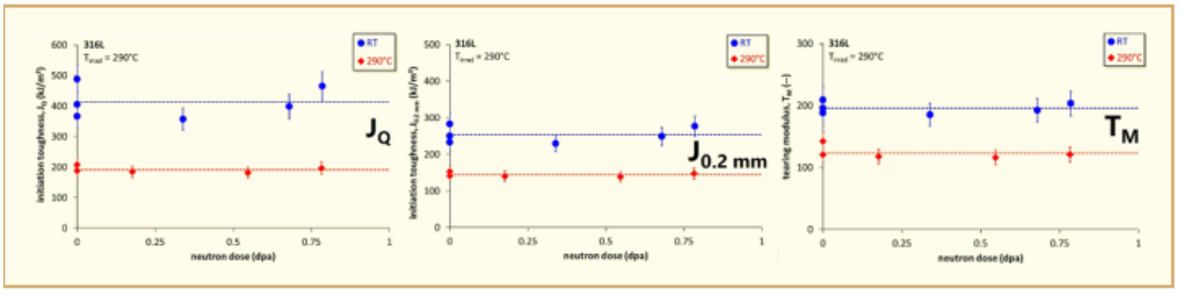

Figure 20-4: Crack resistance test results. No significant effect on initiation toughness (J_Q and $J_{0.2}$ mm) and tearing resistance (T_M) [Chaouadi et al., 2016b].

Fracture surface examination by SEM shows very similar dimple structure (Figure 20-5). The ductility loss is compensated by a strength increase leading to a nearly constant critical void growth rate.

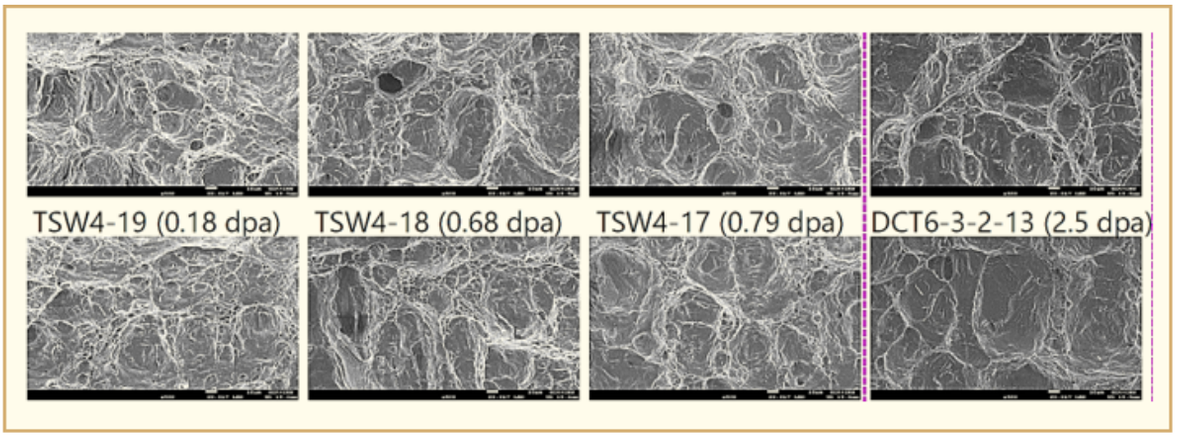

Figure 20-5: SEM examination of the fracture surfaces. No significant effect of irradiation on dimple size suggesting a constant critical void growth rate [Chaouadi et al., 2016b].

BWR components are primarily made of 304L / 316L SS and 308L weld metal, Alloy 600 / 600M and Alloy 82 weld metal & Alloy X-750. Alloy 690, and Alloys 718 and 725 are also considered. Zircaloy-2 is used for fuel cladding, & Aluminum for inspection tooling. The traditional 'subtractive' manufacturing is slow and wasteful whereas powder metallurgy and hot isostatic pressing can create near-net-shape parts with unique properties. Also, additive manufacturing can produce finished parts in complex shapes with very desirable properties. To select a new material, key elements include cost, supply chain, properties, ASME code cases.

The reference [Andresen et al., 2016] presents an experimental SCC Program which aims at evaluating powder metallurgy for alloy 316L SS and Alloy 600M. Are also evaluated in separate tasks:

- Microstructure characterization;
- Tensile properties and
- Charpy fracture toughness.

Two heats of PM 316L and one heat of PM 600M were evaluated in high temperature BWR and PWR water:

- 20% cold worked PM responded similar to wrought material;
- Weld HAZ aligned PM responded similar to wrought material and
- As-received PM exhibited somewhat higher CGRs than wrought material, but not high.

Most reactors in the United States and other countries are expected to continue operation beyond their original 40-year operating license. It is possible that many of these reactors will extend their operation to as many as 80 years and this extended operation will be very demanding on many of the internal structural components and fasteners near the reactor core.

EPRI in collaboration with the Department of Energy and Bechtel Marine Propulsion Co. has initiated the ARRM Program with the objective of developing and testing the next generation of optimized commercial alloys and advanced materials for LWR internals. Clearly considerable testing and screening is needed before a commercial material is qualified or a new advanced alloy developed. Both alloy development processes are relying heavily on ion irradiation experiments during the screening phases prior to neutron irradiations in order to evaluate the maximum number of alloy compositions in the minimum amount of time and cost.

The University of Michigan has characterized the response of selected materials to proton and heavy ion irradiations as well as resistance to irradiation assisted stress corrosion cracking. Proton irradiations have been carried out to 5 dpa for all candidate alloys and to 15 dpa for alloys that show resistance to IASCC in the 5 dpa tests. Heavy ion irradiations have been carried out to at least 150 dpa to investigate the swelling characteristics of an alloy. The reference [Wang et al., 2016] describes the results of proton irradiation and resulting CERT tests, heavy ion irradiations, and microstructural investigations obtained for a range of potential replacement alloys.

The ARRM program started from the graphs of Figure 20-6 and Figure 20-7.

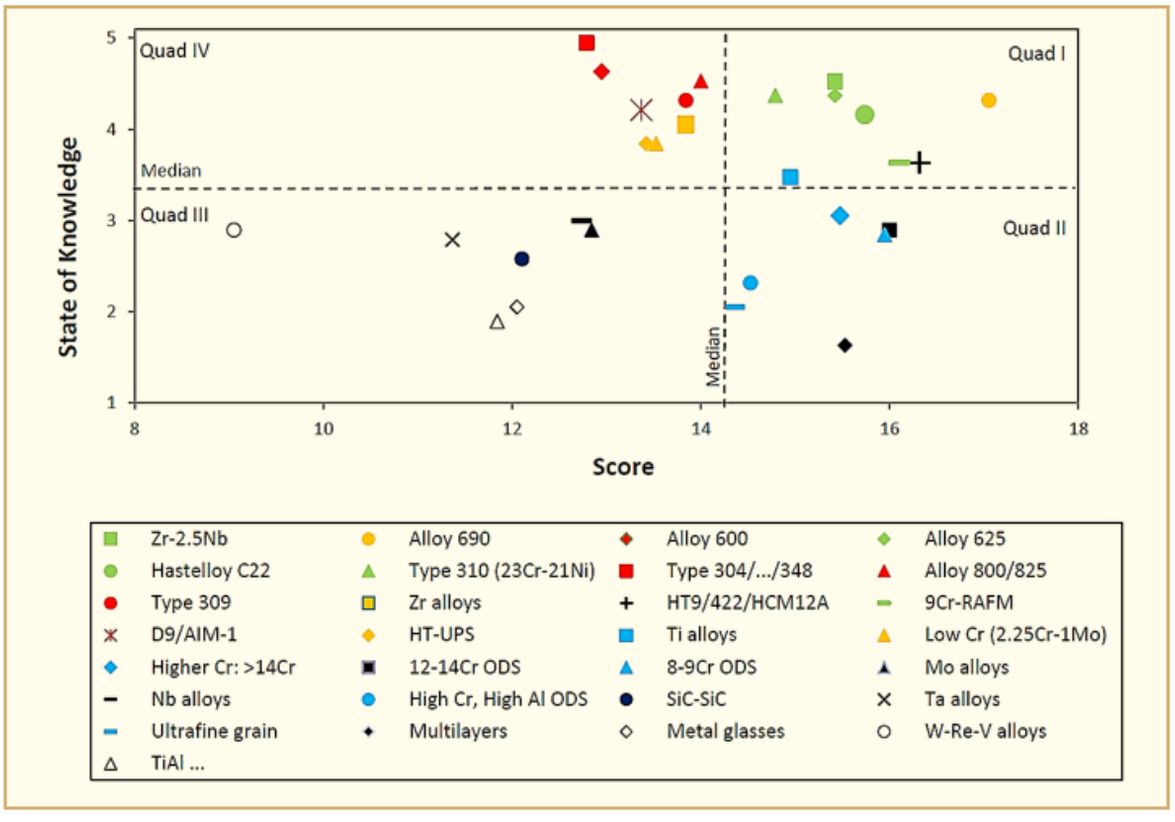

Figure 20-6: Alloy score vs. state of knowledge for low-strength component alloys [Wang et al., 2016].

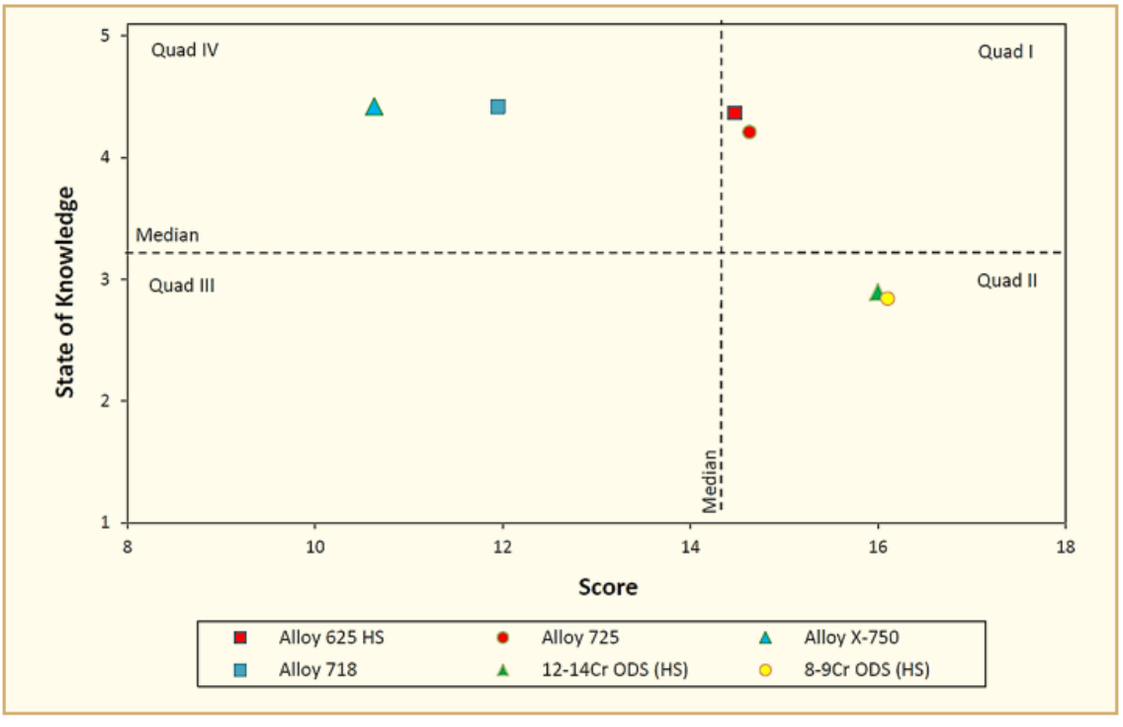

Figure 20-7: Alloy score vs. state of knowledge for high-strength component alloys [Wang et al., 2016].

Based on these figures, the following alloys have been selected (Figure 20-8):

- For low strength applications: 316L, Alloy 625, Alloy 690, Alloy 800, Alloy 310, Zr-2.5Nb, Grade 92 (9 Cr ferritic-martensitic steel) and HT9 (12 Cr ferritic-martensitic steel);
- For high strength applications: Alloy X-750, Alloy 625 plus, Alloy 625 Direct Age, Alloy 725, Alloy 718, 14YWT (14Cr oxide-dispersion-strengthened alloy) and Alloy 439 (18Cr ferritic stainless steel).

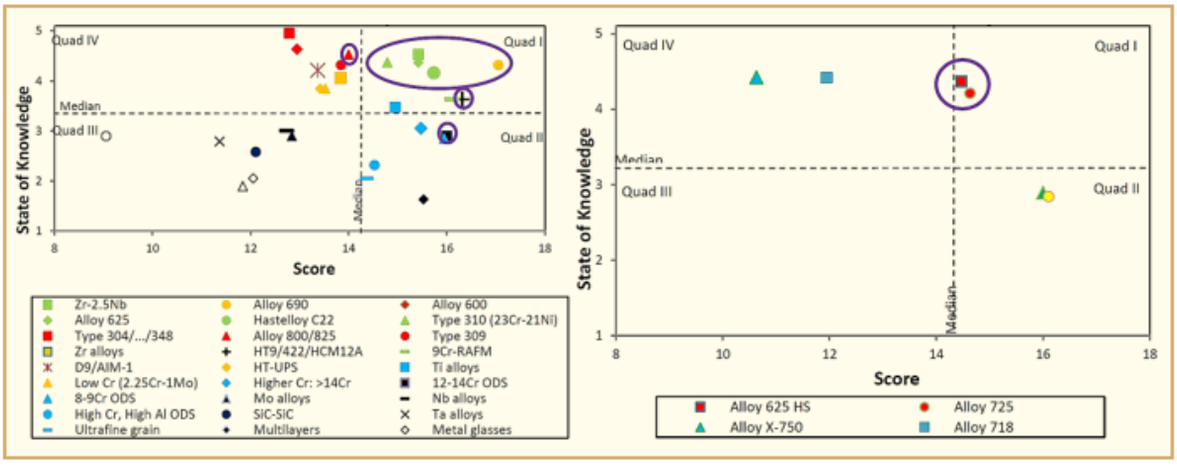

Figure 20-8: Candidate alloys. Left: low-strength alloys. Right: high-strength alloys [Wang et al., 2016].

Alloy 725 has the lowest IASCC susceptibility among all the nickel-base alloys tested in both BWR-NWC (Figure 20-9) and PWR primary water (Figure 20-10) environments.

Alloy 625DA has the highest IASCC susceptibility in both BWR NWC (Figure 20-9) and PWR primary water (Figure 20-10) environments.

21 Steam Generator

As part of a recent effort to model the probability of SG tube rupture as a function of primary-to-secondary side leak rate, material property distributions were developed for several common SG tube materials, including Alloy 600MA, Alloy 600TT, Alloy 690TT (Figure 21-1), and Alloy 800NG (Figure 21-2 and Figure 21-3).

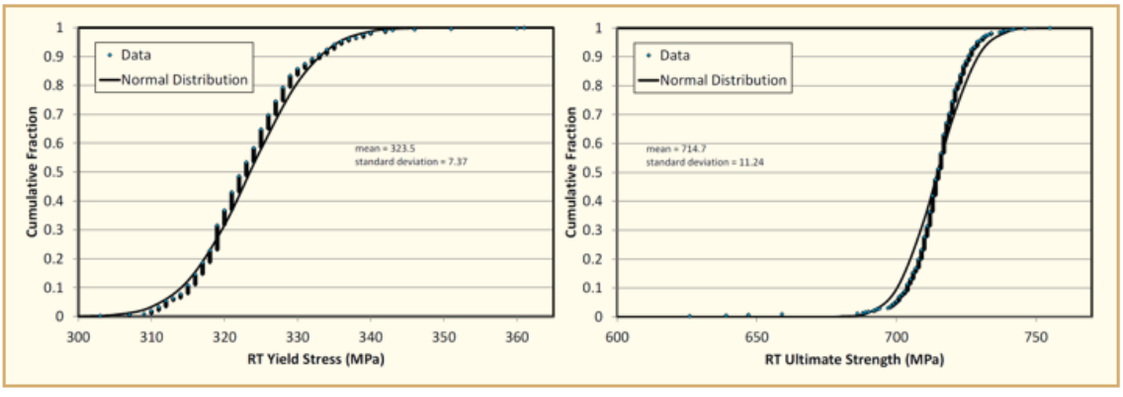

Figure 21-1: Alloy 690TT tubing room temperature mechanical properties. Yield stress = 320 ± 8 MPa. Ultimate tensile stress = 705 ± 11 MPa [Schmitt et al., 2016c].

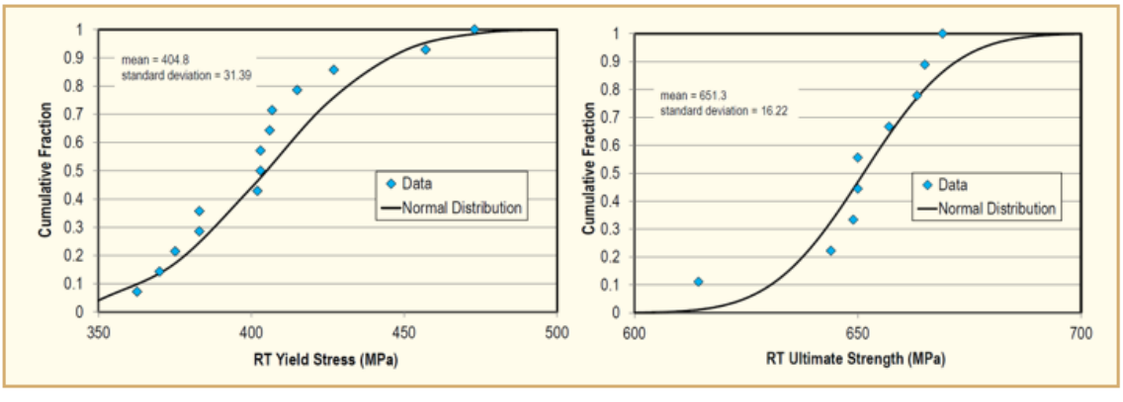

Figure 21-2: Alloy 800CW tubing room temperature mechanical properties. Yield stress = 400 ± 31 MPa. Ultimate tensile stress = 643 ± 16 MPa [Schmitt et al., 2016c].

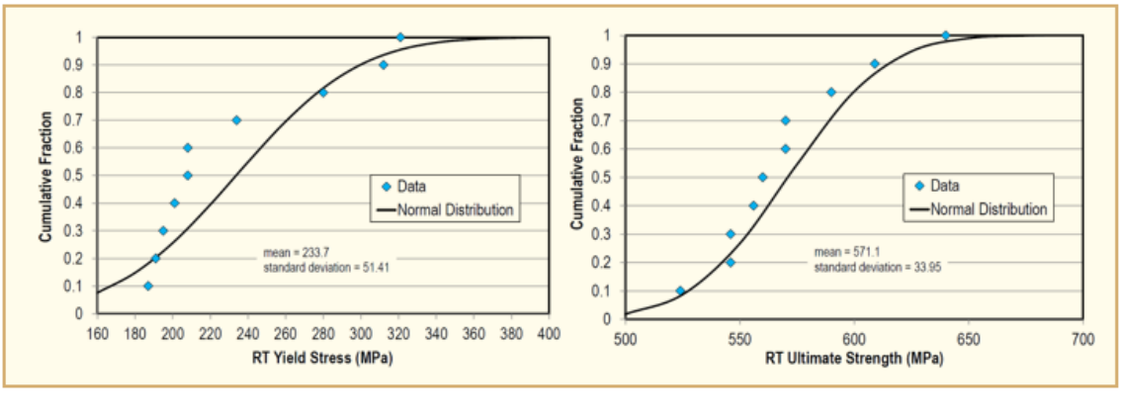

Figure 21-3: Alloy 800MA tubing room temperature mechanical properties. Yield stress = 231 ± 51 MPa. Ultimate tensile stress = 564 ± 34 MPa [Schmitt et al., 2016c].

The material properties of interest included microstructural properties (as observed through SCC crack morphology) that influence the prediction of leak rate (for example, via the Henry-Fauske leak rate prediction) as well as mechanical properties that influence the prediction of tube compliance and rupture. Microstructural properties were developed based on the analysis of material and SCC micrographs (Figure 21-4). Mechanical properties were developed based on the analysis of vendor-supplied test data.

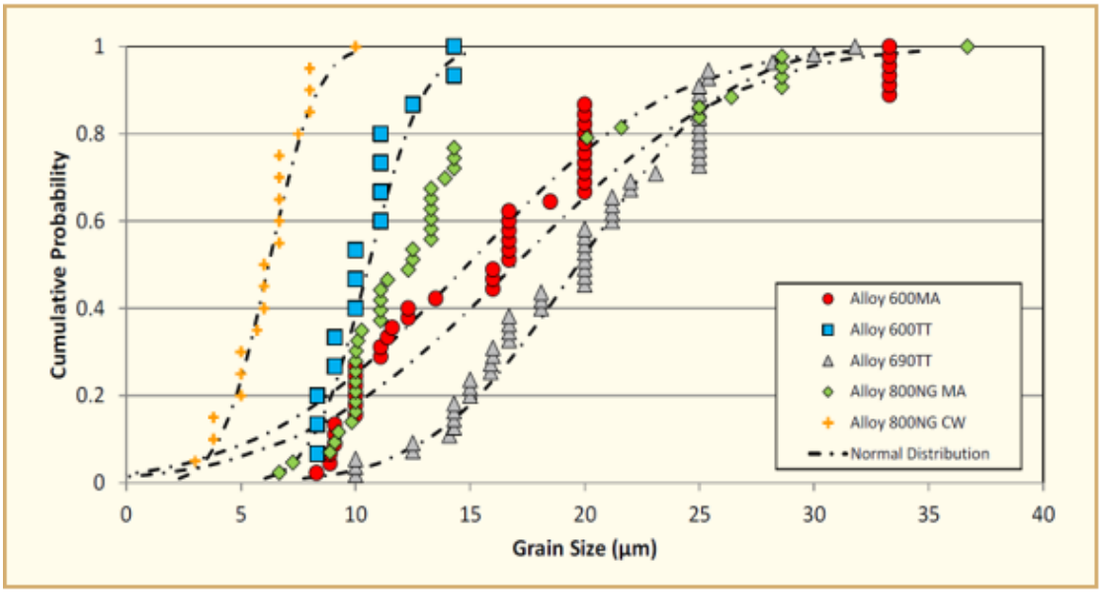

Figure 21-4: Grain size estimation compiled from material micrographs available in the literature. Mean grain size = 17 µm for A600 MA, 10.6 µm for A600 TT, 19.7 µm for A690 TT, 14.9 µm for A800 MA and 6.2 µm for A800 CW [Schmitt et al., 2016c].

Operating temperature mechanical property data for these alloys is somewhat sparse. Therefore, a methodology for predicting high temperature properties from room temperature properties was developed (Figure 21-5).

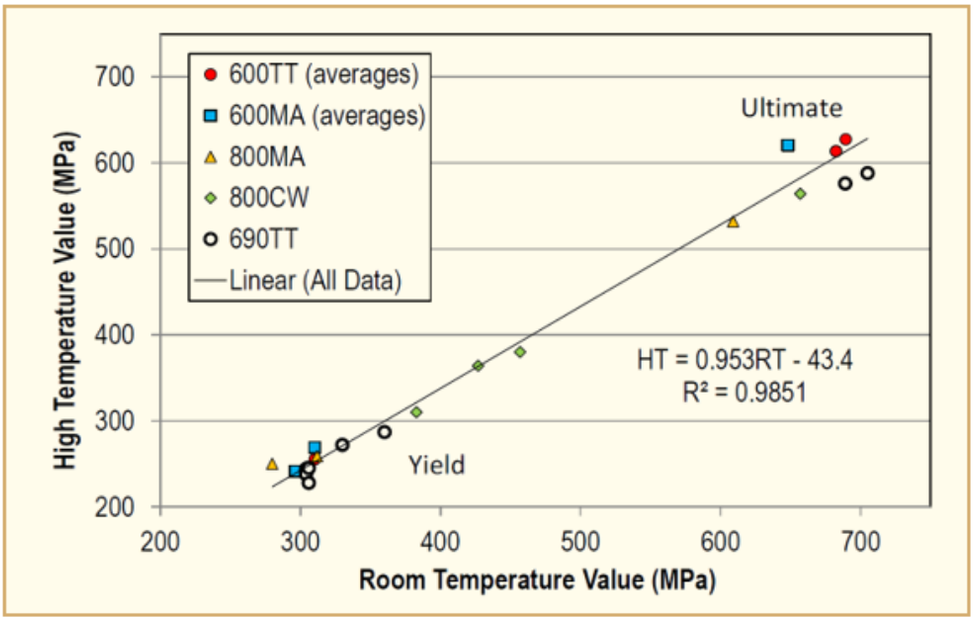

Figure 21-5: Alloys 690 and 800 temperature dependence. A linear model was developed to relate mechanical properties at room-temperature to those at operating temperature HT = 0.953RT - 43.4 MPa [Schmitt et al., 2016c].

The fidelity of these distributions is essential in the analysis of primary-to-secondary side leak rate assessment, but may also be important in numerous other applications.

Following this work, a relationship between leak rate and stress corrosion crack length was developed and validated with leak rate testing data (Figure 21-6).

The model utilized the Henry-Fauske solution as implemented in EPRI's Pipe Crack Evaluation Program to relate leak rate to crack opening displacement and a closed-form elastic solution from the Ductile Fracture Handbook for relating crack opening displacement to crack length (Figure 21-7).

As PICEP was developed for thick-walled piping, it was necessary to validate its usage for thin-walled SG tubes. A total of 72 leak rate tests performed with 30 distinct specimens spanning a range of crack lengths from 3.96 mm to 22.30 mm and leak rates from 0.23 l/h to 329 l/h were identified in the literature and evaluated using the model. For a given leak rate predicated crack lengths were in good agreement with actual crack lengths, demonstrating the validity of the model for thin-walled SG tubes (Figure 21-8).

Additionally, the uncertainty in the testing data was considered through probabilistic methods. The majority of the crack length prediction residual was within the probabilistic bounds associated with uncertainty of the testing data, thereby dismissing the need for additional model uncertainty.

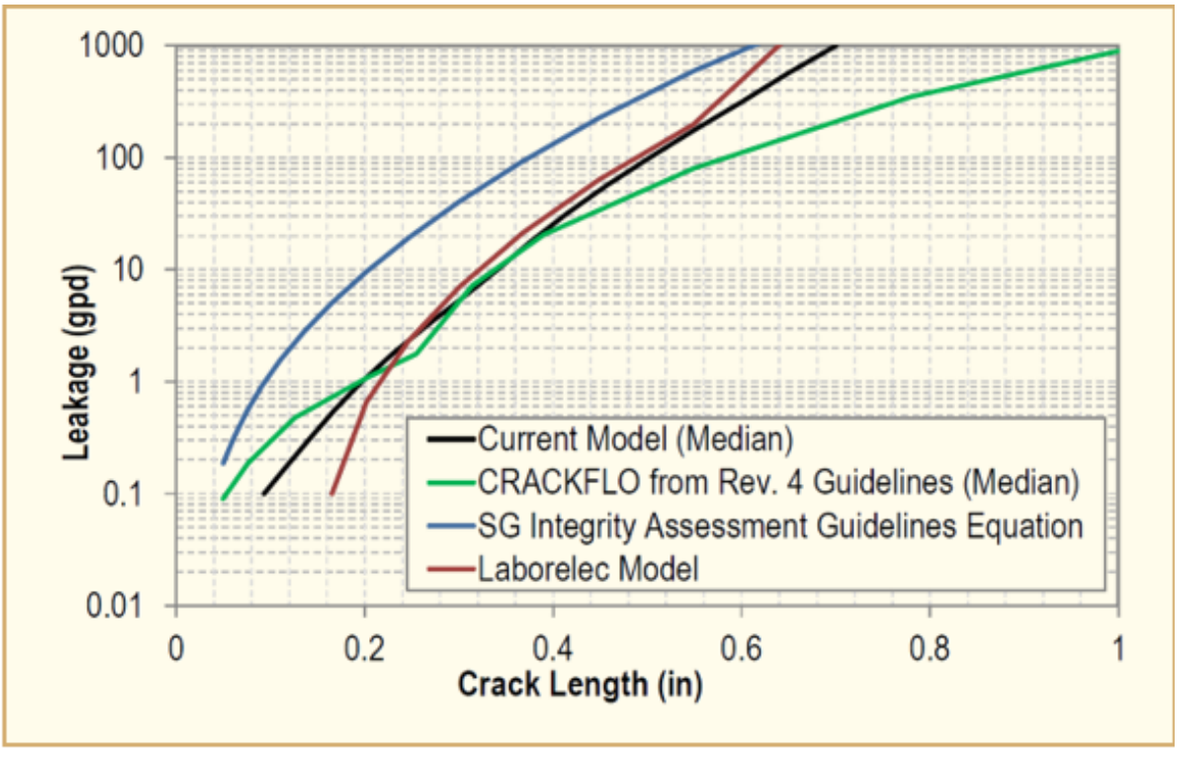

Figure 21-6: Comparison of leakage models for ODSCC flaw in Alloy 600 SG tube with 22.225 mm OD and 1.27 mm thickness at 100 bars pressure differential [Schmitt et al., 2016d].

References

Akkurt H., *Zion Comparative Analysis Project for Assessment of Neutron Absorber Material Performance and Monitoring in Spent Fuel Pools*, Used Fuel & High Level Waste Management Program, EPRI, International Light Water Reactor Materials Reliability Conference and Exhibition 2016, Chicago, Illinois, USA, 1-4 August, 2016.

Alley D., *NRC Perspective and Status of Peening Evaluations*, International Light Water Reactor Materials Reliability Conference and Exhibition 2016, Chicago, Illinois, USA, 1-4 August, 2016.

Andresen P., *Status and Developments with On-line NobleChem*, International Light Water Reactor Materials Reliability Conference and Exhibition 2016, Chicago, Illinois, USA, 1-4 August, 2016.

Andresen P. and Ahluwalia A., *SCC of Alloy 690, Alloy 152/52/52i Weld Metals and Dilution Zones*, International Light Water Reactor Materials Reliability Conference and Exhibition 2016, Chicago, Illinois, USA, 1-4 August, 2016.

Andresen P., Connor M. and Gandy D., *SCC of Powder Metallurgy 316L Stainless Steels & Alloy 600M*, International Light Water Reactor Materials Reliability Conference and Exhibition 2016, Chicago, Illinois, USA, 1-4 August, 2016.

Barborak D., *The Hot Pulse Welding Process for High Integrity Thick Section Welds*, Director of Materials & Welding Technology, International Light Water Reactor Materials Reliability Conference and Exhibition 2016, Chicago, Illinois, USA, 1-4 August, 2016.

Benson M.L. and Homiack M.J., *Uncertainty Characterization of the EPRI/NRC Weld Residual Stress Round Robin Data*, U.S. Nuclear Regulatory Commission, International Light Water Reactor Materials Reliability Conference and Exhibition 2016, Chicago, Illinois, USA, 1-4 August, 2016.

Bjurman M., Ivanchenko M., Ehrnsten U. and Efsing P., *In-service Thermally Aged Cast Stainless Steel – Evolution of Mechanical and Microstructural Properties*, International Light Water Reactor Materials Reliability Conference and Exhibition 2016, Chicago, Illinois, USA, 1-4 August, 2016.

Broussard J. and Crooker P., *Dissimilar Metal Weld Residual Stress Modeling and Guidance*, International Light Water Reactor Materials Reliability Conference and Exhibition 2016, Chicago, Illinois, USA, 1-4 August, 2016.

Cattant F., *Key Emerging Issues and Recent Progress related to Structural Materials Degradation (PWRs, VVERs and CANDUs),* ANT International, LCC11, 2015.

Cattant F., *Key Emerging Issues and Recent Progress related to Structural Materials Degradation*, ANT International, LCC12, 2016.

Chaouadi R. et al., *On the Cu/P and Mn/Ni Interactions during Irradiation of A553B Reactor Pressure Vessel Steels*, International Light Water Reactor Materials Reliability Conference and Exhibition 2016, Chicago, Illinois, USA, 1-4 August, 2016.

Chaouadi R., Stergar E. and Gavrilov S., *Effects of Irradiation on the Tensile and Fracture Properties of 316L Stainless Steel*, International Light Water Reactor Materials Reliability Conference and Exhibition 2016, Chicago, Illinois, USA, 1-4 August, 2016.

Chopra O., *Effects of Thermal Aging and Neutron Irradiation on Crack Growth Rate and Fracture Toughness of Cast Stainless Steels and Austenitic Stainless Steel Welds*, ANL, NUREG/CR-7185, ANL-14/10, 2015.

Crooker P. et al., *Alloy 600/690 SCC Initiation Testing*, International Light Water Reactor Materials Reliability Conference and Exhibition 2016, Chicago, Illinois, USA, 1-4 August, 2016.

Eason E. and Pathania R., *Modeling Environmentally-Assisted Fatigue (EAF) Crack Growth Rates (CGR) in Irradiated Austenitic Stainless Steels in LWR Environments,* International Light Water Reactor Materials Reliability Conference and Exhibition 2016, Chicago, Illinois, USA, 1-4 August, 2016.

Erickson M. et al., *Alternate Toughness Models in ASME CC N830-R1 for use in Appendix A Flaw Evaluation*, International Light Water Reactor Materials Reliability Conference and Exhibition 2016, Chicago, Illinois, USA, 1-4 August, 2016.

Flesner B., *BWR Instrument Penetration J-Groove Weld Examinations – NDE Development & On-site Examination Results*, International Light Water Reactor Materials Reliability Conference and Exhibition 2016, Chicago, Illinois, USA, 1-4 August, 2016.

Focht E., Oberson G., Collins J. and Reichelt E., *Status of U.S. NRC Research Activities for Primary Water Stress Corrosion Crack Growth Rate Testing,* International Light Water Reactor Materials Reliability Conference and Exhibition 2016, Chicago, Illinois, USA, 1-4 August, 2016.

Freyer P., *Focused Ion Beam, Transmission Kikuchi Diffraction, and Transmission Electron Microscopy Characterization of 70 dpa Neutron Irradiated Inconel X-750 Material*, International Light Water Reactor Materials Reliability Conference and Exhibition 2016, Chicago, Illinois, USA, 1-4 August, 2016.

Fruzzetti K. et al., *Potassium Hydroxide for PWR Primary Coolant pH_t Control – Feasibility Assessment*, International Light Water Reactor Materials Reliability Conference and Exhibition 2016, Chicago, Illinois, USA, 1-4 August, 2016.

Fukuta Y., Asada S., Ahluwalia K. and Steininger D, *Study on Effects of Non-Isothermal Condition and Long Hold Time on Environmentally Assisted Fatigue in PWR Primary Water Environment*, International Light Water Reactor Materials Reliability Conference and Exhibition 2016, Chicago, Illinois, USA, 1-4 August, 2016.

Fyfitch S., McDevitt M. and Crooker P., *Evaluation of Craze Cracking Degradation*, International Light Water Reactor Materials Reliability Conference and Exhibition 2016, Chicago, Illinois, USA, 1-4 August, 2016.

Fyfitch S., *Is There Anything New with Alloy A-286 IGSCC in LWRs*?, International Light Water Reactor Materials Reliability Conference and Exhibition 2016, Chicago, Illinois, USA, 1-4 August, 2016.

Garcia S., *IGSCC Mitigation Experience and Application for New Design BWRs*, International Light Water Reactor Materials Reliability Conference and Exhibition 2016, Chicago, Illinois, USA, 1-4 August, 2016.

Garner F. et al., *Use of Ultrasonic Time-of-flight Measurements and BSE Surface Imaging to Non-destructively Measure Void Swelling in PWR Plates and Bolts*, International Light Water Reactor Materials Reliability Conference and Exhibition 2016, Chicago, Illinois, USA, 1-4 August, 2016.

Gilman T. and Alleshwaram A., *Fatigue Aging Management with ASME Code Section XI, Appendix L Flaw Tolerance Evaluation*, International Light Water Reactor Materials Reliability Conference and Exhibition 2016, Chicago, Illinois, USA, 1-4 August, 2016.

Gordon B., *Other Corrosion Concerns Affecting Life Extension of Light Water Reactors*, International Light Water Reactor Materials Reliability Conference and Exhibition 2016, Chicago, Illinois, USA, 1-4 August, 2016.

Gustin H., *Fatigue Management Handbook Training - Fatigue Primer*, International Light Water Reactor Materials Reliability Conference and Exhibition 2016, Chicago, Illinois, USA, 1-4 August, 2016.

Hall B. et al., *Plan for Transitioning RV Integrity to Direct Fracture Toughness*, International Light Water Reactor Materials Reliability Conference and Exhibition 2016, Chicago, Illinois, USA, 1-4 August, 2016.

Nomenclature

appm	atom parts per million
Cr_{eq}	Chromium equivalent for the material
dpa	displacements per atom
GPa	Giga Pascal
HV	Vickers Hardness
J_{Ic}	Value of J near the onset of crack extension
K	Stress intensity factor
K_{Ic}	Critical stress intensity factor
K_{Jc}	Equivalent critical stress intensity factor
K_{max}	Maximum stress intensity factor
K_{min}	Minimum stress intensity factor
l/h	litres per hour
mm	millimetres
MPa	Mega Pascal
Ni_{eq}	Nickel equivalent for the material
nm	nanometer
ppb	parts per billion
ppm	parts per million
UTS	Ultimate Tensile Strength
YS	Yield Strength
δ_c	Ferrite content calculated from the chemical composition of a material (%)
Ø	Diameter
σ_u	Ultimate stress
σ_y	Yield stress
µm	micrometer

List of common abbreviations

ABWR	Advanced Boiling Water Reactor
AD	Areal Density
AM	Additive Manufacturing
AMPs	Aging Management Programs
ANL	Argonne National Laboratory
ANO	Arkansas Nuclear One
APT	Atom Probe Tomography
ARRM	Advanced Radiation Resistant Materials
ASME	American Society of Mechanical Engineers
ASTM	American Society for Testing and Materials
ATEM	Analytical Transmission Electron Microscopy
AWJ	Abrasive Water Jet
B&W	Babcock and Wilcox
BCC	Body Centered Cubic structure
BMI	Bottom Mounted Instrumentation
BMN	Bottom Mounted Nozzles
BMPC	Bechtel Marine Propulsion Co.
BSE	Back Scattered Electrons
BTP	Branch Technical Position
BWR	Boiling Water Reactor
BWRVIP	Boiling Water Reactor Vessel Internals Program
CANDU	CANada Deuterium Uranium
CASS	Cast Austenitic Stainless Steel
CE	Combustion Engineering
CEDM	Control Element Drive Mechanism
CERT	Constant Extension Rate Test
CGR	Crack Growth Rate
CL	Cold Leg
CNL	Canadian Nuclear Laboratories
COD	Crack Opening Displacement
CP	Cathodic Protection
CPF	Conditional Probability of Failure
CR	Cold Roll(ed)
CRD	Control Rod Drive
CRDM	Control Rod Drive Mechanism
CT	Compact Tension
CW	Cold Work(ed)
DBTT	Ductile to Brittle Transition Temperature
DM	Dissimilar Metal
DMW	Dissimilar Metal Weld
DOE	Department Of Energy
EAC	Environmentally Assisted Cracking/Corrosion
EAF	Environmentally Assisted Fatigue
EBSD	Electron BackScattered Diffraction
ECP	Electrochemical Corrosion Potential
EDS	Energy Dispersive Spectroscopy
EMDA	Expanded Materials Degradation Assessment
EOLE	End-Of-License-Extension
EPFM	Elastic-Plastic Fracture Mechanics
EPRI	Electric Power Research Institute
EWR	Excavate and Weld Repair
FAC	Flow Accelerated Corrosion
FAVOR	Fracture Analysis of Vessels, Oak Ridge
FE	Finite Elements
FEA	Finite Elements Analysis
FEM	Finite Element Method/Modeling
FENOC	First Energy Nuclear Operating Company
FIB	Focused Ion Beam
FIV	Flow Induced Vibrations
FME	Foreign Material Exclusion
FOI	Factor Of Improvement
FSWOL	Full Structural Weld OverLay
FTT	Flux Thimble Tube
GALL	Generic Aging Lessons Learned
GB	Grain Boundary
GE	General Electric
GEH	General Electric Hitachi
GMAW	Gas Metal Arc Welding
GTAW	Gas Tungsten Arc Welding
HAZ	Heat Affected Zone
HCF	High Cycle Fatigue
HIP	Hot Isostatic Pressing
HWC	Hydrogenated Water Chemistry
HWC-M	Hydrogen Water Chemistry in Moderate concentrations
IASCC	Irradiation Assisted Stress Corrosion Cracking
ICI	In-Core Instrumentation
ICM	In-Core Monitoring
ID	Inside Diameter
IE	Irradiation Embrittlement
IG	InterGranular

Unit conversion

TEMPERATURE		
°C + 273.15 = K	°C × 1.8 + 32 = °F	
T(K)	T(°C)	T(°F)
273	**0**	32
289	16	61
298	25	77
373	**100**	212
473	**200**	392
573	**300**	572
633	360	680
673	**400**	752
773	**500**	932
783	510	950
793	520	968
823	550	1022
833	560	1040
873	**600**	1112
878	605	1121
893	620	1148
923	650	1202
973	**700**	1292
1023	750	1382
1053	780	1436
1073	**800**	1472
1136	863	1585
1143	870	1598
1173	**900**	1652
1273	**1000**	1832
1343	1070	1958
1478	1204	**2200**

Radioactivity	
1 Sv	= 100 Rem
1 Ci	= 3.7×10^{10} Bq = 37 GBq
1 Bq	= 1 s^{-1}

MASS	
kg	lbs
0.454	**1**
1	2.20

DISTANCE	
x (µm)	x (mils)
0.6	0.02
1	0.04
5	0.20
10	0.39
20	0.79
25	0.98
25.4	**1.00**
100	3.94

PRESSURE		
bar	MPa	psi
1	0.1	14
10	**1**	142
70	7	995
70.4	7.04	**1000**
100	10	1421
130	13	1847
155	15.5	2203
704	70.4	**10000**
1000	100	14211

STRESS INTENSITY FACTOR	
MPa√m	ksi√inch
0.91	**1**
1	1.10